Doctoral Dissertation

Novel Approaches to Elucidate Structure-Performance Relationship in Ziegler-Natta Olefin Polymerization

TOSHIKI FUNAKO

Supervisor: Professor Dr. Minoru Terano

School of Materials Science
Japan Advanced Institute of Science and Technology

March 2015

Contents

Chapter 1 General Introduction 1

1.1 Introduction 2

1.2 Catalyst 3

1.2.1 Catalysis in Chemical Reaction 5

1.2.2 Variety of Catalyst 8

1.2.3 Multifunctional Catalyst 11

1.3 Ziegler-Natta Catalysts 16

1.3.1 Polyolefin 17

1.3.2 Hysterical Development of Ziegler-Natta Catalysts 23

1.3.2.1 First and Second Generation 24

1.3.2.2 Third Generation 25

1.3.2.3 Fourth and Fifth Generation 26

1.3.3 Structure Performance Relationship in Olefin Polymerization 30

1.3.3.1 Role of $MgCl_2$ 31

1.3.3.2 Role of electron donor 34

1.3.3.3 Particle morphology 37

1.4 Statistical analysis 41

1.4.1 Correlation coefficient 42

1.4.2 Principal component analysis 43

1.4.3 Genetic function approximation 44

1.4.4 Application for chemistry 45

1.5 Objective of this study 46

References 48

Chapter 2 ***Multilateral Characterization for Industrial Ziegler-Natta Catalysts toward Elucidation of Structure-Performance Relationship*** 55

2.1 Introduction 56

2.2 Experimental 60

2.2.1 Materials 61

2.2.2 $Mg(OEt)_2$ synthesis 61

2.2.3 Catalyst preparation 62

2.2.4 Polymerization 62

2.2.5 Characterization 63

2.3 Results and discussion 66

2.3.1 $Mg(OEt)_2$ synthesis 66

2.3.2 Catalyst preparation 68

2.3.2.1 Morphology evaluation 68

2.3.2.2 Pore structure evaluation 70

2.3.2.3 Chemical composition 75

2.3.3 Polymerization test 76

2.4 Conclusion 79

References 80

Chapter 3 ***The statistical approaches for elucidation of structure performance relationship in Ziegler-Natta olefin polymerization*** ***83***

3.1 Introduction 84

3.2 Experimental 88

3.2.1 Materials 88

3.2.2 $Mg(OEt)_2$ synthesis 88

3.2.3 Catalyst preparation 89

3.2.4 Polymerization 90

3.2.5 Characterization 90

3.2.6 Statistical analysis 94

3.3 Results and discussion 96

3.2.1 Catalyst preparation and characterization 96

3.2.1.1 $Mg(OEt)_2$ synthesis and their characteristics 96

3.2.1.2 Catalyst preparation and their characteristics 100

3.2.1.3 Olefin polymerization test 109

3.2.2 Dataset evaluation based on statistics 111

3.2.2.1 Dataset evaluation 111

3.2.2.2 One-to-one correlation evaluation using correlation coefficient 113

3.2.2.2 Correlation matrix of structure performance relationship 116

3.4 Conclusion 117

References 119

Chapter 4 *Pore Architecture Engineering of Magnesium Alkoxide based Olefin polymerization Catalysts*

122

4.1 Introduction 123

4.2 Experimental 127

4.2.1 Materials 127

4.2.2 $Mg(OEt)_2$ synthesis 127

4.2.3 Catalyst preparation 128

4.2.4 Polymerization 129

4.2.5 Characterization 129

4.3 Results and discussion 133

4.3.1 Screening of second alcohol for pore architecture control 133

4.3.2 *i*-Propanol incorporation effect on particle structure 138

4.3.2.1 $Mg(OR)_2$ including *i*-propanol 138

4.3.2.2 Catalyst made from $Mg(OR)_2$ including *i*-propanol 144

4.3.3 Polymerization test 150

4.4 Conclusion 153

References 154

Chapter 5 ***Multivariate Analysis of Structure-Performance Relationships in Heterogeneous Ziegler-Natta olefin Polymerization*** 157

5.1 Introduction 158

5.2 Experimental 163

5.2.1 Materials 163

5.2.2 $Mg(OEt)_2$ synthesis 164

5.2.3 Catalyst preparation 167

5.2.4 Polymerization 167

5.2.5 Characterization 168

5.2.6 Statistical analysis 172

5.3 Results and discussion 174

5.3.1 Sample preparation and parameterization 174

5.3.1.1 Catalyst structure characterizations 174

5.3.1.2 Polymerization performances 177

5.3.2 Statistical analysis to elucidate structure performance relationship 179

5.3.2.1 Outlier removal 179

5.3.2.2 Multivariate analysis 184

5.3.2.3 Examination of prediction preciseness 190

5.4 Conclusion 192

References 193

Chapter 6 General Conclusion 196

6.1 General summary 197

6.2 Conclusion 199

Abstract of Minor Research Theme 201

Achievements 216

Acknowledgments 219

Chapter 1
General Introduction

1.1 Introduction

Catalyst is a substance which increases the chemical reaction rate and selectivity. It is able to reduce energy of chemical reaction and improve rate of atom efficiency drastically in the progress of objective chemical reaction. Various catalysts have been used in industrial manufacturing as helpful substances and been made growth along with the industrial expansions by vigorous researches and developments, because of those attractive and important features. Various investigations have been conducted, and enormous kinds of catalysts have been invented and used in industrial manufacturing up to the present time for to satisfy various demands. Therefore, catalysts are working important roles in various industrial fields such as petroleum refining, gas refining, petroleum chemistry, food chemistry, biochemistry, fine chemistry and so on. Thus catalysts are crucial substances which produces from commodities to energies for conservation of our life.

Catalyst is recently focused on not only economic importance by improvement of industrial production efficiencies but also environmental importance by decrease energy and reduction of environmentally hazard substances. Therefore, much further improvement of catalytic performances and addition of novel functions are desired. Thus various catalyst investigations such as elucidation of catalysis mechanism, exploring of

materials which has novel catalysis, designs of catalyst architectures, establishment of preparation methods etc. have been conducted enthusiastically and novel catalysts have been reported continually.

1.2 Catalyst

Catalyst is generic name of substance which can promote chemical reaction without any reduction itself. The definitions of catalyst are as follows [1]:

i) It is a substance which can promote chemical reaction with relatively less amount than reaction and not consume itself during reaction

ii) It is a substance which increase the speed of chemical reaction and not appear in stoichiometric equation

iii) It is a substance which possesses ability of decrease activation energy and makes new route of atom reconstruction.

The substance which can meet the above definitions is regarded as catalyst in scientific field. Thus, the catalyst can be consist of any materials such as organic chemical, inorganic chemical, biochemical and so on. Moreover, it can be any state such as solid, liquid and gas.

Catalyst was used broadly in industrial manufacturing and make enormous benefits by

those helpful features. The growth of industrial benefit which relates to catalyst is shown in Figure 1-1 [1]. Obviously, few production was conducted by using catalyst in the early 1900. Subsequently, inventions and improvements of new catalyst were performed in turn and made industrial range broad. Thus, various new catalysts not only made explosive profits but also these products made our life richness around that time. The enthusiastic developments and researches have been conducted until now. These results progress catalyst chemistry such as improvement of performance, invention of new catalyst, elucidation of catalysis and so on. The current catalyst has been used in most of industrial manufacturing processes by previous enormous efforts.

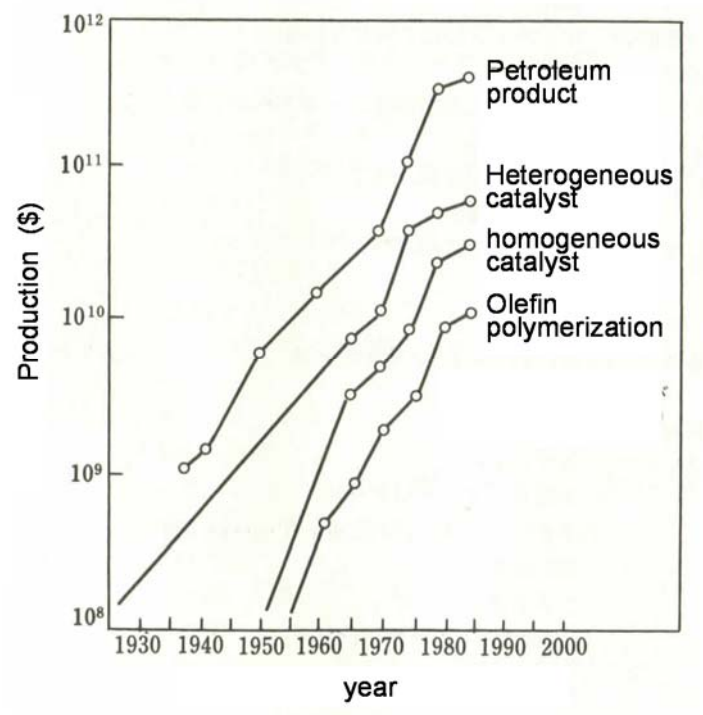

Figure 1-1. Increase of chemical production output related to catalyst using process

1.2.1. Catalysis in chemical reactions

The catalyst does not appear in stoichiometric equation because it never consumes itself during reactions. Originally, the equilibrium of chemical reaction is decided by difference of the state between before reaction and after reaction. It means that equilibrium of chemical reaction independent on reaction route. Hence, the function of catalyst is the acceleration of the reaction speed for closing to equilibrium without change equilibrium state. This phenomena is occurred by decrease of activation energy because the catalyst makes new route of chemical reaction.

This phenomena is explained with the reaction between hydrogen and iodine as example. The stoichiometric equation of this reaction is as follows;

$$H_2 + I_2 \longrightarrow 2HI \qquad (1.1)$$

In the case of progress this reaction without catalyst, it need the temperature more than 300˚C. This high temperature is used for acquisition of higher thermal agitation energy than activation energy, because this reaction is occurred by conversion from transitional state of hydrogen and iodine. Therefore, high temperature is necessary to progress this reaction.

In the case of progress reaction with catalyst, reaction proceeds via successive reaction which was showed below,

$$H_2 \longrightarrow 2H \qquad (1.2)$$

$$I_2 \longrightarrow 2I \qquad (1.3)$$

$$H + I \longrightarrow HI \qquad (1.4)$$

The catalyst can proceed the reaction with greatly lower temperature than non-using catalyst. This is because the catalyst makes activation energy low by generation of new reaction pathway of hydrogen and iodine. The relationship between activation energy and reaction heat at any state is shown in Figure 1-2.

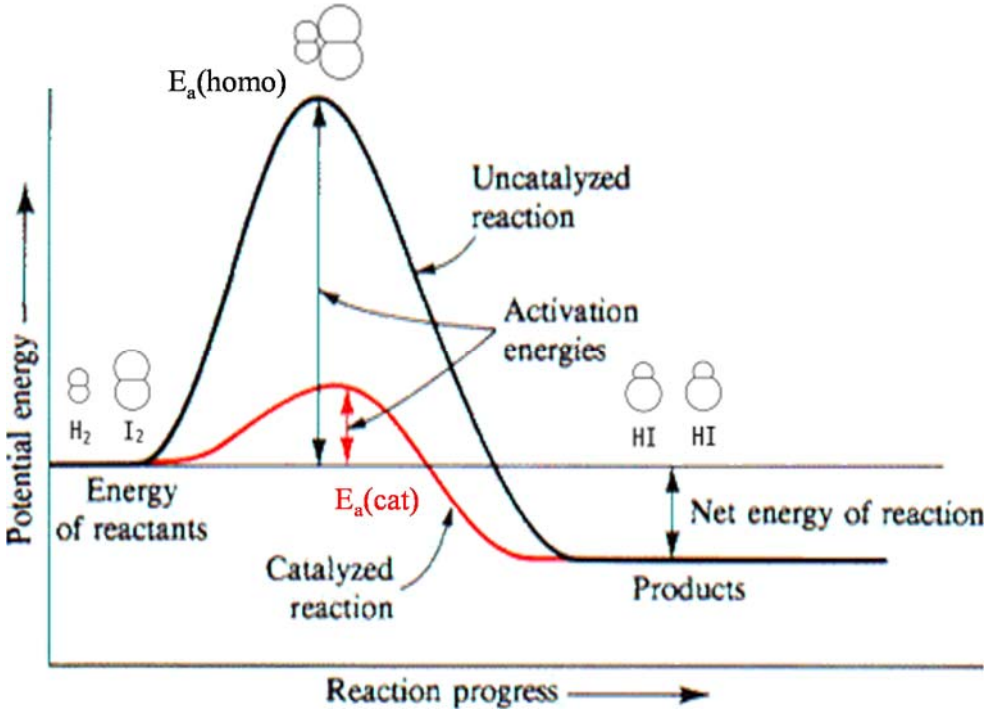

Figure 1-2. Activation energy and reaction heat in chemical reaction with catalyst or noncatalyst

As can be seen from Figure 1-2, conversion of hydrogen and iodine need over $Ea_{(homo)}$ in the reaction without catalyst. However, catalyst decrease activation energy to $Ea_{(cat)}$ to proceed conversion. Thus, existence of catalyst in chemical reaction makes activation energy low and help to proceed reaction to equilibrium state.

The activity energy change in different condition which presence or absence of catalyst and different chemical reaction was shown in Table 1-1. As can be seen, the existence of catalyst in chemical reaction decreases activation energy regardless of reaction species. Moreover, different catalyst change degree of activation energy, even if the reaction is same.

Table 1-1. Activation energy of various reactions and conditions [1]

	Noncatalytic reaction	Catalytic reaction	
Reaction	Activation energy ($kJ \cdot mol^{-1}$)	Activation energy ($kJ \cdot mol^{-1}$)	Catalyst
$2HI \rightarrow H_2 + I_2$	184	59	Pt
		105	Au
$2N_2O \rightarrow 2\ N_2+3H_2$	245	134	Pt
		121	Au
$2NH_3 \rightarrow N_2 + 3H_2$	326	197	Os
		134 ~ 176	Mo
		163	W
		159 ~ 176	Fe

The rate of chemical reaction also related to activation energy. The reaction rate constant k is explained by following equation which is used activation energy.

$$k = A\exp\left(-\frac{E_a}{RT}\right) \qquad (1.5)$$

This equation (1.5) is called Arrhenius equation and often used prediction of the chemical reaction rate. A is pre-exponential factor, E_a is activation energy, R is gas constant and T is temperature. As can be seen from this equation, high temperature and/or low activation energy make rate constant increase. Hence, usage of catalyst not only reduces energy for progress reaction but also increases constant rate of reaction.

1.2.2 Variety of Catalyst

Catalyst is general term of special substance which can improve efficiencies of chemical reaction. It can be identified any state such as solid, liquid and gas phase. Moreover, organic, inorganic and even a living being such as microbe are identified in a broad sense. Therefore, there are welter of catalyst spices in the world.

Catalyst is classified type of process as homogeneous catalyst and heterogeneous catalyst. Homogeneous catalyst was defined catalyst which does not have boundary

surface between catalyst and reaction substrates in a chemical reaction. In the same way, heterogeneous catalyst has boundary surface between substrates. Each of them have available features respectively.

The reaction, which does not have boundary surface between catalyst and substrate, is homogeneous catalytic reaction. Generally, combination is gas-gas or liquid-liquid. The catalyst which is used in homogeneous catalytic reaction is called homogeneous catalyst. Solved metal complex and solid acid-base solid are typical substance as homogeneous catalyst. A lot of technical innovations and inventions were produced in the following rapid and enormous growth of petrochemical industry. For example, olefin polymerization using Ziegler-Natta catalyst (combination of titanium chloride and alkyl aluminum) [2] and alkene hydrogenation using Wilkinson catalyst (Rh complex coordinated by phosphine) [3,4] were one of great inventions and had a big impact on industrial chemistry.

After 1980 decade, homogeneous catalyst came to be used for fine chemicals which has high additional value because of its high controllability of performance. Various accurately designed catalyst which has high selectivity were develop and used for the manufacture the difficult product of separation like a product made by asymmetric synthesis. Those invention makes l-DOPA [5,6], chrysanthemic acid [7], l-menthol [8.9]

and so on were produced in industry by accurate designed catalyst [10]. Thereby, homogeneous catalyst came to be essential substance for synthesis not only fine chemicals but also medicinal product and functional polymer. As stated above, homogeneous catalyst has important roles for synthesis precise synthesis and is expected to use and develop more for produce various chemicals.

On the other hand, the reaction which has boundary between catalyst and substrate were heterogeneous catalytic reaction. And the catalyst which is used in heterogeneous catalytic reaction is called heterogeneous catalyst. Contents of heterogeneous catalyst is various solid species such as transition metal, transition metal compound, metal sulfate, metal salt and so on. [1] Thus, it is not rare that heterogeneous catalyst consisted of multicomponent. Moreover, porous material such as zeolite and aerogel, and unique crystal structure like a perovskite are often used for getting high and/or novel performance. In comparison with heterogeneous catalyst and homogeneous catalyst, heterogeneous catalyst has better feature such as low cost for operation, easiness of using, easiness of separation with substrate, activity and lifetime than homogeneous catalyst. Synthesis ammonium using Haber–Bosch process (Fe_3O_4 including small amount of K_2O and Al_2O_3) [11], high stereoregularity propylene production using Ziegler-Natta process ($TiCl_4/InD/MgCl_2 + AlEt_3 + ExD$) [12, 13] are one part of most famous solid catalyst

which innovated industrial manufacturing at that time. Other various reactions such as hydrogenation, dehydrogenation, oxidation, reduction, alkylation, isomerization, purification and etc. support industrial manufacturing by wide variety of applicable heterogeneous catalyst.

1.2.3 Multifunctional Catalyst

Various industrial catalyst generated profits and change our life more rich by a lot of energetic research and development after industrial innovation. In recently, industrial process has been strongly desired more economic efficiency in the following rising of a newly emerging country which is represented and more reduction space for reaction to expand to micro reactor like a private electric generator. Application of multifunctional catalyst for processes is one of solution. Multifunctional catalyst is one of a catalyst spices which has more than one performances. Applications of this catalyst for chemical reaction are expected not only improvement of process efficiency but also reduction of additional operation and the plural number of reactor.

The plural number of performances are established by catalyst structure designs. Multifunctional catalyst is generally designed and prepared with “multicomponent” and/or ”designing hierarchical structure”.

Multicomponent means that more than one active spices are used for preparation catalyst as active sites. These catalyst has some kinds of active sites which can progress different reaction respectively and makes performances higher and/or progress consecutive reaction which need some active species with a reactor and a step. For example, Al_2O_3 supported Pt catalyst is one of multifunctional catalyst for catalytic reforming of naphtha [14]. Reforming is a chemical process used to convert naphtha (low octane products) into high octane products for giving additional values. Various reaction such as dehydrogenation, isomerization, cyclization and hydrogenation are conducted in this process. Therefore, catalyst was desired various performances at same phase. Table 1-2 shows the catalytic activity and selectivity of methylcyclopentane reforming by combination of Pt catalyst and acid support as example [15]. Silica/alumina supports did not progress any reaction, and Pt catalyst itself progress only dehydrated products. However, benzene is generated by existence of Pt and Silica/alumina at same catalyst. Hence, Pt/Alumina for catalytic reforming is bifunctional catalyst whose Pt has function of dehydration and Aluminum has function of isomerization [16]. From above reports, multicomponent catalyst comes to have multisite which can progress successive reaction with one step.

Table 1-2. Mechanism of bifanctional catalyst in reforming reaction of C6 paraffin

Catalyst	Production (mol%)			
	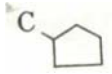	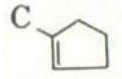	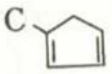	
SiO_2-Al_2O_3	98	0	0	0.1
Pt/ SiO_2	62	20	18	0.8
SiO_2-Al_2O_3 + Pt/ SiO_2	65	14	10	0.4

A hierarchical structure means an organizational architecture of catalyst substances like an assembled toy building blocks. These structures such as pore, surface, crystal structure and particle sharp were much bigger scales than active site. However, these can improve catalyst performance such as selectivity [17], activity [18-20] and life time [21,22] so on. For example, the control of reactant selectivity by architectonics of porous zeolite is introduced as an example. The zeolite pore improves not only activity by increase active specific surface area but also selectivity of reactant by molecular shape selectivity. The selectivity is derived from correlation between reactant and pore, however various reaction mechanism is conducted [17]. Three mechanism is explained as an example. The compound which has eight-membered pore such as Ca-A and H-erionite decomposes only liner alkane without reaction of alkane which has methyl side chain [24]. Figure 1-3 shows the image of its reaction. This phenomena is called reactant selectivity which is decided correlation size between molecular and pore. The cause of reactive difference

between reactant is derived from reaction inside pore [25]. Next phenomena is called product selectivity which is selectivity derived from diffusion limitation of reactant in pore.

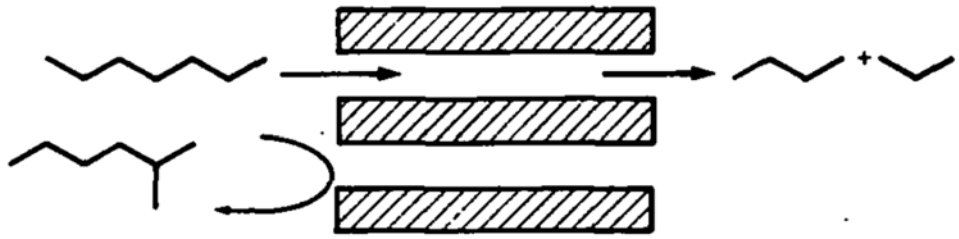

Figure 1-3. Images of molecular shape selectivity derived from reactant selectivity

The images of disproportionation of toluene using ZSM-5 is depicted in Figure 1-4. As can be seen, small reactant such as *p*-xylene and benzene is obtained selectively by reaction in ZSM-5 pore [26]. Various reactant were generated in the pore, however big reactant is not able to diffuse freely and trapped until become small molecules. Therefore, this catalyst makes small molecules selectively. Last phenomena is called restricted transition state selectivity which is selectivity derived from limitation of transition form.

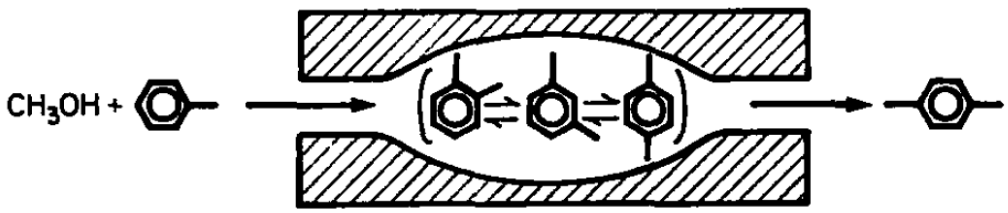

Figure 1-4. Images of molecular shape selectivity derived from product selectivity

The image of disproportionation of m-xylene using H-mordenite is shown in Figure 1-5 as example. In the case of this reaction, 1,3,5 trimethylbenzen is able to go through pore channel, however transition state of compounds for production of 1,3,5-trimethylbenzen is too bulky to form in pore [27]. Thus, 1,3,4 trimethylbenzen, whose intermediate is not bulky compound, is obtained selectively. As mentions above, catalyst hierarchical structure has important role for control catalytic functions.

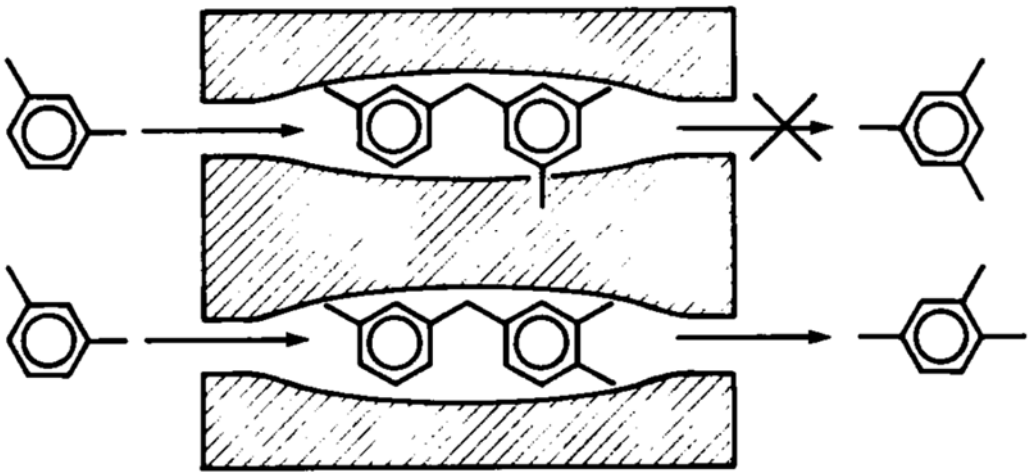

Figure 1-5. Images of molecular shape selectivity derived from restricted transition state selectivity

Multifunctional catalyst has excellent performance and improve processes drastically. Thus, a lot of investigation is conducted energetically to respond industrial demands. However, it is hard work that accomplishment of accurate designing and prepare desired multifunctional catalyst whose architecture ranges micro to macro scales. Hence, the

reaction which is unclear structure performance relationship and the preparation methods which is not able to accurate control make multifunctional catalyst development difficult. Therefore researches and developments of multifunctional catalyst are not only synthesis and performance test but also elucidation of structure performance relationship and exploring method for accurate architecture synthesis.

1.3 Ziegler-Natta catalysts

Ziegler-Natta catalyst is a one of industrial catalyst for polyolefin manufacturing. Especially, this catalyst is used for 99% of polypropylene production in industry. From the following importance of polypropylene in the world, this catalyst comes to have very important role of industrial field.

The first report of this catalyst was success of ethylene polymerization without high pressure and temperature using combination of $TiCl_4$ and alkylaluminum compounds at first in 1953 by Karl Ziegler [2]. Subsequently, propylene polymerization was also succeeded by combination of $TiCl_3$ and alkylaluminium compounds in 1954 by Giulio Natta [12]. These techniques were able to liner polyolefin without high temperature and pressure, and innovated industrial polyolefin manufacture drastically. Therefore, this catalyst is named by implementer who are Ziegler and Natta. After invention, enormous

researches and developments have been conducted and those catalytic performances have kept improving in following industrial importance of polyolefin [28]. Thereby, various polyolefin such as wide variety of commodity grade, copolymer grade which polymerized with higher α-olefine and so on were invented by enormous efforts and produced in industry for sell. In recent year, specialty grade which has high additional values like ultra-high molecular weight polyethylene and impact copolymer was invented and produced. Therefore various Ziegler-Natta catalysts are developed to produce the wide range of polyolefin grade.

1.3.1 Polyolefin

Polyolefin is generic term of synthesized polymer made from alkene as monomer. Especially, polyethylene and polypropylene are well known as commodity plastics. Polyolefin possesses not only great mechanical property but also easiness of fabrication, cheap process cost from synthesis to molding. Therefore, polyolefin is used in broad wide of field as material and product more than 200 million tons every year in the following its industrial and practical conveniences [29]. Moreover, the fact that polyolefin is a material which processes low impact on environment is acknowledged again because polyolefin is composed by only carbon and hydrogen without any toxic material such as

chloride and aromatic groups. From these backgrounds, the increase of polyolefin usage is predicted. The trends of polyolefin production amount were shown in Figure 1-6 [30]. This data suggested that demands of polyolefin keep growth about 5% every year nevertheless a huge amounts of production. [31] Therefore, improvement of production efficiencies and material properties are strongly desired.

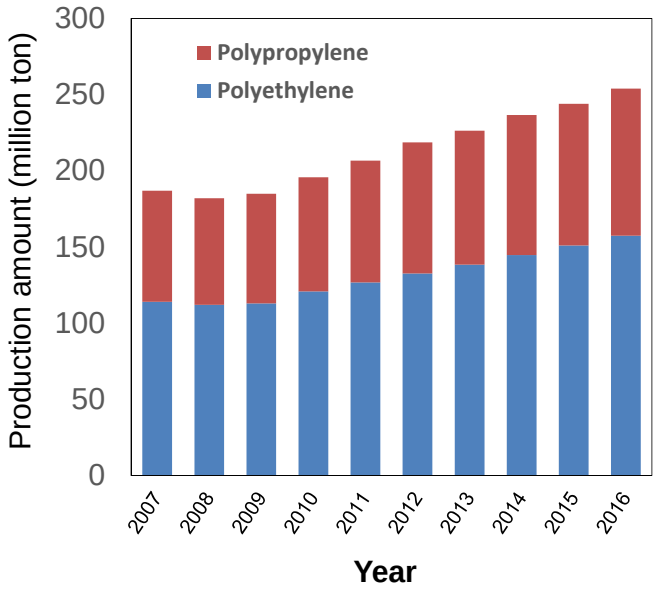

Figure 1-6. Past and future trends of polyolefin production

Polyethylene is a polymer of ethylene and produced the largest amount in the plastics spices. Polyethylene is synthesized by various kinds of catalyst because mechanical property is depends on those structure of molecular chain such as length and branches. Polyethylene is classified according to their molecular chain structure into three categories. The images of molecular structure of classified polyethylene is shown in

Figure 1-6 and those general properties are shown in Table 1-3 [32].

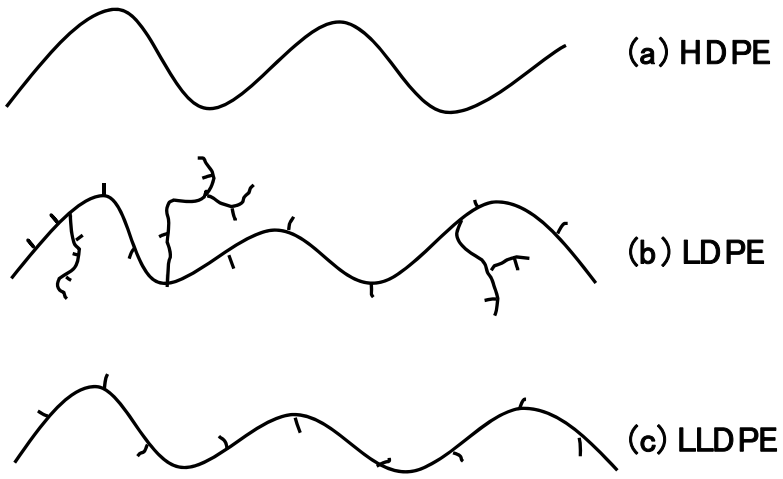

Figure 1-7. Images of molecular structure of polyethylene;
(a) HDPE, (b) LDPE, (c) LLDPE

Table 1-3. Approximate range of properties of different types of PE [32]

	density ($g \cdot cm^{-3}$)	melting point (°C)	crystallinity (%)
HDPE	0.940-0.965	125-135	65-80
LDPE	0.915-0.930	106-120	40-60
LLDPE	0.910-0.940	120-125	40-60

First, high density polyethylene (HDPE) is liner polyethylene without any branches and able to be synthesized by Ziegler-Natta catalyst or fillips catalyst. Properties were dependent of molecular weight and molecular weight distribution. These trend to become different using catalyst spices and polymerization conditions. The features of this polymer is higher crystallinity and density than the other polyethylene spices. Thus this possesses

higher righty and opaque state. Taking advantage of those features, this is used film, plastic bag, some case, pipe and so on. Second, low density polyethylene possesses long chain branches and is synthesized by Philips catalyst. The feature of LDPE is lower density and crystallinity than HDPE. Mechanical properties are dependent not only information of main molecular chain structure but also amount and length of branches. Thus, this mechanical property is flexible and soft. Additionally molding fabrication is easier than the other polyethylene. Form those features, LDPE is used as a material for making film, plastic bags. Third, linier low density polyethylene is liner polyethylene with some amount of short branches and is synthesized by copolymerization between ethylene and α-olefin spices using various catalysts. Mechanical properties are dependent of molecular weight, α-olefin incorporation amount and spices. Therefore selection for α-olefin is one of important factor. Basically metallocene catalysts is able to make LLDPE with high contents ofα-olefin and narrow molecular weight distributions. Thus this possesses is the middle of HDPE and LDPE. From those features, LLDPE is used as a material for making for films and cases. Thus, Polyethylene spices are used broad range by changing these structures and properties.

Polypropylene is polymer made from propylene and synthesized huge amount as an available material all over the world. 99% of propylene is produced by Ziegler-Natta

catalysts in industrial manufacturing although one part of metallocene spices can synthesis polypropylene. Because propylene synthesized by Ziegler-Natta catalysts is cheaper and able to possess broad range of mechanical properties by using different catalyst type. Mechanical properties are dependent not only molecular weight and molecular weight distribution but also stereoregurarity. Stereoregurarity is orientation of polymer decided by coordination of molecules. The images of three kinds of polypropylene with different stereoregurarity is shown in Figure 1-8 [33].

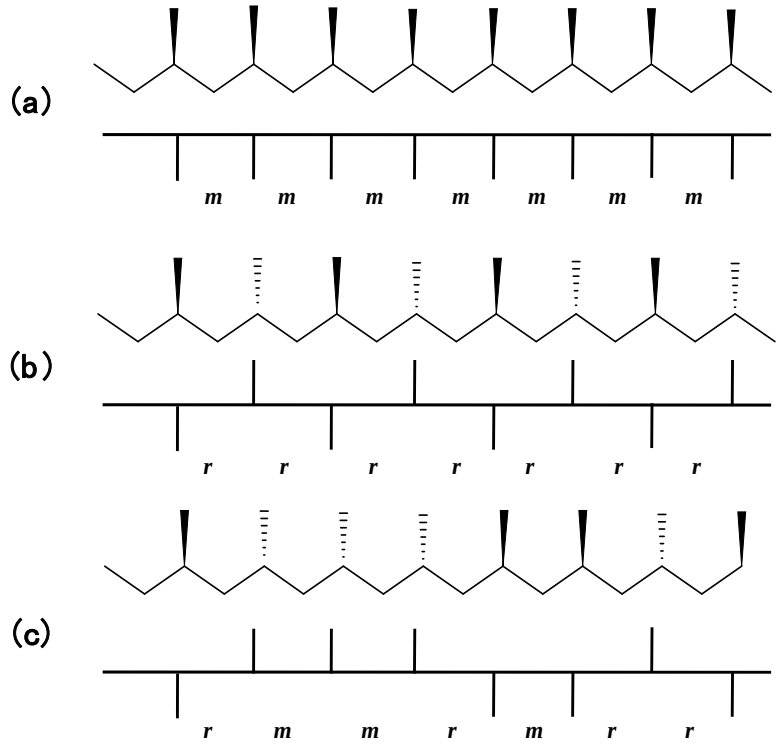

Figure 1-8. Images of stereoregularity of polypropylene; (a) isotactic polypropylene, (b) syndiotactic polypropylene, (c) atactic polypropylene

Isotactic is state that all methyl groups are positioned at the same side with respect to the main chain. Syndiotactic is state that position of methyl group is alternative. Atactic is state that position of methyl group is random [34]. Generally, ratio of isotactic part is called tacticity as degree of molecular orientation. It is one of most important factor to effect on mechanical properties. The higher tacticity polypropylene is, higher rigidity it possesses. From those background, Wide range of polypropylene grades are produced and used for support any request using various type of Ziegler-Natta catalyst

Most of polyolefin products are generic and cheap. However some kinds of polyolefin grade possess excellent property which put out additional values. For example, ultra high molecular weight polyethylene (UHMWPE) has great rigidity, self‐lubricating, abrasion resistance regardless of high temperature conditions [35]. This polymer is one part of HDPE with extremely high molecular weight. This is made from polymerization using Ziegler-Natta catalyst [36,37] or metallocene [38] with reduction of chain transfer reaction frequency as little as possible. Nevertheless difficulty of molding fabrication because of its rigidity and high melting temperature [39], it is used as special materials for gear, fiber, film, artificial bone and so on . Impact copolymer is also well known as high value added polyolefin. It is made by multistep polymerization which process is propylene polymerization as first step and propylene-ethylene polymerization as second

step [39,40]. This multistep process makes polypropylene particles with high dispersed ethylene-propylene rubber [41,42]. This polymer possesses high shock resistance under low temperature conditions without loss of propylene properties. Because of its excellent properties, impact polypropylene is used as a materials for bumper of automobile, sporting goods, construction materials and so on.

1.3.2 Hysterical development of Ziegler-Natta catalysts

Ziegler-Natta catalyst is industrial catalyst to product various kinds of polyolefin materials. Especially, this catalyst is used for 99% of polypropylene production in industry. From the following importance of polyolefin in the world, this catalyst comes to have very important role of industrial field and has kept to be conducted researches and developments for improvement catalyst performances since invention. The performance improvements of Ziegler-Natta catalyst for propylene polymerization is shown in Figure 1-9. As can been seen, its performances has kept to improve and continue to grow from now on.

Here, the history of Ziegler-Natta catalyst developments are explained in this section.

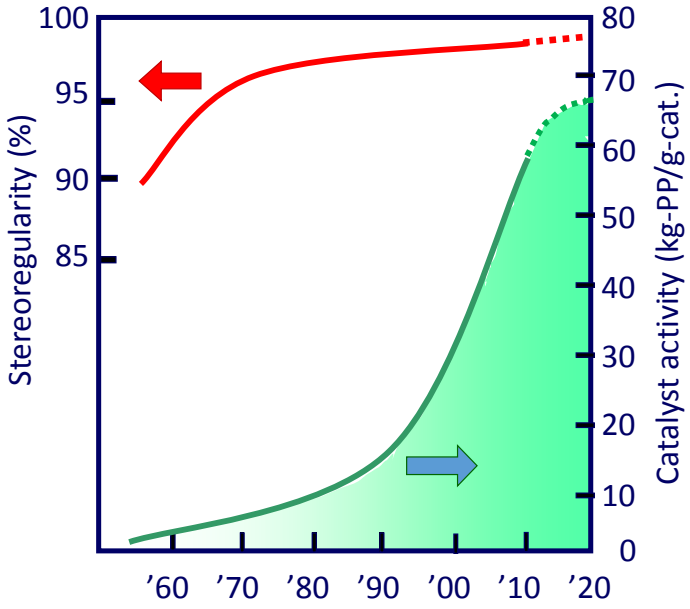

Figure 1-9. The performance improvements of Ziegler-Natta catalyst for propylene polymerization

1.3.2.1 First and second generation

In 1953, Karl Ziegler found out that the combination of $TiCl_4$ and alkylaluminum compound can synthesize polyethylene under ordinary temperature and pressure [2]. Subsequently, Giulio Natta succeeded to obtain polypropylene using $TiCl_4$ and $AlEt_2Cl$ under ordinary temperature and pressure [12]. These catalysts which are simple combination of titanium chloride and alkylaluminum were called first generation catalyst. These inventions contributed polyolefin industrial manufacturing drastically. However, the catalyst of those days is too low activity and stereoregularity to sell out polymers without any post treatments. Hence, decalcification of catalyst residues and separation of

atactic part must be conducted to sell. By the way, regioselectivity was high sufficiently and was not investigated about more control from the early stage because originally only 1-2 insertion is occurred by polymerization of titanium catalyst [43,44]. Therefore, improvement of activity and stereotacticity was tired to improve. In order to increase catalyst stereospecificity, various electron donating compounds were tired to coordinate in titanium chloride spices. As results, it is found that amine and ester compounds can increase catalyst stereospecificity. Thus, taking advantage of the features, high surface area and stereospecific Ziegler-Natta catalyst was developed by cogrinding with $TiCl_3$ and donor compounds. Like these catalysts which were electron doner added Ziegler-Natta catalyst were called second generation catalyst. This catalyst performances were improved. Activity became so high that decalcification was not necessary by combination of bulk polymerization. Additionally, rate of atactic part were reduced only 3-4% by improvement of tacticity [28].

1.3.2.2 Third Generation

In early 1960, support material was started to use in Ziegler-Natta catalyst. At the most early stage, some materials which had high specific surface area such as silica, alumina, magnesium hydroxide and chlorinated magnesium oxide were used as supports and

coordinated with $TiCl_4$. These developed catalysts were used as ethylene polymerization catalyst [45]. Soon after, the combination of $TiCl_4$ and activated $MgCl_2$ were found out and used as high activity catalysts [46,47]. However, this catalyst possessed too low activity and stereoselectivity to use industrial manufacturing in propylene polymerization. The investigation for exploring high performances lewis base as donor in order to solve problem of low performance for propylene polymerization. In 1970s, it was achieved to develop novel solid catalyst which was made by grinding among $TiCl_4$, $MgCl_2$ and lewis base compounds (called internal donor). And this catalyst was activated by alkylaluminum compound and another lewis base (external donor), and showed high activity and stereoselectivity in propylene polymerization. This catalyst systems came to be used in industrial manufacturing from 1978 and catalyst performances were increased drastically [45]. These catalytic systems which is $TiCl_4$ / Internal donor / $MgCl_2$ + alkylaluminum + external donor is used as fundamental combination even now.

1.3.2.3 Fourth and Fifth Generation

Development of Ziegler-Natta catalyst was mainly conducted by exploring new donor and morphological control after invention of combination which was $MgCl_2$ supported $TiCl_4$ and Internal donor activated by alkylaluminum and external donor before

polymerization. The general performances of Ziegler-Natta catalyst with different donor were shown in Table 1-4 [13,44].

Table 1-4. General performances of Ziegler-Natta catalyst with different systems

Internal donor	External donor	PP yield (PP-Kg·cat·g^{-1})	X.I. (%)	*mmmm* (%)	*Mw/Mn*	H_2 responce
Phthalate	Silane	70-40	96-99	94-99	6.5-8	Medium/Low
Diether	None	130-100	96-98	95-97	5-5.5	Excellent
Diether	Silane	100-70	98-99	97-99	4.5-5	Excellent/High
Succinate	Silane	70-40	96-99	95-99	10-15	Medium/Low

The industrial catalyst which used by Montecatini company at first in 1978 is used ethyl benzoate and methyl-p-toluate as internal and external donor respectively. Ester compounds were often used like this in early stage of using $MgCl_2$ supported Ziegler-Natta catalyst. Especially ethylbenzoate was often used as internal and external donor. Then, the combination of phthalate compounds and alkoxysilane was founded out as internal and external donor. This combination possessed superior activity and stereoselectivity than combination of ester compounds. From development of this combinations, activity and steroreguratiry came to become high enough. Therefore, new donor is demanded various performances with good balances which are activity, steroselectivity, lifetime, molecular weight length and molecular weight distributions.

After that, new donor kept to be explored and founded out. For example, diether compounds (especially 1,3 diether) can show higher activity and narrower molecular weight distribution than the other donor without using any external donor [48]. Additionally, succinate compounds can synthesis polypropylene which has broader molecular weight distribution than any other donors [49]. As mentions above, improvements and developments of donor comes to not only improve efficiency of industrial processes but also synthesize desired polypropylene structure in order to control property from first order structure. From its usefulness, exploring new donor is currently also performed to control polymer structures accurately.

On the other hand, more efficient and simplified processes were desired in early 1970s after polymer which is high yield and tacticity could be acquired constantly. Therefore improvement of these properties were also conducted by control of catalyst particle morphology apart from donor improvement. This catalyst is made by grinding among solid catalyst compositions and those particle morphologies were irregular and small at that time. Thus, these catalyst performances were high activity and seteroselectivity, however low activity stability and irregular morphology made operation difficult. Therefore improvement of catalyst performances is demanded and tried to control morphology. In early 1980s, precipitation method [50] and chemical reaction method [51]

were developed and used for control catalyst morphology. Precipitation method is one of methods which prepare catalyst by precipitation from solved catalyst in solution. Especially, the method which precipitation from $MgCl_2$/alcohol solution is often used because of high performances of resultant catalyst. The features of this catalyst are particle density and stiffness. Thus, this catalyst is often used in homo polymerization by bulk process and gas process. Other method is chemical reaction methods which prepare catalyst by conversion from magnesium precursor to $MgCl_2$ and coordination $TiCl_4$ and donor. $Mg(OEt)_2$ is often used for chemical reaction method. The features of this catalyst are high morphology control ability because catalyst morphology depends on precursor morphology. Thus, catalyst has high control ability of polymer morphology ability. Additionally, it has high comonomer insertion ability in copolymerization because catalyst has high porosity. From these features, catalyst made by chemical reaction method is better suited production of copolymer, Impact copolymer and so on.

As mentions above, Ziegler-Natta catalyst developments were mainly conducted by exploring new donor and control particle morphologies and made performances higher. Development of catalyst achieved not only to improve production efficiency but also to product high added value polyolefin like UHMWPE and impact copolymer. Current catalyst developments keep to be conducted with same objective which are exploring new

donor and control particle morphologies for more improvements of Ziegler-Natta catalyst.

1.3.3 Structure performance relationship in olefin polymerization

Ziegler-Natta catalyst was simple combination of $TiCl_3$ and alkylaluminum compounds at first invention. However, usage of donor and $MgCl_2$ made structure complex instead of improvement performances. Therefore, elucidation of correlation between structures and performances became difficult. The main causes were three. First is difficulty of characterization on catalyst structure. Ziegler-Natta catalyst is composed of multicomponent and irregularly hierarchic structures which ranges from angstrom scale to millimeter. Second is difficultly of systematic change of catalyst morphology because current industrial preparation methods are not able to control only one structure parameters. Third is difficulty of quantitative elucidation of structure effect because catalytic performances were determined by various structural parameters with concerted or opposed mechanism. Therefore elucidation of structure performance relationship is very difficult task from above problem. However, a lot of investigation reported role of structures for performances by importance of Ziegler-Natta catalyst. Here, the role of catalyst structural information is explained.

1.3.3.1 Role of $MgCl_2$

In 1970s, Ziegler-Natta catalyst which was called third generation came to use $MgCl_2$ as support material. It worked not only immobilization of active species and increase active surface like other catalyst systems but also electron donation effect to active species. The effect of various metal chloride ($MnCl_n$) in propylene polymerization activities were compared from $Ti(OBu)_4/AlEt_2Cl$ systems which active site is not easy to change by Soga and coworkers. As a results, correlation between activity and electronegativity of M^{n+} ($\chi_n = \chi_0(1+2n)$; χ_0 = electronegativity of metal, n=oxidation number) were founded out. This correlation is shown in Figure 1-10 [52]. As can be seen, $MgCl_2$ had the highest activity and lowest electronegativity. Therefore, $MgCl_2$ is best support for Ziegler-Natta catalyst.

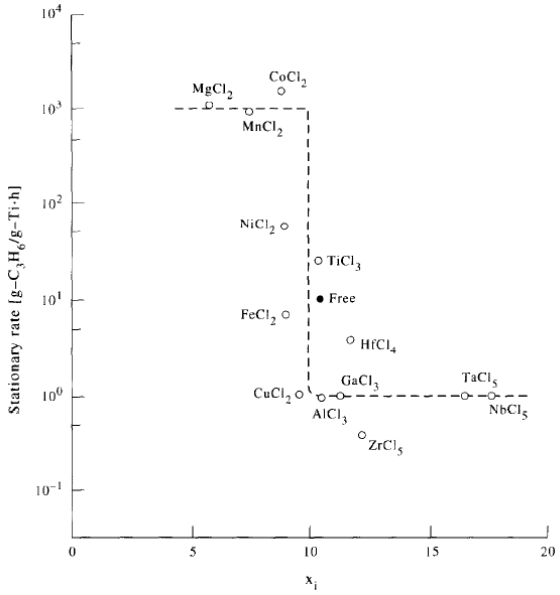

Figure 1-10. Correlation between activity and electronegativity of metal ion

δ-$MgCl_2$ is used for Ziegler-Natta catalyst as support [53,54]. It is called activated $MgCl_2$ and those crystalline structures are different between usually used $MgCl_2$. XRD patterns for various $MgCl_2$ are shown in Figure 1-11 [55]. As can be seen, only δ-$MgCl_2$ spectra is broad. It means that crystal size is small and peak is too broad to identify crystal structure [56]. Therefore, characterization of $MgCl_2$ is very difficult, especially $TiCl_4$ and donor supported $MgCl_2$ is not able to determine those crystalline structures perfectly now.

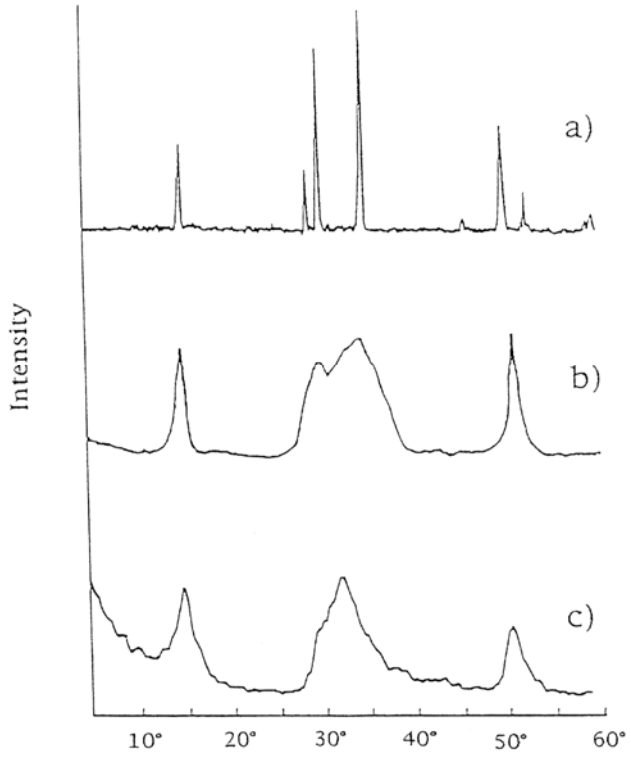

Figure 1-11. XRD pattern of various $MgCl_2$; (a) α -$MgCl_2$ (b) δ-MgCl2 activated from α -$MgCl_2$ by ballmilling, (c) δ-MgCl2 activated α -$MgCl_2$ by chemical reaction method

δ-$MgCl_2$ has high energy surface which are (110) and (104). This images are shown in Figure 1-12 [57]. $TiCl_4$ and donor are considered to adsorb these surface. When $TiCl_4$ is adsorbed to $MgCl_2$, structure is changed from tetrahedral to octahedral and coordinated with $TiCl_4$ mononuclear and/or Ti_2Cl_6 dinuclear. Thus, it is considered that titanium can be coordinated any site and form various state irregularly. This is causes that Ziegler-Natta catalyst has multisite.

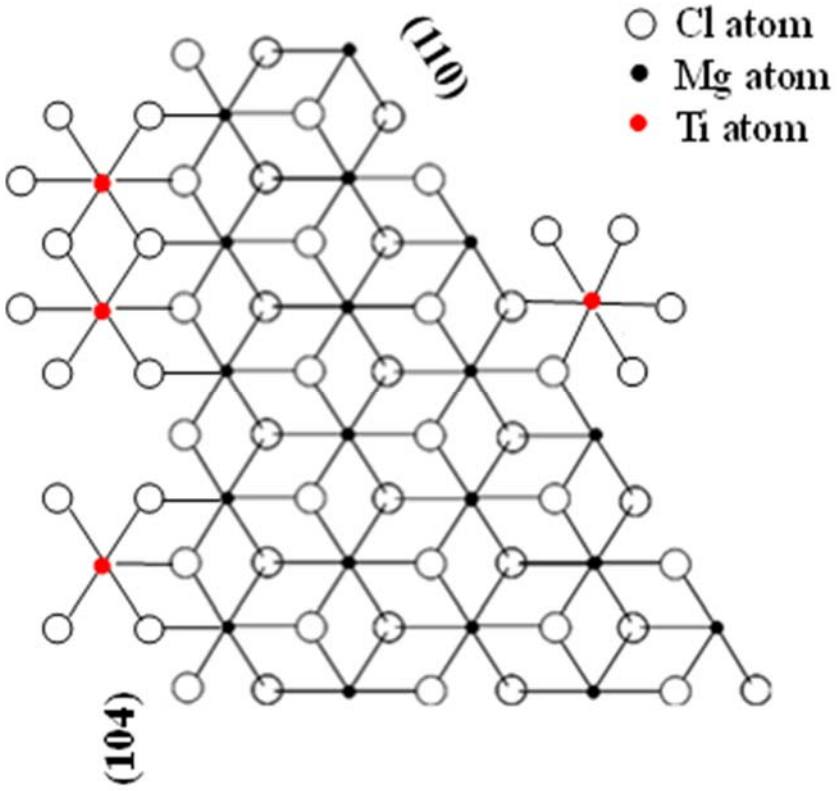

Figure 1-12. Model of mono and dinuclear $TiCl_4$ species on the (104) surface and mononuclear $TiCl_4$ species on the (110) lateral surfaces

As mentions above, the role of $MgCl_2$ in Ziegler-Natta catalyst is immobilization of titanium species, increase active surface area, regulation of active site symmetry and electron donation. All effects are important role for preparation high performance Ziegler-Natta catalyst.

1.3.3.2 Role of electron donor

Olefin polymerization using Ziegler-Natta catalyst is progressed by coordinate anionic polymerization which is showed in Figure 1-13 [58].

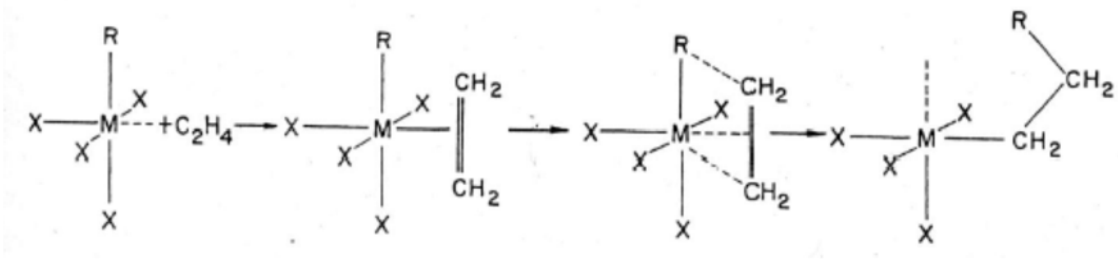

Figure 1-13. Cossee Mechanism. R and X indicate a growing chain and chlorine atom respectively.

The state of titanium spices effect on polymerization performance greatly. A donor is a substance to which the state of titanium and $MgCl_2$ structure can be changed and improves catalytic performance. Catalyst performances were improved by donor property not only electro donation for active site but also stabilization of activated $MgCl_2$ surface and steric hindrance. The role of donor in Ziegler-Natta polymerization is as follows

Role of internal donor [28]

1. stabilization of activated $MgC1_2$, resulting in an enhancement of the effective surface area

2. preventing formation of non-stereospecific sites by adsorbing on the $MgC1_2$ surface, where $TiCI_4$ is supported to form non-stereospecific sites

3. taking part in the formation of highly isospecific sites

4. replaced by external donors, to form more isospecific sites.

Roles of external donors [28]:

1. poisoning of non-stereospecific sites selectively;

2. conversion of non-stereospecific sites into highly isospecific sites

3. conversion of isospecific sites into more highly isospecific sites

4. increase the reactivity of the isospecific sites.

The elucidation of effect on performance was difficult to identified because characterization difficulty of irregular active site. Nevertheless, enormous effort to elucidate, it has not resulted to clarify quantitative structure performance relationship until now by only experimental results. However, Busico and coworker propose active site model by obtained enormous data. This model is called three site model and shown

in Figure 1-14 [59]. This model describes that the stereospecificity is not determined $TiCl_4$ coordinated surface such as (110) or (104) and nuclearity (mono- or dinuclear), and according to coordinate or not of bulky regents (donor,Cl) in $L_{1,2}$ site at near the coordinated metal sites (Mg, Ti, or Al). After, Terano and coworker improve more expansive and accurate this model [60].

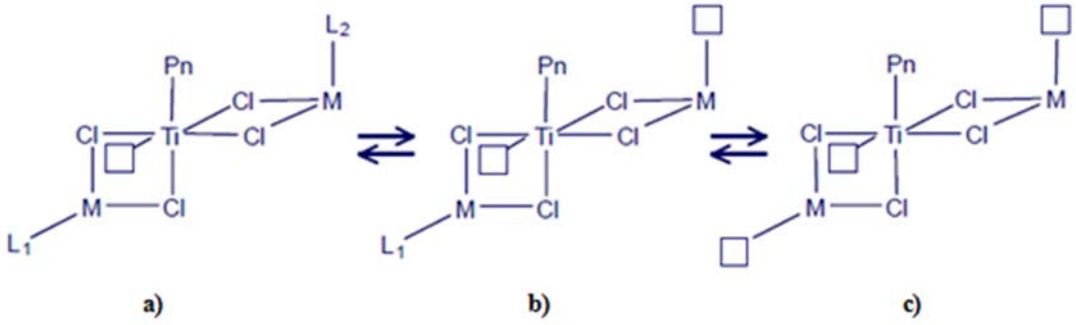

Figure 1-14. Three-site model of active Ti species for highly isospecific (a), poorly isospecific (b), and syndiospecific (c). M = Ti, Mg, or Al, $L_{1,2}$ = donor or Cl, □ = vacant site, and Pn = growing polymer chain.

Recently, cluster DFT calculation comes to be powerful tools for investigation of accurate micro active site structure following great development of computer science. this method proved that adsorption of two succinate compounds at the L_1 and L_2 site can convert the aspecific titanium species into isospecific active site on the $MgCl_2$ (110) surface [61]. Additionally, Taniike reported that monoester donor is adsorbed to (110) surface with $TiCl_4$ and improve not only stereospecificity but also regioregularity and

polymer molecular weight which are proved by obtained experimental results [62,63].

1.3.3.3 Particle morphology

The performances of Ziegler-Natta catalyst was desired not only activity and stereospecificity but also operation easiness and application other polymerization method from usage of $MgCl_2$ as a support. Therefore, many researcher tried to improve performance such as stability of activity, copolymerization performance, catalyst stiffness, control ability of synthesized polymer and so on. Thus, precipitation method and chemical reaction method which can control catalyst morphology were developed to satisfy demands [50,51]. Recently, control of particle morphology comes to be demanded not only shape but also inner hierarchical structure because more accurate control of performance. Then correlation between particle structures and performances to obtain design criteria of particle morphology.

The cause which $MgCl_2$ morphology has more number of roles than other catalyst is changed morphology by fragmentation during polymerization. Fragmentation is a phenomenon which is particle braking by internal pressure from generated polymer inside pore [64,65]. The image of fragmentation progress is shown in Figure 1-15 [66].

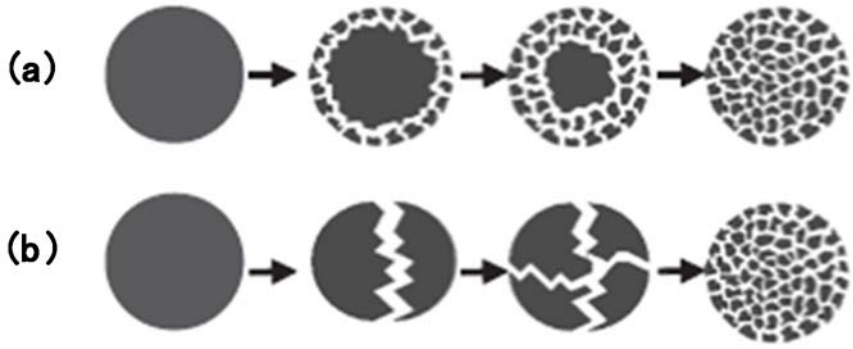

Figure 1-15. Two limiting modes of the fragmentation of catalyst carriers: (a) shrinking core, (b) continuous bisection

The fragmentation behavior is decided by size of pore, stiffness of catalyst particle and polymer generation speed. Fragmentation behaver is roughly divined by shrinking pore model and continues bisectional model. Shrinking pore model is fragmentation form outside of particle to inside gradually. This fragmentation behavior tends to be occurred when particle pore is small and particle stiffness is high. On the other hand, continues bisectional model is fragmentation from inside and fragment particle gradually became small. This fragmentation tends to be occurred when particle stiffness is low and polymer is easily synthesis inside pore by low diffusion limitation. In practice case, fragmentation is occurred with combination of both models and strongly depends on not only particle structure but also polymerization species and conditions [67].

The behavior of fragmentation has strong effect on stability of activity behavior. Catalyst activity is determined by active site number with balance of activations and

deactivations by alkylaluminium compounds. Some active sites are deactivated by excessive oxidization and some active sites are generated from new surface by fragmentation. Therefore control of activate and deactivate balance by fragmentation process is very important role of control activity behavior [68]. The activity behaviors which is performed by irregular shaped catalyst and shape controlled catalyst is shown in Figure 1-16 [69]. As can been seen, the activity behavior of irregular shaped catalyst is confirmed rapid activation and deactivation. The cause of this phenomena is derived from preparation method. Irregular shaped catalyst is made by cogrinding method and most of active site is placed on near surface. Therefore active site is activated and deactivated at one time. As results, activity become increase rapidly and decrease soon. On the other hand, activity of morphology controlled catalyst is stable because the balance of activation and deactivation is maintain.

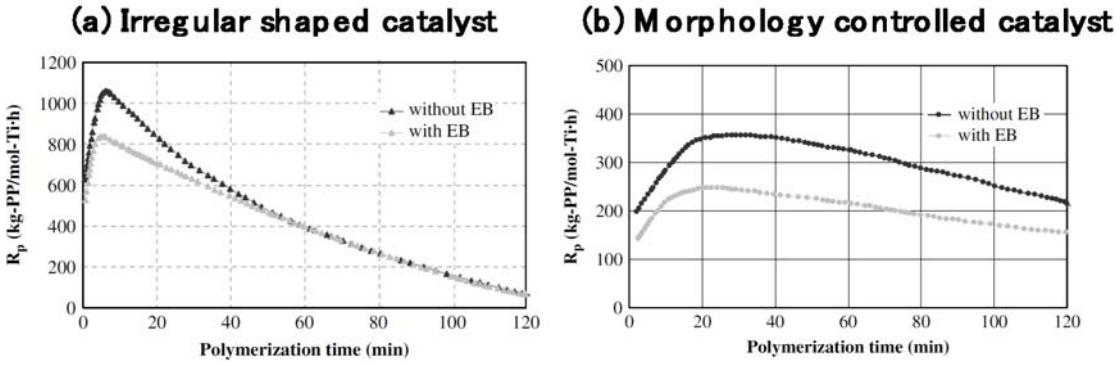

Figure 1-16. Kinetic profiles of propylene polymerization using catalyst whose morphology was different; (a) Irregular shaped catalyst, (b)Morphology controlled catalyst

Additionally, catalyst has an ability to control synthesized polymer morphology. This ability is derived from phenomena which the morphology of polymer is dependence on catalyst morphology in Ziegler-Natta olefin polymerization. This phenomena is said replication phenomenon. The mechanism of replication phenomenon is shown in Figure 1-17 [70,71]. At the initial stage of polymerization, catalyst fragments are dispersed uniformly in polymer particle. As polymerization proceeds, polymer subparticle growth with fragmented catalyst. As polymerization proceeds further, fragmented catalyst fragment more and growth new subperticle. Polymer particle is grown by these mechanism in olefin polymerization. Thus, polymer grows with keeping catalyst morphology. From these reason, the morphology of industrial catalyst is demanded spherical shape and narrow particle size distribution because demanded polymer morphology is spherical shape and narrow particle size distribution for ease operations.

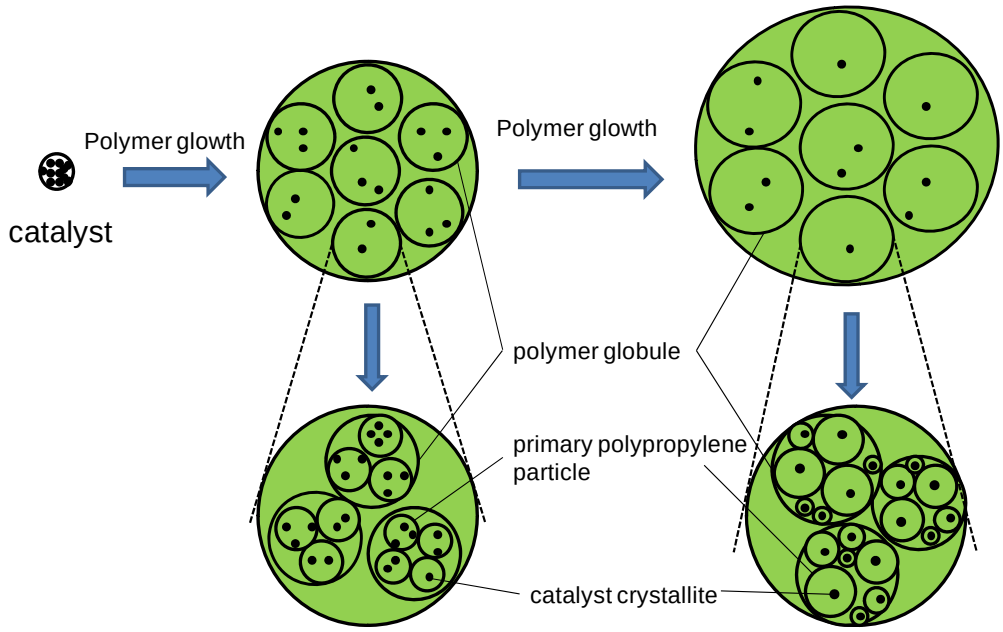

Figure 1-17. Polymer growth mechanism with Ziegler-Natta catalyst fragmentation

As mentioned above, the performance of Ziegler-Natta catalyst is dependent on not only micro structure such as chemical composition and active site structure, but also catalyst morphology such as pore, particle size, shape and stiffness. Therefore, morphology control method keeps to be investigated for improvement of Ziegler-Natta catalyst.

1.4 Statistical analysis

Statistics is the study of big data processing which are collection, analysis, interpretation, presentation and organization using applied mathematics. This study comes to be used in a broad filed such as medical science, industrial science, social

problem and so on in accordance with growth of an information-oriented society by development of computer and popularization of Internet. Currently, this becomes indispensable study in the various field. Statistical analysis is data treatment process based on statistics. This is a generic term of the methods which analysis the enormous and complex data to obtain right information by various ways. Here, statistical analysis is explained.

1.4.1 Correlation coefficient

Correlation coefficient is statistical indicator which indicates liner correlation between two variable. Generally, the value approaches +1 or –1, the correlation extent becomes higher in a positive or negative direction, respectively. And the value approaches 0, the correlation extent becomes lower.

Correlation coefficient is determined by covariance of two variable and variance of each variable. The correlation coefficient r, between two variables (x and y) is defined as

$$r = \frac{C_{(x,y)}}{\sqrt{V_x \times V_y}} \qquad (1.6)$$

$C_{(x,y)}$, V_x and V_y are the covariance and the variances for x and y, respectively. They are defined as

$$C_{(x,y)} = \sum_{i=1}^{n} \frac{(x_i - \bar{x})(y_i - \bar{y})}{n} \qquad (1.7)$$

$$V_x = \sum_{i=1}^{n} \frac{(x_i - \bar{x})^2}{n} \qquad (1.8)$$

$$V_y = \sum_{i=1}^{n} \frac{(y_i - \bar{y})^2}{n} \qquad (1.8),$$

where n is the number of data.

1.4.2 Principal component analysis

Principal component analysis (PCA) is one of multivariate analysis which can reduce large number of variables to smaller number without any information losses. This method was invented in 1901 by Karl Pearson [72], and investigated various investigators for made improvement of itself [73,74] and development of new analysis systems like a Principal Component Regression (PCR) [75,76] . This analysis is reduction of variables identification of the plural number of variables within multi-dimensional state which explain the maximum value of variances in the whole data set in the minimum number of dimensions for easy to understand big data. Using this analysis results has great information as follows [77];

1. Reduction of the dimensions of dataset, enabling a greater quantity of information to be visualized.

2. Study of the relation between different descriptors

3. Preparation data for further analysis for removing descriptor or samples which has collinearity.

From this merit, PCA is used only conforming of sample features and classification of dataset [78] but also finding out outlier [74,79] and collinearity descriptor combinations [80] for pretreatment of other multivariate analyses.

1.4.3 Genetic function approximation

Genetic function approximation (GFA) is one of multivariate analysis which can construct quantitative structure-performance relationship with genetic algorithm. This method was established by Rogers and Hopfinger in 1994 [81]. GFA is not the method which is calculation from partial regression coefficient and residual parameters of assigned descriptors like a Multi Linear Regression (MLS), but a method which is search and determination by checking large number of equation models based on genetic algorism. Genetic algorism [82] is a search algorism which models on natural genetics and evolutions. This algorithm works with a group of variables which called population. This population is evolved to next generation in processes which are selection, crossover and mutation. Where selection is determination of residual variables by fitting degree like a

survival in nature, crossover is blend between survived variables each other and creation new variables which has inherit features from both of last variables like a making child, mutation is creation variables randomly in order to avoid algorithm stuck suboptimal point, generation is the number of trial. These processes are conducted until model fitness value becomes convergence [77].

This method can approach to best fitting model equation with selection of a plenty number of models which has various descriptor combinations. Therefore, this method appropriates the cases that there are poor information about influence degree of each descriptors to performance. It can determine best fitness model efficiently from infinity number of descriptors information.

1.4.4 Application for material science

Statistics is the study for investigation about population and economics originally and started to be use in the 17th century. In the later part of 20th century, growth of an information-oriented society by development of computer and popularization of Internet made this study more useful for other field. The material science was one of them, and pharmaceutical chemistry was first example to use statistics for material science. Statistical analysis was used as screening of new chemical about evaluation in

investigation for new medicine development and performed big contributions to increase efficiency of experiment. Its utility became more important by introduction of high-throughput techniques and used more fields including material science. There are few report and example of usage is limited, however statistical analysis becomes to be used for prediction about rigidity of polymer material [79], prediction of chemical property [83,84], prediction of homogeneous catalyst activity [85,86]and so on.

In recently, usage of statistical analysis was admitted for Registration of Toxic Substances Control Act database (TSCA) and application Registration, Evaluation, Authorisation and Restriction of Chemicals (REACH restriction) because validity and utility of this study becomes well known. Additionally, new chemistry which set high-through put technique and statistical analyses as principal techniques for automatic and efficient development of new materials are proposed and developed [87]. Form those background, usage of statistical analysis will be developed itself and used in more broad fields.

1.5 Objective of this study

Multifunctional catalyst is one of a catalyst spices which has more than one performances. Applications of this catalyst for chemical reaction are expected not only improvement of catalytic performances but also reduction of additional operation and the

plural number of reactor.

Ziegler-Natta olefin polymerization catalyst is one of multifunctional catalyst. This catalyst has been improved by usage of multicomponent and construction of hierarchical structure to enhance their properties until now. However, its catalyst structure becomes complex and irregular. Structure performance of current catalyst systems relationship is not elucidated clearly. Therefore, catalyst development has been conducted by only experimental developments with enormous try and error, and performance increase rate becomes low recently. The cause of this problem is mainly three. First is difficulty of characterization on catalyst structure. Ziegler-Natta catalyst is composed of multicomponent and irregularly hierarchic structures from micro to macro. It is hard to characterize structures only one measurement. Second is difficultly of systematic change of catalyst morphology because current industrial preparation methods are not able to control only one structure parameters. Third is difficulty of quantitative elucidation of structure effect because catalytic performances were determined by various structural parameters with concerted or opposed mechanism. Therefore elucidation of structure performance relationship is very hard task from above problem

From those backgrounds, the purpose of this study was elucidation of structure performance relationship by multilateral characterization which is a variety of

characterization methods in order to achieve structural parameterization over multi scales and statistical analysis which is the powerful tool for elucidation of multivariate factor form enormous datasets. The results of this study will be expected to contribute not only establishment of systematic Ziegler-Natta catalyst development but also preparation of tailor-made catalyst, proposal of new catalyst construction indications which has novel performance and so on.

References

[1] E. Kikuchi, K. Segawa, A. Tada, Y. Imizu, H. Hattori, "Atarashii shokubaikagaku (新しい触媒化学)" 1988 sankyo shuppan (三共出版)

[2] K. Ziegler, E. Holzkamp, H. Breil, H. Martin, *Angew. Chem.,* 67 (1955) 541

[3] J. A. Osborn, F. H. Jardine, J. F. Young. G. Wilkinson, *J. Chem. Soc. A*, (1966) 1711–1732.

[4] A. J. Birch, D. H. Williamson, *Org. React.*, 24 (1976) 1-95.

[5] W. S. Knowles, M. J. Sabacky, B. D. Vineyard, US patent, (1974) 4008281 A (monsanto company)

[6] W. S. Knowles, *Adv. Synth. Catal.*, 345 (2003) 3-13

[7] Susan B. Rivera*, B. D. Swedlund, G. J. King, R. N. Bell, C. E. Hussey, Jr., D. M. Shattuck-Eidens, W. M. Wrobel, G. D. Peiser, and C. D. Poulter, Proc. *Natl. Acad. Sci. U.*

S. A., 98 (2001) 4373-4378

[8] S. Akutagawa, *Appl. Catal.*, A, 128 (1995) 171-207

[9] H. Kumobayashi, *Recl. Trav. Chim. Pays- Bas* 115 (1996) 201-210

[10] H.U. Blaser, F. Spindler, M. Studer, *Appl. Catal.*, A, 221 (2001) 119–143

[11] A. Nanicini, "synthesis of ammmonia" (D.J. Borgars ed.) (1961) MacMillan

[12] G. Natta, P. Pino, P. Corradini, F. Danusso, E. Mantica, G. Mazzanti, G. Moraglio, *J. Am. Chem. Soc.,* 77 (1955) 1708.

[13] J. C. Chadwick, Macromol. *React. Eng.*, 3, (2009) 428-432

[14] F. G. Ciapettaa, D. N. Wallacea, *Catal. Rev.*, 5 (1972) 67-158

[15] P. B. Weisz, *Actes 2me Congr, Int. Catal.*, Edition Technip (1961) Paris

[16] G. A. mills, H. Heinemann, T. H. Milliken and A.G. Oblad, *Ind. Eng.Chem.* 45, 1953 134-137

[17] S. M. Csicsery, *Zeolites*, 4, (1984) 202-213

[18] T. Tatsumi, N. Jappar, *J. Phys. Chem. B* 102 (1998) 7126-7131.

[19] N. van der Puil, F.M. Dautzenberg,H. van Bekkum, J.C. Jansen. *Microporous Mesoporous Mater*. 27, (1999) 95-106

[20] M. V. Tweigg, *Catal. Chem. Processes*, (1981) 11

[21] M. Andersson, L. Österlund, S. Ljungström, A. Palmqvist, *J. Phys. Chem. B*, 106

(2002) 10674-10679

[22] S. Matsumoto, *Catal. Today* 90 (2004) 183-190.

[23] J. Kašpar,, P. Fornasiero, M. Graziani, *Catal. Today* 50 (1999) 285-298.

[24] S.M. Csicsery, Zeolite chemistry and catalysis (J. A. Ravo ed.) (1976) 680

[25] P.B. Weisz V. J. Frilette, R. W. Maatman, E. B. Mower., *J. Catal.*, 1 (1963) 307-312

[26] J. Weitkamp, S. Eenst, *Catal. Today*, 19 (1994) 107-149

[27] S.M. Csicsery, *J. Catal.*, 23 (1971) 124-130

[28] K. Soga, T. Shiono, *Prog. Polym. Sci.*, 22, (1997) 1503-1546

[29] P. Galli, G. Vecellio, *J. Polym. Sci., Part A, Polym. Chem.* 42 (2004) 396-415

[30] Society of Polyolefin Science and Industry, Japan "Comprehensive investigation for next generation polyolefin Vol.7" (次世代ポリオレフィン総合研究 Vol.7) (2013)

[31] Ministry and Economy, Trade and industry (Japan), The trend of petrochemicals production and demands in the world (世界の石油化学製品と今後の需要動向) 2014 Jun.

[32] P. S. Chum, K. W. Swogger, *Prog. Polym. Sci.*, 33 (2008) 797-819

[33] Chain Structure and Conformation of Macromolecules, J. C. Randall, Ed., Academic Press, New York, 1977

[34] P. Corradini, G. Guerra, L. Cavallo, *Acc. Chem. Res.*, 37 (2004) 231-241

[35] R. A. Phillips, *J. Polym. Sci., Part B: Polym. Phys.*, 36 (1998) 495-517

[36] S. Padmanabhan, K. R. Sarma, and S. Sharma, *Ind. Eng. Chem. Res.*, 48 (2009) 4866–4871

[37] R. Jamjah, G. H. Zohuri, M. Javaheri, M. Nekoomanesh, S. Ahmadjo, A. Farhadi, *Macromol. Symp.*, 274 (2008) 148–153

[38] S. Ronca, G. Forte, H. Tjaden, Y. Yao, S. Rastogi, *Polymer*, 53 (2012) 2897-2907

[39] F. M. Mirabella Jr., *Polymer* 34, (1993), 1729-1735

[40] H. Tana,L. Li, Z. Chenb, Y. Songa, Q. Zheng., *Polymer* 46 (2005) 3522–3527

[41] M. Nakae, H. Uehara, T. Kanamoto, T. Ohama, R. S. Porter, *J. Polym. Sci., Part B: Polym. Phys.*, 37 (1999) 1921-1930

[42] K. Katayama, S. Tanase, N. Ishihara, *J. Appl. Polym. Sci.*, 122 (2011) 632–638

[43] C. Vasile, Ed.,"Handbook of Polyolefins" Marcel Dekker: New York, 2000.

[44] V. Bucico, R. Cipullom P. Corradini, *Macromol. Chem.*, 194 (1993) 1079-1093

[45] N. Pasquini Ed, "Polypropylene handbook"(ポリプロピレンハンドブック) Nikkankougyoushinbunsha (日刊工業新聞社) Japan (2012)

[46] British Patent 1286867 (1968) Montedison

[47] JP Patent 1031698 (1968) Mitsui Petrochemicals

[48] G. Morini, E. Albizzati, G. Balbontin, I. Mingozzi, M. C. Sacchi, F. Forlini, and I. Tritto, *macromol*., 29 (1996) 5770-5776

[49] X. Wen, M. Ji, Q. Yi, H. Niu, J. Y. Dong, *J. Appl. Polym. Sci*., 118 (2010) 1353-1358

[50] JP1981011908 (1981) Mitsui Petrochemical Industries,Ltd.

[51] JP Patent 1987158704 (1987) Toho Catalyst Co. Ltd.

[52] Y. Doi, K. Soga, M. Murata,E. Suzuki, Y. Ono,T. Keii. *Polym. Commun.*, 24 (1983) 244-246

[53] V. D. Noto, S. Bresadola, *Macromol. Chem. Phys.*, 197 (1996) 3827-3835

[54] M. Vittadello, P. E. Stallworth, F. M. Alamgir, S. Suarez, S. Abbrent, C. M. Drain, V. D. Noto, S. G. Greenbaum, *Inorg. Chi. Acta* 359 (2006) 2513-2518

[55] V. D. Noto, S. Lavina, D. Longo, M. Vidali, *Electrochim. Acta*, 43 (1998) 1225-1237

[56] R. Zannetti, C. Marega, A. Marigo, A. Martorana, *J. Polym. Sci. Part B. Phys*, 26 (1988) 2399.

[57] V. Busico, P. Corradini, L. De Martino, A. Porto, V. Savino, E. Albizzati, *Macromol. Chem. Phys.*, 186 (1985) 1279-

[58] P. Cossee, *J. Catal.*, 3 (1964) 80

[59] V. Busico, R. Cipulo, G. Monaco, G. Talarico, M. Vacatello, J. C. Chadwick, A. L. Segre, O. Sudmeijer, *Macromol.*, 32 (1999) 4173-4182

[60] B. Liu, T. Nitta, H. Nakatani, M. Terano, *Macromol. Chem. Phys.*, 204 (2003) 395-402

[61] A. Correa, F. Piemontesi, G. Morini, L. Cavallo, *Macromol.*, 40 (2007) 9181-9189

[62] V. Busico, R. Cipullo, P. Corradini, *Makromol. Chem.* 194 (1993) 1079-1093

[63] V. Busico, R. Cipullo, V. Romanelli, S. Ronca, *J. Chem. Soc. A,* 127 (2005) 1608-1609

[64] T. Taniike, M. Terano, *Macromol. Rapid. Commun.*, 28 (2007) 1918-1922

[65] T. Taniike, M. Terano, *Macromol. Rapid. Commun.*, 29 (2008) 1472-1476

[66] B. Horáčková, Z. Grof, j. Kosek, *Chem. Eng. Sci.*, 62 (2007) 5264-5270

[67] G. Weickert, G. B. Meier, J. T. M. Pater, R. K. Westerterp, *Chem. Eng. Sci.*, 54 (1999) 3291-3296

[68] M. Hassan Nejad, P. Ferrari, G. Pennini, G. Cecchin, *J. Appl. Polym. Sci.* 108 (2008) 3388-3402.

[69] A. Dashti, A. Ramazani SA., Y. Hiraoka, S. Y. Kim, T. Taniike and M. Terano, *Polym. Int.* 58 (2009) 40–45.

[70] M. Kakugo, H. Sadatoshi, J. Sakai, Catalytic Olefin Polymerization 56 (1989) 345-354.

[71] M. Kakugo, H. Sadatoshi, J. Sakai, M. Yokoyama, *Macromol.* 22 (1989) 3172-3177

[72] K. Pearson, *Phil. Mag.* 2 (1901) 559-572.

[73] H. Hotelling, *J. Educ. Psych.*, 26 (1933) 417-441

[74] P. Filzmoser, K. Hron, C. Reimann, *Environmetrics* 20 (2009) 621–632

[75] I. T. Jolliffe, *J. R. Stat. Soc. C* 31 (1982) 300-303

[76] P. Comon, *Signal Processing* 36 (1994) 287-314

[77] material studio 6.0, Accelrys

[78] S. Rezzi, D. E. Axelson, K. Héberger, F. Reniero, C. Mariani, C. Guillou, *Anal. Chim. Acta*, 552 (2005) 13–24

[79] M. Hakkarainen, G. Gallet, S. Karlsson, *Polym. Degrad. Stab.*, 64 (1999) 91-99

[80] T. Næs, B. H. Mevik, *J. Chemom.*, 15 (2001) 413–426

[81] D. Rogers, A. J. Hopfinger, *J. Chem. Inf: Comput. Sci.*, 314 (1994) 854-866

[82] J. Holland, "Adaptation in Artificial and Natural Systems"University of Michigan Press: Ann Arbor, MI (1975)

[83] S. A. Mirkhani, F. Gharagheizi, N. Farahani, K. Tumba, *J. Mol. Liq.*, 179 (2013) 78–87

[84] S. A. Mirkhani, F. Gharagheizi, P. I. Kashkouli, N. Farahani, *Fluid Phase Equilib.*, 324 (2012) 50-63

[85] X.Hu, M. L. Foo, G. K. Chuah, S. Jaenicke, *J. Catal.* 195 (2000) 412-415

[86] G. Occhipinti, H. R.´ Bjørsvik, V. R. Jensen, *J. Am. Chem. Soc.*, 128, (2006), 6952-6964

[87] S. Senkan, *Angew. Chem. Int. Ed.*, 40 (2001) 312-329

Chapter 2

Multilateral Characterization for Industrial Ziegler-Natta Catalysts toward Elucidation of Structure-Performance Relationship

2.1 Introduction

"Multi-components" and "structural hierarchy" are key issues to realize multifunctional and performant heterogeneous catalysts. The word, multi-components, represents that active components, support materials, modifiers and cocatalysts in a system play different roles, while "structural hierarchy" dictates the significance of the structural design over multi length scales. The most illuminative example, the three-way catalyst [1,2] for automotive catalytic converters typically consists of cordierite honeycomb support, whose structure is optimized to enhance the contact efficiency without penalizing airflow resistance, and a few-micron-thick washcoat deposited on the support. The washcoat consists of BaO-stabilized porous γ-Al_2O_3 as a carrier, CeO_2 (/ZrO_2) as an attenuator for the oscillation of the air-to-fuel ratio, and nano-sized noble metal or metal alloy (Pt/Pd/Rh) as active catalytic materials [1,3,4]. These multifunctional catalysts have been invented and developed mainly in an empirical manner from viewpoints of performance optimization in terms of activity, selectivity catalytic lifetime, and so on. In most of cases, roles of each component and impacts of each structural factor on the whole catalytic performance are roughly or qualitatively understood, while it is still challenging to embody quantitative structure-performance relationships (SPR) [5-7]. The difficulty comes from several reasons: A catalyst performance is usually affected by several chemical and structural factors in a complicated way, while to vary one of these factors without changing the other factors is not easy in usual preparation procedures [8,9]. Furthermore, prepared catalysts contain different extents of chemical and structural heterogeneity over multi scales, making it extremely demanding to unexceptionally

parameterize factors that affect a catalytic performance [4,10].

The heterogeneous Ziegler-Natta catalyst for industrial olefin polymerization is a representative example of such those catalysts. Manufacturing high-quality polymer products under efficient plant operation generally requires for a catalyst to simultaneously fulfill various performances such as high activity at an elevated temperature, (extremely) high selectivity, an appropriate kinetic profile, uniform particle sizes with spherical morphology, high hydrogen response for the polymer molecular weight control and so on [11,12]. While there are a huge variety of preparation routes empirically established in terms of performance optimization [13], Ziegler-Natta catalysts at the level of industry generally possess the following structural features.

1) Pro-catalysts consist of $TiCl_4$ and a Lewis basic compound co-supported on activated $MgCl_2$ support, where the Lewis base called as internal donor is a key component to drastically improve the catalyst stereospecificity as well as to activate the $MgCl_2$ support during preparation [14-17].
2) Catalyst macroparticles possess spherical morphology with narrow particle size distributions typically between 10-100 μm. They are made by hierarchical agglomeration of primary structural units of $TiCl_4$/internal donor/$MgCl_2$, whose dimensions are believed to be around 1-10 nm [18,19].
3) The said hierarchical agglomeration leads to the formation of a range of porosity from micro to macropores, whose distributions and shapes are sensitively affected by employed preparation methods and conditions [20,21]. In Ziegler-Natta olefin polymerization, polymer initially formed in accessible pores build up mechanical

stresses inside catalyst particles to trigger particle fragmentation (called as pore-breakage process), due to which fresh catalyst surfaces which are originally hidden in inaccessible pores are continuously exposed. These processes enable industrial catalysts to retain stable polymerization activity over hours. In this way, inner structures of catalyst macroparticles significantly affect the way of fragmentation [22,23] and the kinetic behavior during polymerization [12].

Roughly saying, the first structural feature at the atomic scale is mainly related to the primary structure and polydispersity of produced polymer through the performance of active sites [13,24], while the latter two at larger scales from nm to μm mainly affect the kinetic profile of a catalyst and the resultant polymer particle morphology through fragmentation and replication phenomena during polymerization [11,25,26]. However, from a quantitative viewpoint, all these issues are believed to more or less exert influences on each said performance.

Though several researches have been undertaken with the aim to understand relationships between catalyst structures and performances in Ziegler-Natta olefin polymerization, quantitative structure-performance relationships have not been reached yet. One of the main drawbacks in the previous studies can be attributed to the absence of multilateral characterization: They determined only one or a few structural parameter(s) of catalyst samples such as crystalline disorder of $MgCl_2$ [27], surface area [28], total pore volume [12,29], and average pore size [12], without considering other parameters which also affect a targeted performance. Characterization and parameterization of the structures of Ziegler-Natta catalysts are actually not trivial in

terms of the complexity and heterogeneity in chemical and physical structures as well as of their extreme sensitivity to moisture. Nevertheless, reliable quantitative structure-performance relationships are not to be acquired without parameterizing catalyst structures as precisely as possible with various characterization methods.

Based on these backgrounds, we have set our primary objective to firstly establish and apply multilateral characterization for structures of Ziegler-Natta catalysts. Four catalysts were prepared based on the chemical conversion of $Mg(OEt)_2$ precursor, which is one of the most employed preparation routes in industry due to superior activity and copolymerization ability of resultant catalysts. They were subjected to a variety of characterization methods in order to achieve structural parameterization over multi scales such as electron microscopy, N_2 adsorption/desorption, Hg intrusion, and UV/vis spectroscopy, and gas chromatography. We also examined impacts of the determined structural parameters on the ethylene/1-hexene copolymerization ability of the catalysts.

2.2 Experiment

2.1.1 Materials

Anhydrous $MgCl_2$, triethylaluminium (TEA), and four kinds of poreless Mg particles (termed Mg A-D) were donated from Toho Titanium Co., Ltd., Tosoh Finechem Corporation and Yuki Gousei Kogyo Co., Ltd., respectively. The morphologies of Mg A and C are flake-like, while those of Mg B and D are spherical (Figure 2-1). Characterization results of the Mg particles are shown in Table 2-1. The size of Mg particles becomes smaller in the order of A→C→B→D.

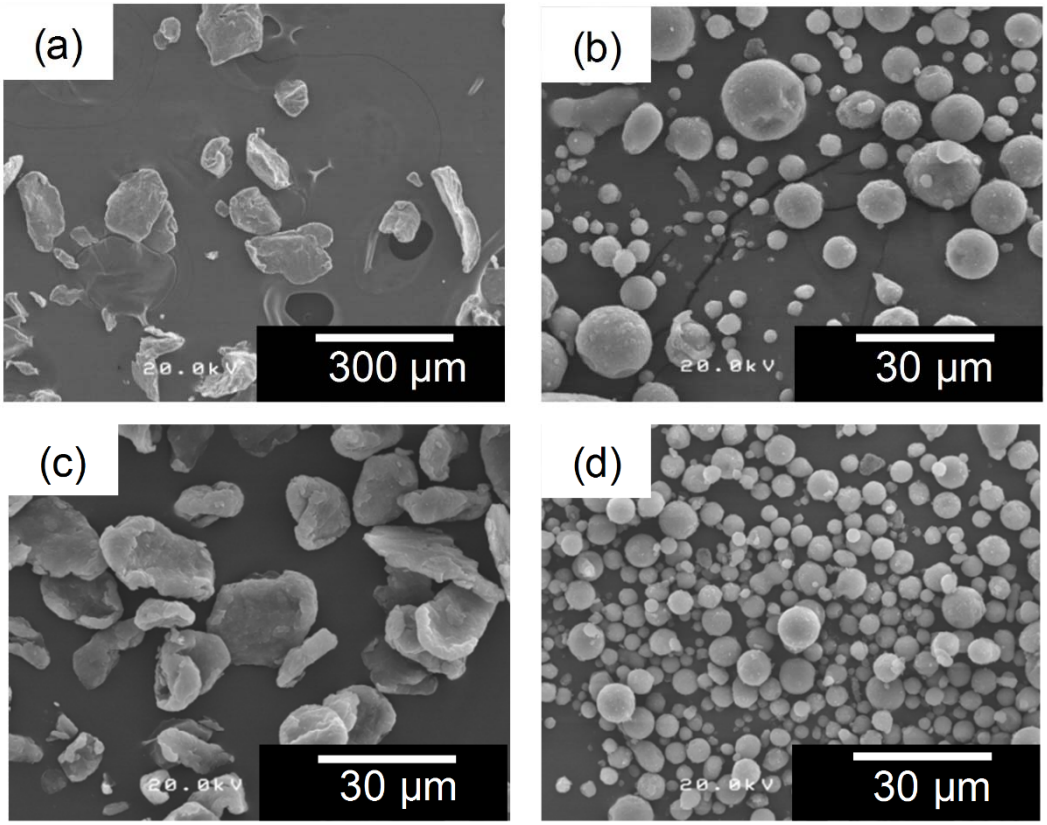

Figure 2-1. SEM images of Mg particles: (a) Mg A (x100), (b) Mg B (x1000), (c) Mg C (x1000), and (d) Mg D (x1000)

Table 2-1. Characterization results of Mg particles

Sample	D_{10}[a] (μm)	D_{50}[a] (μm)	D_{90}[a] (μm)	RSF[d]
Mg A	15.7	39.7	132	2.93
Mg B	5.15	10.0	23.4	1.82
Mg C	7.94	17.2	28.6	1.78
Mg D	5.13	8.61	18.5	1.56

[a] D_{10}, D_{50} and D_{90} are the particle diameters at 10%, 50% and 90% in the cumulative number-base particle size distribution obtained by the analysis of SEM images over 500 particles.
[b] Determined based on Eq. (1).

Ethanol (purity > 99.5%) was dried over 3A molecular sieve with N_2 bubbling. Heptane (purity > 99.5%), toluene (purity > 99.5%) and di-*n*-butylphthalate (DBP) (purity > 98%) were dried over 4A molecular sieve with N_2 bubbling. Cyclohexylmethyldimethoxysilane (CMDMS) was purified by distillation under reduced pressure. Ethylene of research grade donated by Sumitomo Chemical Co., Ltd. was used as delivered.

2.2.2 $Mg(OEt)_2$ synthesis

$Mg(OEt)_2$ was synthesized based on a patent [30] with several modifications. 0.25 g of $MgCl_2$ (as an initiator) and 31.7 mL of dehydrated ethanol were introduced into a 500 mL jacket-type separable flask equipped with a mechanical stirrer rotating at 180 rpm under N_2 atmosphere. After the dissolution of $MgCl_2$ at 75°C, 2.5 g of Mg and 31.7 mL of ethanol were introduced. 2.5 g of Mg and 31.7 mL of ethanol were again added 10 min after the reaction was initiated by $MgCl_2$. Thereafter, 2.5 g of Mg and 31.7 mL of ethanol were added repeatedly 4 times every 10 min, followed by aging at 75°C for 2 h. Finally,

the temperature was decreased to 40°C, and the product was washed with ethanol. In this study, four kinds of $Mg(OEt)_2$ particles (MGE 1-4) were synthesized from Mg A-D under the same conditions.

2.2.3 Catalyst preparation

The preparation of Ziegler-Natta catalysts from $Mg(OEt)_2$ was conducted again based on a patent [31] with several modifications. 10 g of $Mg(OEt)_2$ and 140 mL of toluene were charged in a 300 mL 3-neck flask equipped with a mechanical stirrer rotating at 180 rpm under N_2 atmosphere. 20 mL of $TiCl_4$ was dropwisely added, where the temperature of the suspension was kept within 0-5°C. Thereafter, the temperature was once elevated to 90°C to add 3.0 mL of DBP and then brought to 110°C. The reaction slurry was continuously stirred at 110°C for 2 h. Subsequently, the reaction product was washed with toluene twice at 90°C and further treated with 20 mL $TiCl_4$ at 90°C for 2 h. After that, the product was washed with *n*-heptane 7 times to get the final catalyst. Four kinds of Ziegler-Natta catalysts (Cat 1-4) were obtained from MGE 1-4 under the same conditions.

2.3.4 Polymerization

Ethylene/1-hexene copolymerization was performed in a 1 L autoclave equipped with a mechanical stirrer rotating at 350 rpm. 407 mL of *n*-heptane was introduced into the reactor. TEA ([Al] = 10 mmol/L), CMDMS (Al/ExD = 10) and 93 ml of 1-hexene (corresponding to 0.75 mol) were introduced into the reactor, and the solution was saturated with 0.5 MPa of ethylene at 50°C. A catalyst ([Ti] = 0.005 mmol/L) was fed

into the reactor by a bomb injection technique to initiate the polymerization. The polymerization was conducted for 30 min with a continuous supply of ethylene gas at 0.5 MPa. The polymer was recovered by pouring the reaction slurry into mixture of acetone and methanol kept at 0°C and subsequent filtration.

2.3.5 Characterization

• Scanning electron microscopy

Particle morphological characteristics of $Mg(OEt)_2$ and catalyst particles were studied with scanning electron microscopy (SEM, Hitachi S-4100) operated at an accelerating voltage of 20 kV. Before the measurements, particles were subjected to Pt sputtering for 100 s. To quantify observed particle morphology, SEM images (> 500 particles) were analyzed by a software (eizokun software , Ashahikasei). D_{10}, D_{50} and D_{90} were defined as the particle diameters at 10%, 50% and 90% in the cumulative number-base particle size distribution. The relative span factor (RSF) and the circularity degree were respectively calculated based on Eqs. (1) and (2),

$$relative\ span\ factor\ (RSF) = \frac{D_{90} - D_{10}}{D_{50}} \quad (1),$$

$$circularity\ \ degree = \frac{4 \times \pi \times area}{(boundary\ \ length)^2} \quad (2),$$

where the area and boundary length for a two-dimensionally projected particle were determined over 500 particles.

• N_2 adsorption/desorption measurement

N_2 adsorption and desorption isotherms at 77 K were acquired on BELSORP-max

(BEL JAPAN, INC.). *Ca*. 50-100 mg of catalyst powder in a pyrex tube with a rubber cap was outgassed at 80°C over 3 h in vacuo, prior to the measurement. Since the BET analysis does not work properly for typical Ziegler-Natta catalysts with a plenty of micropores (pore diameter (D) < 2 nm) [17], the specific surface area was not determined. Instead, the micropore volume (V_{micro}) was approximated with

$$V_{micro} = V_{0.4} \times \frac{V_{liquid}}{V_{gas}} - \int_{2}^{50} \frac{2}{D} \cdot \frac{V_{meso}(D)}{dD} dD \qquad (3),$$

where $V_{0.4}$, V_{liquid}, V_{gas}, and $V_{meso}(D)$ are the N_2 adsorption volume at $p/p_0 = 0.4$, the volumes of a N_2 molecule in gaseous and liquid states, and the mesopore volume at the diameter of D nm determined by the method described in the next paragraph. V_{micro} was estimated by subtracting the contribution of multilayer N_2 adsorption onto mesopore surfaces from the adsorption volume at $p/p_0 = 0.4$ (converted to the liquid N_2 volume). Note that the thickness of the multilayer adsorption at $p/p_0 = 0.4$ was approximated as 2 nm, and the contribution from the multilayer adsorption onto macropore and external surfaces was regarded as negligible. The latter is true for typical industrial Ziegler-Natta catalysts, whose pore dimensions are mainly micro and/or meso scale(s).

The mesopore size distributions (2.1 nm < D < 50 nm) were analyzed by the BJH method or by the INNES method. Even though the two methods are based on the same Kelvin equation for the N_2 condensation, cylinder-type and slit-type mesopores are assumed in the BJH and INNES methods, respectively. Hence, the BJH method is suitable for the hysteresis types H1 and H2 respectively for size-uniform and size-irregular cylindrical-type mesopores, while the INNES method for the types H3 and H4

respectively for size-uniform and size-irregular slit-type mesopores .

• Mercury intrusion measurement

The meso and macro pore size distributions (7 nm < diameter < 1000 nm) were measured with the mercury intrusion technique (Pascal 440 Porosimeter, Thermo Scientific). The pore size was evaluated from the intrusion pressure according to the Washburn-Laplace equation. The surface tension (γ) and contact angle (θ) were respectively set to 0.480 N / m and 141.3°.

• Chemical analysis

The Ti content was determined with UV-vis spectroscopy (V-670 JASCO), where a measured amount of a catalyst sample was dissolved in $HCl/H_2SO_4/H_2O_2$ solution and the intensity of a ligand metal charge transfer band at 410 nm was measured. The DNBP content was determined by IR spectroscopy (FT/IR-4100, JASCO): A measured amount of a catalyst sample was once dissolved in HCl solution, then DNBP was fully phase transferred to *n*-heptane, and finally the carbonyl absorption band was integrated to determine the DNBP content.

• ^{13}C NMR

The 1-hexene incorporation amount, *i.e. n*-Bu branch content, in ethylene/1-hexene copolymer was measured by ^{13}C NMR (Bruker 400 MHz) operating at 100 MHz with proton decoupling at 120°C using 1,2,4-trichlorobenzene as a diluent and 1,1,2,2-

tetrachloroethane-d_2 as an internal lock and reference.

2.3 Results and discussion

2.3.1 $Mg(OEt)_2$ synthesis

Four kinds of $Mg(OEt)_2$ particles were synthesized from different Mg particles (whose characteristics were given in Figure 2-1 and Table 2-1). Their representative SEM images are shown in Figure 2-2. The particles of four $Mg(OEt)_2$ samples more or less possessed spherical shapes. However, spheroidal particles, which were probably formed by agglomeration of the spherical particles and/or fine particles (< 1 μm) were occasionally observed. Magnified images (Figure 2-2c) revealed that the particles were composed by aggregation of thin plate-like building blocks, whose dimension and shape were highly inhomogeneous. The lateral dimension of the building blocks varied in the range of 100-1000 nm and the thickness was about 10 nm. Among the four samples, MGE 1,3 were relatively spherical compared with MGE 2,4. On the other hand, there was no quantitative difference in their surface textures.

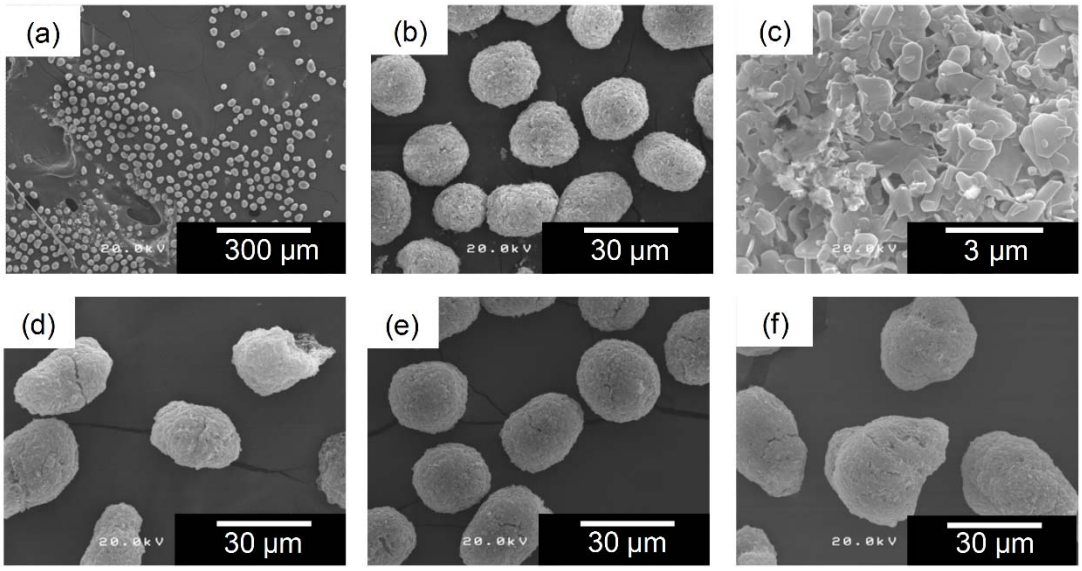

Figure 2-2. SEM images of $Mg(OEt)_2$ particles: (a) MGE 1 (x100), (b) MGE1 (x1000), (c) MGE 1 (x10000), (d) MGE 2 (x1000), (e) MGE 3 (x1000), and (f) MGE 4 (x1000)

The particle characteristics of the $Mg(OEt)_2$ samples such as the particle size distribution and the circularity obtained from SEM images are summarized in Table 2-2. The average particle size (D_{50}) became in the order of MGE 4 > 3 > 2 > 1. MGE 1,3 synthesized from flake-like Mg had higher circularity and narrower particle size distribution than MGE 2, 4 synthesized from spherical Mg. Moreover, smaller flake-like or spherical Mg particles respectively led to larger MGE particles (*i.e.* MGE 3 > 1 and MGE 4 > 2). Tanase and coworkers proposed a particle growth mechanism in the $Mg(OEt)_2$ synthesis that $Mg(OEt)_2$ seed particles formed on Mg surfaces fall off from the surfaces and aggregate with each other to shape the macroscopic particle morphology. According to the mechanism, it was thought that the morphological differences of the original Mg particles exert influences on the said detachment and agglomeration behaviors of the seed particles through the viscosity (shear force) of the reacting slurry,

and differentiate the particle size distribution and circularity. At the best of our knowledge, these are the first academic results for the influences of the reaction conditions on the morphology of formed $Mg(OEt)_2$ particles. It is notable that additional experiments on MGE 3' (reproduction of MGE 3) proved quantitative reproducibility not only for the analysis but also for the synthesis.

Table 2-2. Particle characteristics for $Mg(OEt)_2$

Sample	D_{10} (μm)	D_{50} (μm)	D_{90} (μm)	RSF	Circularity degree[a]
MGE 1	19.6	22.3	26.2	0.298	0.911
MGE 2	12.1	26.1	35.7	0.904	0.828
MGE 3	21.0	26.6	30.5	0.359	0.901
MGE 4	26.6	36.8	46.9	0.554	0.847
MGE 3'	21.2	27.7	31.4	0.370	0.915

[a] Determined based on Eq. (2).

2.3.2 Catalysts characterization

2.3.2.1 Morphology evaluation

From the four $Mg(OEt)_2$ samples, four catalysts were prepared in the same conditions, whose SEM images are shown in Figure 2-3. The shapes and sizes of the catalyst particles approximately replicated those of the $Mg(OEt)_2$ particles for each. Though the replication more or less held at the level of the building blocks, their corners and edges became smeared after the catalyst preparation. Thus, macroscopic structural features of the particles were more nicely replicated, while structures at a smaller scale likely underwent some variation. These tendencies were similar among the four catalyst samples.

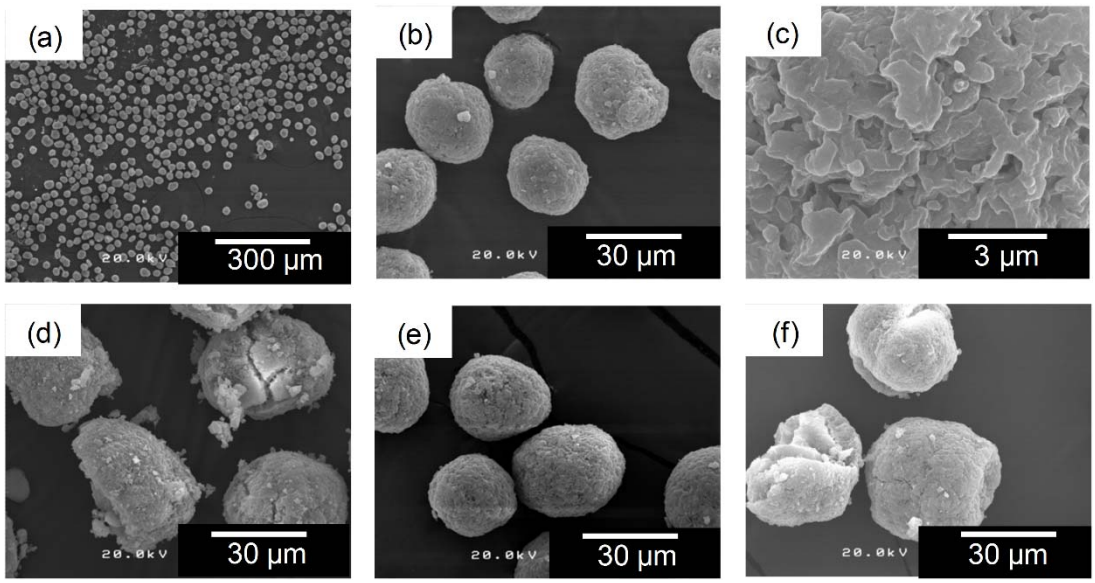

Figure. 2-3. SEM images of catalyst particles: (a) Cat 1 (x100), (b) Cat 1 (x1000), (c) Cat 1 (x10000), (d) Cat 2 (x1000), (e) Cat 3 (x1000), and (f) Cat 4 (x1000)

Table 2-3 shows the results of the particle analyses for SEM images of the catalyst particles. Again, Cat-3' prepared from MGE C' had similar particle characteristics with Cat 3 from MGE 3, proving the reproducibility of the catalyst synthesis. The results in Table 2-3 are discussed in a comparative way with those in Table 2-3 to clarify correlations of the particle morphology between the $Mg(OEt)_2$ and catalyst samples. The orders of the particle characteristics among the four samples were slightly altered. For example, D_{50} had the order of Cat 2 > 4 > 3 > 1 against MGE 4 > 3 > 2 > 1, RSF had the order of Cat 2 > 4 > 3 > 1 against MGE 2 > 4 > 3 > 1, and so on. The RSF values became larger for all of the samples after the catalyzation. Especially, Cat 2,4 formed non-negligible amounts of fine and agglomerated particles, resulting in more broadening in the particle size distribution compared with Cat 1,3. It was believed that the particles of MEG 1,3 were mechanically tough probably because the plate-like morphology of Mg

1,3 might impose greater shear force during the particle formation. On the contrary, the particles of MEG 2,4 formed under lower shear force from the spherical Mg particles might be mechanically fragile, causing disintegration and re-agglomeration of the particles during the catalyst synthesis.

Table 2-3. Particle characteristics for catalysts

Sample	SEM				
	D_{10} (μm)	D_{50} (μm)	D_{90} (μm)	RSF	Circularity degree
Cat 1	22.3	25.6	31.0	0.343	0.835
Cat 2	12.4	37.6	55.5	1.15	0.740
Cat 3	26.8	30.9	41.9	0.490	0.896
Cat 4	22.0	36.6	49.8	0.761	0.787
Cat 3’	29.9	34.7	45.8	0.457	0.882

2.3.2.2. Pore structure evaluation

The catalyst pore structures were studied comparatively based on N_2 adsorption and Hg porosimetry. The N_2 adsorption is routinely employed not only for the determination of the (BET) specific surface area but also for the micro and mesopore analyses [10]. On the other hand, the Hg porosimetry is employed for the meso and macropores analyses [32]. Cross-validation between the two pore analysis methods becomes possible by using overlapping dimensions of the two methods at the mesopore range.

Representative N_2 adsorption / desorption isotherms are shown for Cat 3 in Figure 2-4 (the other samples had qualitatively similar isotherms). The adsorption isotherms for all the catalysts belonged to the type II of the IUPAC classification for macroporous (D > 50 nm) or non-porous materials. Meanwhile, the hysteresis loop made by the adsorption and desorption branches belonged to the type H3, suggesting the capillary condensation for

slit-shaped mesopores (2 nm < D < 50 nm), whose sizes and shapes are non-uniform [33,34]. This is consistent with the lamellar morphology of the building blocks observed in SEM (Figure. 2-2c). The presence or absence of micropore filling (D < 2 nm) at low p/p_0 was not readily understandable from the isotherms, since it overlaps with the monolayer and multilayer adsorption. We have recently clarified that typical Ziegler-Natta catalysts including $Mg(OEt)_2$-based one contain at least two classes of micropores by means of the α_s-plot method, which prevents reliable determination of the monolayer capacity in the BET surface area analysis. To be worse, typical methods for the determination of the micropore volume or size distribution (such as HK and SF method) were not applicable to Ziegler-Natta catalysts either due to the absence of material-specific parameters for $MgCl_2$ or due to the continuity between the condensation micropore filling and mesopore filling in the adsorption isotherm [35,36]. Consequently, Eq. (3) was proposed as an intuitive method to estimate the micropore volume in Ziegler-Natta catalysts.

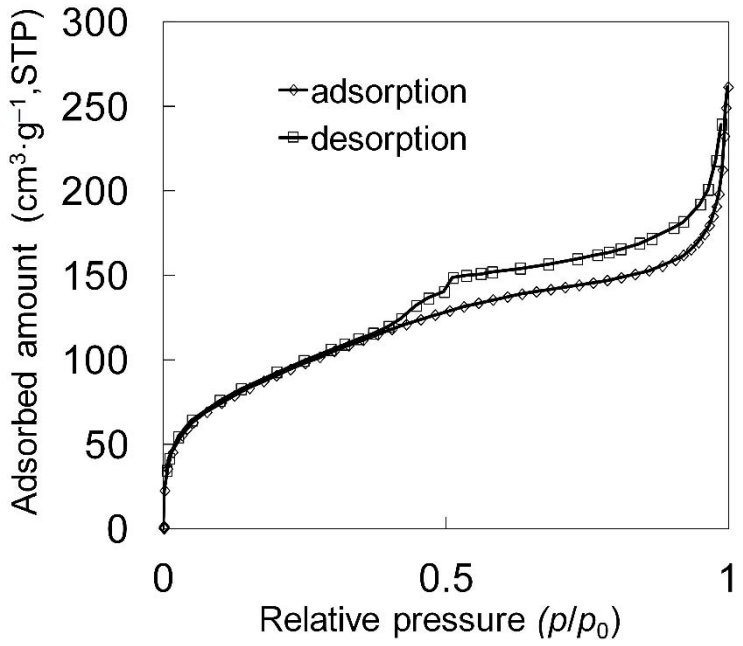

Figure 2-4. Nitrogen adsorption/desorption isotherms for Cat C

Figure 2-5 represents the Hg intrusion data for Cat-3 (again the other samples had similar intrusion curves). Typically for $Mg(OEt)_2$-based Ziegler-Natta catalysts, significant intrusion occurred at around 0.1 MPa. Comparison between the size scale for 0.1 MPa (10-20 μm) and a catalyst particle size (20-30 μm) dictates that the corresponding intrusion mainly arises from interparticle voids. After the intrusion into interparticle voids, second intrusion started at around 10 MPa, which was mainly due to intraparticle pores. Though it was not possible to clearly distinguish between the intrusion into interparticle voids and that into intraparticle pores, we have decided to regard the intrusion above 7.4 MPa (corresponding to below 200 nm) as one which mainly arose from intraparticle pores.

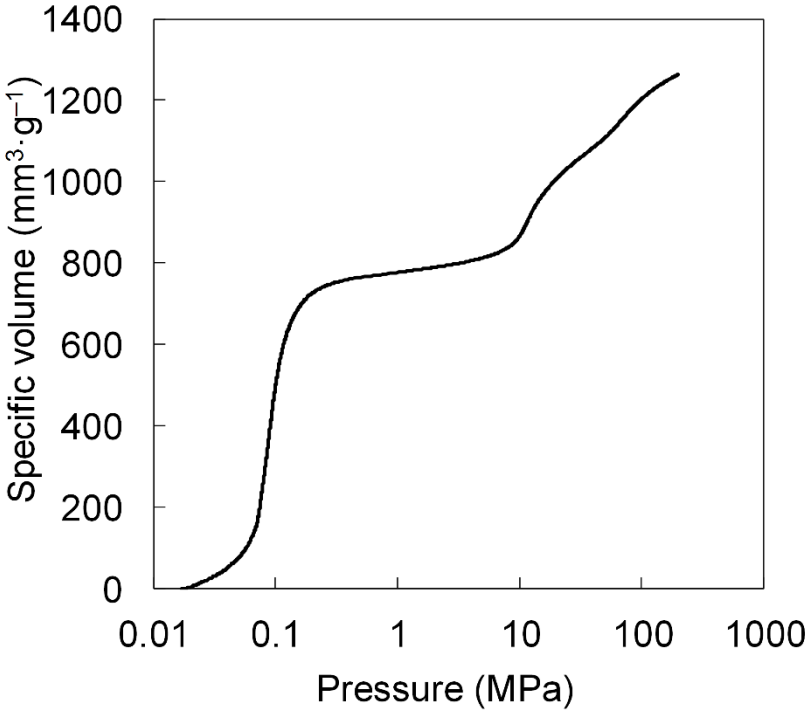

Figure 2-5. Hg intrusion curve for Cat-C

The INNES method [37] was employed for the mesopore analysis instead of the most popular BJH method [38]. The former assumes slit-type pores in agreement with the H3 hysteresis observed for the catalysts (Figure 2-4), while the latter assumes cylindrical pores. Figure 2-6 compares the mesopore volumes obtained by the N_2 adsorption and Hg porosimetry in the range of 10 nm < D < 50 nm for the four catalysts. The INNES method for slit-type pores exhibited relatively nice linear correlation with the pore volume determined by the Hg intrusion, while no correlation was detected for the BJH method. The deviation in the absolute volumes between the N_2 adsorption and the Hg intrusion came from different pore network filling mechanisms [39]. The Hg intrusion underestimates pore sizes in the presence of bottleneck pores within the pore network,

while it is not the case for the N_2 adsorption. Thus, the meanings of 10 nm < D < 50 nm are not necessarily equal for the N_2 adsorption and Hg porosimetry.

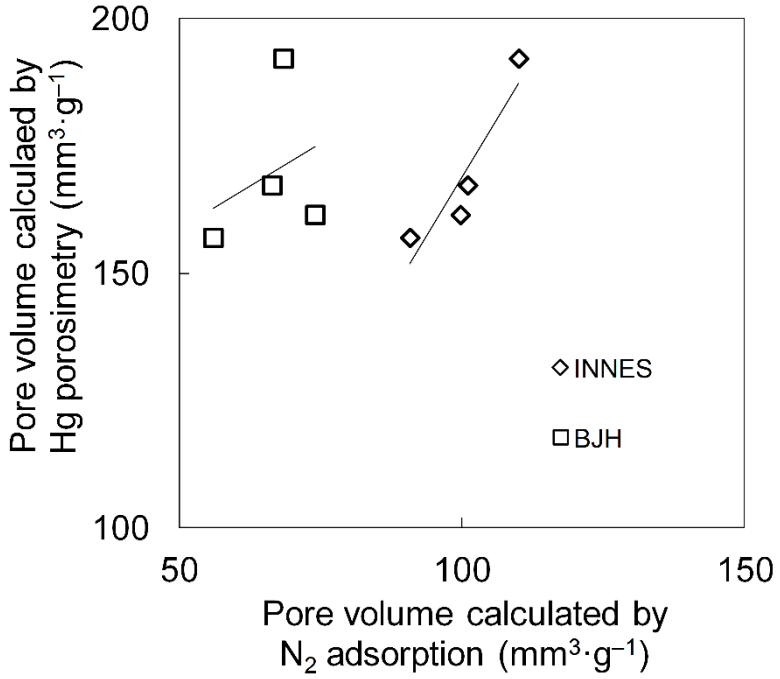

Figure 2-6. Comparison of mesopore volumes (10 nm < D < 50 nm) between N_2 adsorption and Hg porosimetry. The mesopore volume for N_2 adsorption was analyzed either by the INNES or BJH method.

The results of the analyses for the N_2 adsorption and Hg porosimetry are summarized in Table 2-4. As is seen in Table 2-4, $Mg(OEt)_2$-based Ziegler-Natta catalysts have a wide range of porosity from micro to macropores. While the four catalysts exhibited quite similar pore volumes in the micropore region, the difference in the pore volume among Cat A-D became greater at a larger pore dimension. Compared with Cat B,D that were prepared from spherical Mg sources, Cat A,C that were prepared from flake-like Mg sources had larger pore volumes in the meso and macropore regions. Since such a tendency was not observed at the stage of $Mg(OEt)_2$, it is reasonable to consider that the

different meso and macro porosity arose in the course of catalyzation. However, its mechanistic origin is yet unclarified without capturing intermediate structures during the catalyzation.

Table 2-4. Pore volumes for catalyst particles

	Pore volume ($mm^3 \cdot g^{-1}$)		
	V_{micro} (D < 2 nm)[a]	V_{meso} (2 nm < D < 50 nm)[b]	V_{macro} (50 nm < D < 200 nm)[c]
Cat A	111	194	216
Cat B	114	187	172
Cat C	112	196	220
Cat D	120	166	171

[a] Calculated based on Eq. (3) from the N_2 adsorption isotherm.
[b] Calculated by the INNES method from the N_2 adsorption isotherm.
[c] Calculated based on the Washburn-Laplace equation from the Hg intrusion curve.

2.3.2.3 Chemical composition

Table 2-5 summarizes the results of the chemical composition analyses. The chemical composition including the Ti and DNBP contents was not significantly different among Cat 1-4, where the DNBP/Ti molar ratio always fell in a range of 1-1.2, typical for $Mg(OEt)_2$-based Ziegler-Natta catalysts. Thus, macroscopic structural differences in $Mg(OEt)_2$ particles did not affect microscopic chemical parameters of the resultant catalysts, which enabled us to isolate influences of structural parameters on the polymerization performances.

Table 2-5. Chemical composition of catalysts

	Ti contents (wt%)	DBP contents (wt%)
Cat A	2.4	17
Cat B	2.5	18
Cat C	2.7	18
Cat D	2.7	15

2.3.3 Etylene/1-hexene copolymerization

In order to investigate correlations between catalyst structural parameters and polymerization performances, ethylene/1-hexene copolymerization was conducted. Though previous studies pointed out the significance of catalyst pore structures on the incorporation efficiency of bulky 1-hexene, quantitative examination has been hardly established [40]. The polymerization results are summarized in Table 2-6. The copolymerization activity was far the highest for Cat A, and the remaining three showed the order of Cat C > B ~ D. Although it was considered that a variety of structural factors affected the activity, catalysts with smaller particle sizes tended to show higher activities (Figure 2-7a). This fact plausibly suggests the importance of the diffusion limitation in ethylene polymerization: when all the catalyst particles were covered by the polymer, smaller particles shorten the diffusion length of ethylene in the radial direction.

Table 2-6. Polymerization results[a]

Sample	Activity ($kg \cdot Ti\text{-}mol^{-1} \cdot h^{-1} \cdot atm^{-1}$)	*n*-Bu branch content[b] (mol%)
Cat A	1.5×10^3	6.3
Cat B	8.6×10^2	5.5
Cat C	1.1×10^3	6.3
Cat D	8.5×10^2	5.0

[a] Ethylene/1-hexene copolymerization was conducted at 50ºC in heptane with 10 mmol/L of TEA, 1.0 mmol/L of CMDMS, 1.5 mol/L of 1-hexene, and 0.5 MPa of continuously supplied ethylene for 30 min.
[b] Determined by ^{13}C NMR.

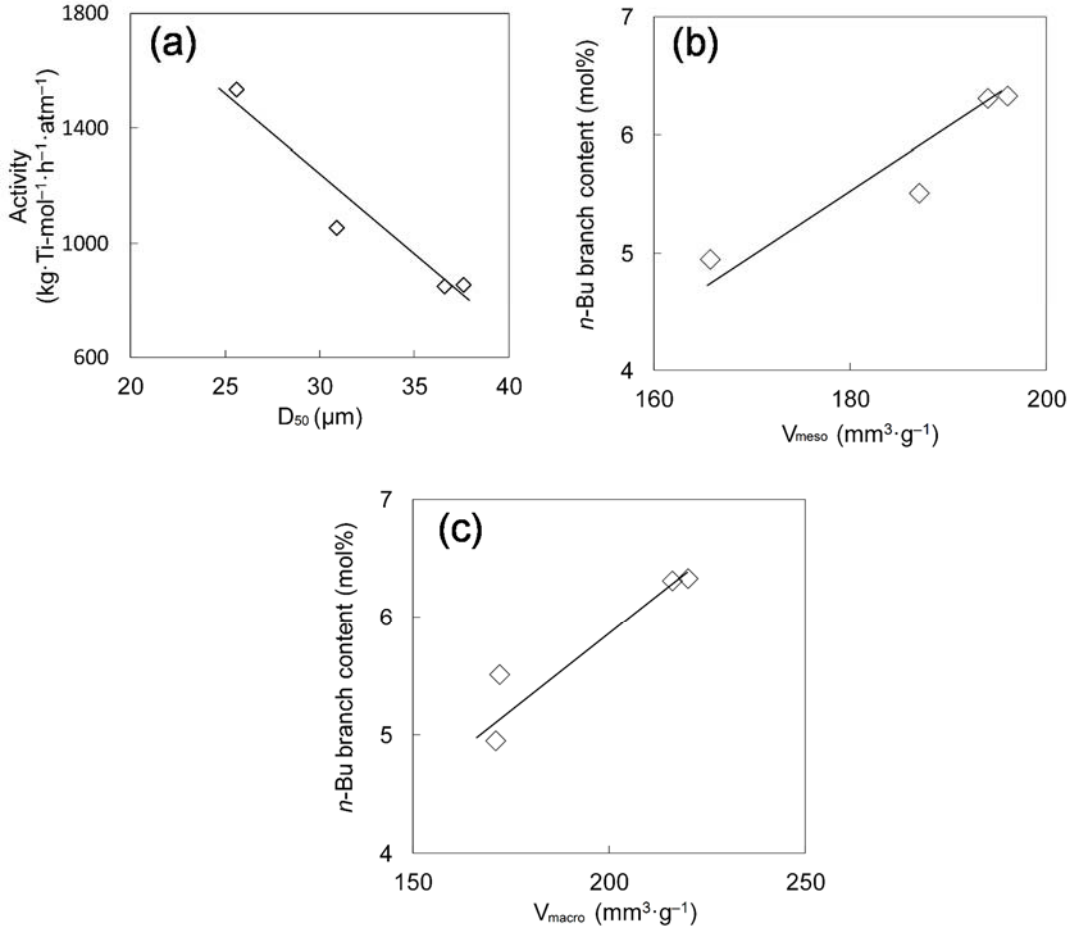

Figure 2-7. Correlations between catalyst structural parameters and ethylene/1-hexene copolymerization performances: (a) D_{50} (number-base) vs. activity, (b) V_{meso} vs. *n*-Bu branch content, and (c) V_{macro} vs. *n*-Bu branch content

The 1-hexene incorporation efficiency followed the order of Cat C > A > B > D, in spite of the similarity of the catalyst composition, *i.e.* the active site nature. Since it was expected that the incorporation efficiency would be related to the ease of the diffusion for bulkier 1-hexene, the *n*-Bu branch contents were plotted against the pore-related parameters (Figures 2-7b and 2-7c). Positive correlations were found for the mesopore volume determined by N_2 adsorption and for the macropore volumes by Hg intrusion. As reported in recent literature, accessible pores are readily filled by formed polymer at the very initial stage of polymerization (roughly corresponding to grams of polymer per gram of catalyst) [41]. Therefore, the pore volume is likely to exert its influences on the 1-hexene incorporation efficiency only at the initial stage. The most plausible scenario is as follows: At the initial timing of polymerization when catalyst pores are not filled yet, 1-hexene needs to reach active sites in competition with ethylene. Pores with the dimension comparable with the molecular size of 1-hexene decelerate its diffusion, and the number of pores with the dimension larger than the size of 1-hexene directly affects the 1-hexene incorporation at the initial stage. Copolymer formed at the initial stage fills accessible pores to become diffusion resistance at a later stage of polymerization. In general, the diffusion barrier becomes lower when the crystallinity of the polymer gets lower by the incorporation of more 1-hexene, subsequently leading to larger 1-hexene incorporation even after the initial stage [42]. In conclusion, it was considered that the mesopore and macropore volumes affected the 1-hexene incorporation efficiency through the crystallinity of the initially formed polymer. The scenario is consistent with a known fact that the formation of less crystalline polymer in a pre-polymerization stage drastically

enhances the α-olefin incorporation efficiency of a catalyst [43].

2.4 Conclusions

In this study, multilateral characterization was applied to state-of-the-art Ziegler-Natta catalysts featured with ill-defined hierarchical structures. Precise parameterization of the catalysts through scanning electron microscopy, Hg porosimetry, N_2 adsorption/desorption, and chemical analyses enabled us to tackle structure-performance relationships in heterogeneous olefin polymerization.

$Mg(OEt)_2$-based Ziegler-Natta catalysts possessed nearly spherical particle morphology, whose size distribution roughly replicated that of $Mg(OEt)_2$ precursor particles. The catalyst particles contained a wide class of internal pores: macropores, slit-shaped mesopores, and micropores. On the contrary to macroscopic parameters (particle size, macropore volume), microscopic parameters (micropore volume, chemical composition) were hardly affected by structures of $Mg(OEt)_2$ particles. Among the obtained chemical and structural parameters, we found that the number-average particle size of the catalysts was negatively correlated with the activity in ethylene/1-hexene copolymerization, and that the meso and macropore volumes were positively correlated with the 1-hexene incorporation efficiency. These two correlations suggested not only the importance of the monomer diffusion in ethylene/1-hexene copolymerization, but also the validity of multilateral characterization over multi length scales to depict structure-performance relationships for such a complicated catalyst whose ill-defined hierarchical structure has been empirically optimized.

References

[1] S. Matsumoto, *Catal. Today*, 90 (2004) 183–190.

[2] J. Kašpar, P. Fornasiero, M. Graziani, *Catal. Today*, 50 (1999) 285–298.

[3] H.S. Gandhi, G.W. Graham, R.W. McCabe, *J. Catal.*, 216 (2003) 433–442.

[4] R.M. Heck, R.J. Farrauto, *Appl. Catal. A: Gen.,* 221 (2001) 443–457.

[5] G. Occhipinti, H.R. Bjørsvik, V.R. Jensen, *J. Am. Chem. Soc.*, 128 (2006) 6952–6964.

[6] M.A. Pena, J.L.G. Fierro, *Chem. Rev.*, 101 (2001) 1981–2017.

[7] A. Corma, J.M. Serra, P. Serna, M. Moliner, *J. Catal*., 232 (2005) 335–341.

[8] E.J. Dil, S. Pourmahdian, M. Vatankhah, F.A. Taromi, *Polym. Bull*. 64 (2010) 445–457.

[9] J. Kim, M. Choi, R. Ryoo, *J Catal*., 269 (2010) 219-228

[10] T. Tatsumi, N. Jappar, *J. Phys. Chem. B,* 102 (1998) 7126–7131.

[11] A. Dashti, A. Ramazani, Y. Hiraoka, S.Y. Kim, T. Taniike, M. Terano, *Polym. Int*., 58 (2009) 40–45.

[12] M. Hassan Nejad, P. Ferrari, G. Pennini, G. Cecchin, *J. Appl. Polym. Sci.,* 108 (2008) 3388–3402.

[13] Y. Hiraoka, S.Y. Kim, A. Dashti, T. Taniike, M. Terano, *Macromol. React. Eng*., 4 (2010) 510–515.

[14] E. Albizzati, U. Giannini, G. Collina, L. Noristi, L. Resconi, in: E.P. Moore, Jr. (Ed.), Polypropylene Handbook, Hanser-Gardner Publications: Cincinnati, OH, 1996, Chapter 2.

[15] K.K. Kang, T. Shiono, Y.T. Jeong, D.H. Lee, *J. Appl. Polym. Sci*., 71 (1999) 293–

301.

[16] A. Andoni, J. C. Chadwick, H. J.W. Niemantsverdriet, P. C. Thüne, *J. Catal*., 257 (2008) 81-86.

[17] T. Taniike, M. Terano, *J.Catal.,* 293 (2012) 39–50

[18] R. Zannetti, C. Marega, A. Marigo, A. Martorana, *J. Polym. Sci. Part B: Polym. Phys*., 26 (1988) 2399–2412.

[19] M. Kakugo, H. Sadatoshi, J. Sakai, in: T. Keii, T. Soga (Eds.), Catalytic Olefin Polymerization, H Kodansha-Elsevior: Tokyo, 1990, p. 345–354.

[20] T. Taniike, P. Chammingkwan, V.Q. Thang, T. Funako, M. Terano, *Appl. Catal. A: Gen.*, 437–438 (2012) 24–27.

[21] Y. Cheneviere, F. Chieux, V. Caps, A. Tuel, *J. Catal.,* 269 (2010) 161–168

[22] X. Zheng, M.S. Pimplapure, G. Weickert, J. Loos. *Macromol. Rapid Commun*., 27 (2006) 15–20.

[23] X. Zheng, J. Loos, *Macromol. Symp*., 236 (2006) 249–2258.

[24] T. Wada, T. Taniike, I. Kouzai, S. Takahashi, M. Terano, *Macromol. Rapid Commun*., 30 (2009) 887–891.

[25] T.F.L. McKenna, A. Di Martino, G. Weickert, J.B.P. Soares, *Macromol. React. Eng*., 4 (2010) 40–64.

[26] P. Pokasermsong, P. Praserthdam, *Eng. J*., 13 (2009) 57-64.

[27] P. Galli, P. Barbè, G. Guidetti, R. Zannetti, A. Martorana, A. Marigo, M. Bergozza A. Fichera, *Eur. Polym. J.*, 19 (1983) 19–24.

[28] A. Marigo, C. Marega, R. Zannetti, G. Morini, G. Ferrara, *Euro. Polym. J.*, 36 (2000)

1921–1926.

[29] L.A. Almeida, M.F.V. Marques, *Macromol. React. Eng.*, 6 (2012) 57–64.

[30] H. Nomura, N. Kurihara, K, Higuchi, JP Patent 1991-74341 (1991) (to COLCOAT Engineering Co., Ltd.).

[31] M. Terano, A. Murai, M. Inoue, K. Miyoshi, JP Patent 1987-158704 (1987) (to Toho Catalyst Co., Ltd.).

[32] A. Martínez, G. Prieto, J. Rollán, *J. Catal*., 263 (2009) 292–305

[33] K.S.W. Sing, D.H. Everett, R.A.W. Haul, L. Moscou R.A. Pierotti, J. Rouquérol, T. Siemieniewska, *Pure & Appl. Chem*., 57 (1985) 603–619.

[34] K.S.W. Sing, *Pure & Appl. Chem.*, 54 (1982) 2201–2218.

[35] J.H. de Boer, B.G. Linsen, Th.J. Osinga, *J. Catal.*, 4 (1965) 643–648.

[36] N. Setoyama, T. Suzuki, K. Kaneko, *Carbon*, 36 (1998) 1459–1467.

[37] W.B. Innes, *Anal. Chem.,* 29 (1957) 1069–1073.

[38] E.P. Barrett, L.G. Joyner, P.H. Halenda, *J. Am. Chem. Soc*., 73 (1951) 373–380.

[39] K.L. Murray, N.A. Seaton, M.A. Day, *Langmuir*, 15 (1999) 8155–8160.

[40] P. Kumkaew, L. Wu, P. Praserthdam, S.E. Wanke, *Polymer*, 44 (2003) 4791–4803.

[41] T. Taniike, V.Q. Thang, N.T. Binh, Y. Hiraoka, T. Uozumi, M. Terano, *Macromol. Chem. Phys.,* 212 (2011) 723–729.

[42] C. Przybyla, B. Tesche, G. Fink, *Macromol. Rapid Commun*., 20 (1999) 328–332.

[43] Y.S. Ko, S.I. Woo, J. *Polym. Sci. Part A: Polym. Chem.,* 41 (2003) 2171–2179.

Chapter 3

The statistical approaches for elucidation of structure performance relationship in Ziegler-Natta olefin polymerization

3.1 Introduction

Recent catalysts become to be desired to equip the multifunctional performance, because industrial demands for catalyst become not only increase activity but also improvement of reaction selectivity, easiness of operation, longer life time and so on [1]. Thus, the enormous researches and developments of multifunctional catalysts were briskly conducted to obtain benefits for industrial manufacturing such as abbreviation of reactor number in multistage reaction, extreme control of product characteristics, reduction of operation energies and so on. In resent investigations, “multicomponent” and “hierarchical structure” were key issues of development and/or improvement multifunctional catalyst. The automotive catalyst is excellent multifunctional catalyst and explained as example [2,3]. This catalyst possesses “multicomponent” and ”hierarchical structure” ranges from micro scale to macro is prepared by washcoat of support chemical (ex CeO_2) and active metal species (ex. Rh/Pt/Pd) composition on ceramics which has honeycomb structures. This catalyst possesses not only the three kinds of active site for three kinds of redox reaction but also poisoning resistance, good substrate diffusion, high stiffness and so on [4,5]. As in the example catalyst, designing and control “multicomponent” and ”hierarchical structure” is most important and essential factor for development of multifunctional catalyst which can be used in industry.

Ziegler-Natta catalyst is one of multifunctional catalyst used in industrial polyolefin manufacturing and possess “multicomponent” and “hierarchical structure” [6,7]. This catalyst composed of simple combination between $TiCl_3$ (active species) and alkylaluminium (activator) at early development stage [8]. However, this simple systems had too low polymerization performances to produce polyolefin of good property with efficiently. Since then, enormous researches and developments were conducted to improve olefin polymerization performances following importance of polyolefin. Those investigations established new multicomponent catalyst which is $TiCl_4$ (active species) and donor (active site modifier) supported $MgCl_2$ (support) and new preparation method for control hierarchical structures [9]. Those developments not only improve catalyst performances drastically and added new functions such as stable activity behavior [10], high comonomer insertion [11], long lifetime [9], high particle stiffness [9] and so on. As in mentioned, usage of various chemicals and particle hierarchy construction makes Ziegler-Natta catalyst performances excellent.

Catalyst developments keeps to be conducted and desired to control structure more accurately for further improvement of olefin polymerization performances at the present stage, because polyolefin usage expands more widely fields. Thus, elucidation of correlation between catalyst structures and polymerization performances is strongly

desired to obtain development index, however, correlation has not elucidated quantitatively until now. Because polymerization performances were determined from various structural factors with concerted and/or opposed effects in Ziegler-Natta catalyst olefin polymerization. Additionally, recent catalyst improvement by preparing catalyst multicomponent and hierarchy makes correlation more complex. Therefore, elucidation of structure performance relationship is extremely hard task against academic and industrial desires [12]. Various investigations tried to elucidate industrial catalyst structure performance relationships such as between specific surface area [13,14] and activity, pore architecture [15,16] and activity etc. and reported previously. However reported correlations had even leaves a big question for the quantitativity as well as statistical validity. A serious drawback in previous attempts to find structure performance relationships is attributed to severe limitation in the numbers of employed structural parameters and samples, while the Ziegler-Natta catalysts are characterized by complicated structural hierarchy over multi-length scales as well as a multivariate nature in determining their polymerization performances. Essentially, full characterization of structural parameters which has possibility to effect on performance and increase of sample number until correlation becomes independence on the number sample any more must conduct to elucidate structure performance relationship.

From those backgrounds, this study aims to prepare dataset and establish evaluation way for obtain correct values in multivaliable reaction using statistical techniques for elucidation of structure performance relationship which has not elucidated until now. In particular, we have accomplished full structural characterization [12] and polymerization tests for 16 catalyst samples, which were prepared from $Mg(OEt)_2$ precursor particles. Thus obtained dataset was utilized to examine statistical validity of correlation coefficients between any arbitrary structural parameter and polymerization performance in terms of the sample number that was used to calculate the correlation coefficients.

3.2 Experiment

3.2.1 Materials

Anhydrous $MgCl_2$, triethylaluminium (TEA), and four kinds of poreless Mg particles (termed Mg C) were donated from Toho Titanium Co., Ltd., Tosoh Finechem Corporation and Yuki Gousei Kogyo Co., Ltd., respectively. The morphologies of Mg C are flake-like, while those of Mg B and D are spherical which are same as Magnesium samples in Chapter 2. Ethanol (purity > 99.5%) was dried over 3A molecular sieve with N_2 bubbling. Heptane (purity > 99.5%), toluene (purity > 99.5%) and di-*n*-butylphthalate (DBP) (purity > 98%) were dried over 4A molecular sieve with N_2 bubbling. Cyclohexylmethyldimethoxysilane (CMDMS) was purified by distillation under reduced pressure. Ethylene of research grade donated by Sumitomo Chemical Co., Ltd. was used as delivered.

3.2.2 $Mg(OEt)_2$ synthesis

$Mg(OEt)_2$ was synthesized based on a patent [17] with several modifications. 0.67 g of I_2 (as an initiator) and 31.7 mL of dehydrated ethanol were introduced into a 500 mL jacket-type separable flask equipped with a mechanical stirrer rotating at 180 rpm under N_2 atmosphere. After the dissolution of I_2 at 75°C, 2.5 g of Mg and 31.7 mL of ethanol

were introduced. 2.5 g of Mg and 31.7 mL of ethanol were again added 10 min after the reaction was initiated by $MgCl_2$. Thereafter, 2.5 g of Mg and 31.7 mL of ethanol were added repeatedly 4 times every 10 min, followed by aging at 75°C for 2 h. Finally, the temperature was decreased to 40°C, and the product was washed with ethanol. In this study, 16 kinds of $Mg(OEt)_2$ particles (MGE 1-16) were synthesized from Mg A-D under the different conditions.

3.2.3 Catalyst preparation

The preparation of Ziegler-Natta catalysts from $Mg(OEt)_2$ was conducted again based on a patent [18] with several modifications. 15 g of $Mg(OEt)_2$ and 200 mL of toluene were charged in a 500 mL 3-neck flask equipped with a mechanical stirrer rotating at 180 rpm under N_2 atmosphere. 30 mL of $TiCl_4$ was dropwisely added, where the temperature of the suspension was kept within 0-5°C. Thereafter, the temperature was once elevated to 90°C to add 4.5 mL of DBP and then brought to 110°C. The reaction slurry was continuously stirred at 110°C for 2 h. Subsequently, the reaction product was washed with toluene twice at 90°C and further treated with 30 mL $TiCl_4$ at 90°C for 2 h. After that, the product was washed with *n*-heptane 7 times to get the final catalyst. 16 kinds of Ziegler-Natta catalysts (Cat 1-16) were obtained from MGE 1-16 under the same conditions.

3.2.4 Polymerization test

Propylene and ethylene homopolymerization and copolymerization with 1-hexene. Homopolymerization was performed in a 1 L autoclave equipped with a mechanical stirrer rotating at 350 rpm. 500 ml of *n*-heptane was introduced into the reactor. TEA ([Al] = 10 mmol/L) and CMDMS (Al/ExD = 10) were introduced into the reactor, and the solution was saturated with 0.5 MPa of monomer at 50°C. 30 mg of a catalyst was fed into the reactor by a bomb injection technique to initiate the polymerization. The polymerization was conducted for 60 min with a continuous supply of monomer gas at 0.5 MPa. At the end of the reaction, monomer was vented and the polymer slurry was filtered immediately. In the case of copolymerization with 1-hexene, 500 ml mixture of *n*-heptane (407 ml) and 1-hexene (93 ml, corresponding to 0.75 mol) were used instead of 500 ml of *n*-heptane. The polymerization was conducted for 30 min with 15 mg of a catalyst. The other conditions were the same as those for the homopolymerization.

3.2.5 Characterization

• Scanning electron microscopy

Particle morphological characteristics of $Mg(OEt)_2$ and catalyst particles were studied

with scanning electron microscopy (SEM, Hitachi S-4100) operated at an accelerating voltage of 20 kV. Before the measurements, particles were subjected to Pt sputtering for 100 s. To quantify observed particle morphology, SEM images (> 500 particles) were analyzed by a software (Image J software, NIH). D_{10}, D_{50} and D_{90} were defined as the particle diameters at 10%, 50% and 90% in the cumulative number-base particle size distribution. The relative span factor (RSF) and the circularity degree were respectively calculated based on Eqs. (1) and (2),

$$relative\ span\ factor\ (RSF) = \frac{D_{90} - D_{10}}{D_{50}} \qquad (3-1)$$

(1),

$$circularity\ \ degree = \frac{4 \times \pi \times area}{(boundary\ \ length)^2} \qquad (3-2)$$

(2),

where the area and boundary length for a two-dimensionally projected particle were determined over 500 particles.

• N_2 adsorption/desorption measurement

N_2 adsorption and desorption isotherms at 77 K were acquired on BELSORP-max (BEL JAPAN, INC.). *Ca*. 50-100 mg of catalyst powder in a pyrex tube with a rubber cap was outgassed at 80°C over 3 h in vacuo, prior to the measurement. Since the BET analysis does not work properly for typical Ziegler-Natta catalysts with a plenty of micropores (pore diameter (D) < 2 nm) [20,21], the specific surface area was not

determined. Instead, the micropore volume (V_{micro}) was approximated with

$$V_{micro} = V_{0.4} \times \frac{V_{liquid}}{V_{gas}} - \int_2^{50} \frac{2}{D} \cdot \frac{V_{meso}(D)}{dD} dD \qquad (3-3)$$

(3),

where $V_{0.4}$, V_{liquid}, V_{gas}, and $V_{meso}(D)$ are the N_2 adsorption volume at $p/p_0 = 0.4$, the volumes of a N_2 molecule in gaseous and liquid states, and the mesopore volume at the diameter of *D* nm determined by the method described in the next paragraph. V_{micro} was estimated by subtracting the contribution of multilayer N_2 adsorption onto mesopore surfaces from the adsorption volume at $p/p_0 = 0.4$ (converted to the liquid N_2 volume). Note that the thickness of the multilayer adsorption at $p/p_0 = 0.4$ was approximated as 2 nm, and the contribution from the multilayer adsorption onto macropore and external surfaces was regarded as negligible. The latter is true for typical industrial Ziegler-Natta catalysts, whose pore dimensions are mainly micro and/or meso scale(s) [12].

The mesopore size distributions (2.1 nm < D < 50 nm) were analyzed by the BJH method or by the INNES method. Even though the two methods are based on the same Kelvin equation for the N_2 condensation, cylinder-type and slit-type mesopores are assumed in the BJH [22] and INNES [23] methods, respectively. Hence, the BJH method is suitable for the hysteresis types H1 and H2 respectively for size-uniform and size-irregular cylindrical-type mesopores, while the INNES method for the types H3 and H4

respectively for size-uniform and size-irregular slit-type mesopores .

• Mercury intrusion measurement

The meso and macro pore size distributions (7 nm < diameter < 1000 nm) were measured with the mercury intrusion technique (Pascal 440 Porosimeter, Thermo Scientific). The pore size was evaluated from the intrusion pressure according to the Washburn-Laplace equation which was shown in equation (3-1). The surface tension (γ) and contact angle (θ) were respectively set to 0.480 N / m and 141.3°.

$$D = \frac{2\gamma \cos\theta}{P} \qquad (3-4)$$

• Chemical analysis

The Ti content was determined with UV-vis spectroscopy (V-670 JASCO), where a measured amount of a catalyst sample was dissolved in $HCl/H_2SO_4/H_2O_2$ solution and the intensity of a ligand metal charge transfer band at 410 nm was measured. The DNBP content was determined by IR spectroscopy (FT/IR-4100, JASCO): A measured amount of a catalyst sample was once dissolved in HCl solution, then DNBP was fully phase transferred to *n*-heptane, and finally the carbonyl absorption band was integrated to determine the DNBP content.

•^{13}C NMR

The 1-hexene incorporation amount, *i.e. n*-Bu branch content, in ethylene/1-hexene copolymer was measured by ^{13}C NMR (Bruker 400 MHz) operating at 100 MHz with proton decoupling at 120°C using 1,2,4-trichlorobenzene as a diluent and 1,1,2,2-tetrachloroethane-d_2 as an internal lock and reference.

3.2.6 Statistical analysis

The correlation coefficient is one of statistical index and directly expresses the correlation extent between the two variables. As the *r* value approaches +1 or –1, the correlation extent becomes higher in a positive or negative direction, respectively. In general, the correlation coefficient, *r*, between two variables (*x* and *y*) is defined as

$$r = \frac{C_{(x,y)}}{\sqrt{V_x \times V_y}} \qquad (3.5)$$

$C_{(x,y)}$, V_x and V_y are the covariance and the variances for *x* and *y*, respectively. They are defined as

$$C_{(x,y)} = \sum_{i=1}^{n} \frac{\left(x_i - \bar{x}\right)\left(y_i - \bar{y}\right)}{n} \qquad (3.6)$$

$$V_x = \sum_{i=1}^{n} \frac{\left(x_i - \bar{x}\right)^2}{n} \qquad (3.7)$$

$$V_y = \sum_{i=1}^{n} \frac{\left(y_i - \bar{y}\right)^2}{n} \qquad (3.8),$$

where n is the number of data.

3.3 Results and discussion

3.3.1 Catalyst preparation and characterization

3.3.1.1 $Mg(OEt)_2$ synthesis and their characteristics

Sixteen kinds of $Mg(OEt)_2$ particles were synthesized from different conditions. Table 1 summarized synthesis conditions of $Mg(OEt)_2$ samples..

Table 3-1. Reaction condition for $Mg(OEt)_2$ synthesis

sample	Halide	Mg source	Stirring speed (rpm)	Total amount of Mg (g)	Total amount of halide (mmol)
MGE1	$MgCl_2$	A	180	12.5	2.64
MGE2	$MgCl_2$	B	180	12.5	2.64
MGE3	$MgCl_2$	C	180	12.5	2.64
MGE4	$MgCl_2$	D	180	12.5	2.64
MGE5	$MgBr_2$	C	180	12.5	2.64
MGE6	MgI_2	C	180	12.5	2.64
MGE7	I_2	C	180	12.5	2.64
MGE8	I_2	C	180	16.7	3.51
MGE9	I_2	C	180	10.0	2.13
MGE10	I_2	C	180	16.7	2.64
MGE11	I_2	C	180	10.0	2.64
MGE12	I_2	C	180	12.5	2.13
MGE13	I_2	C	180	12.5	3.51
MGE14	I_2	C	120	12.5	2.64
MGE15	I_2	C	240	12.5	2.64
MGE16	I_2	C	300	12.5	2.64

MGE1-4 corresponds to the samples in chapter 2 which were prepared using different samples. Mg-3 (used for MGE3) were used as standard Mg source and fixing the other

conditions at the standard one, the kinds of initiators was altered for MGE5-7. At the fixed ethanol amount, the amount of Mg source, and iodine amount (as halide initiator) were altered for MGE8-13. For MGE14-16, the stirring speed was varied without changing the other conditions form those for MGE7. Their SEM pictures were shown in Figure 3-1. Moreover, particle morphological characteristics acquired from the statistical analysis of SEM images analysis over 500 particles were shown in Table 3-2.

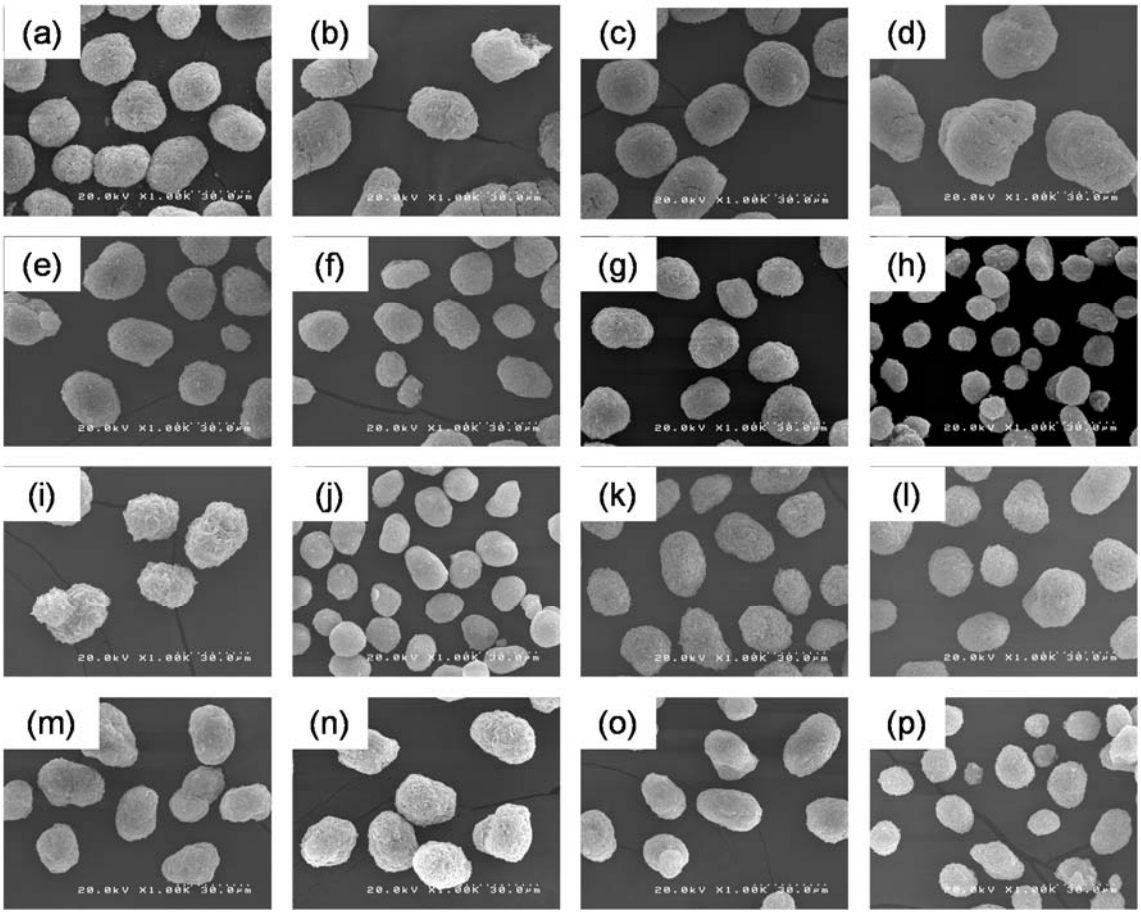

Figure 3-1. SEM images of $Mg(OEt)_2$ samples.

Table 3-2. $Mg(OEt)_2$ morphological characteristics[a]

Sample	D_{10}[b] (μm)	D_{50}[b] (μm)	D_{90}[b] (μm)	RSF[c]	Circularity[d]
MGE1	19.6	22.3	26.2	0.30	0.91
MGE2	12.1	26.1	35.7	0.90	0.83
MGE3	26.3	31.2	39.7	0.43	0.92
MGE4	26.6	36.8	46.9	0.55	0.85
MGE5	15.9	20.9	27.8	0.57	0.88
MGE6	16.8	18.6	28.4	0.63	0.88
MGE7	17.2	20.7	34.2	0.82	0.89
MGE8	10.1	12.4	16.5	0.52	0.82
MGE9	20.5	24.7	30.7	0.41	0.84
MGE10	12.6	15.2	20.4	0.51	0.87
MGE11	18.7	22.1	26.8	0.37	0.89
MGE12	17.0	20.1	27.2	0.51	0.91
MGE13	17.8	22.1	29.5	0.53	0.91
MGE14	19.7	24.6	44.5	1.01	0.87
MGE15	14.9	19.0	25.6	0.56	0.87
MGE16	12.2	16.7	22.2	0.60	0.90

[a] Particle morphological characteristics were acquired by a statistical analysis of SEM images over 500 particles. [b] Particle diameters at 10%, 50% and 90% in the cumulative number particle size distribution. [c] Relative span factor (RSF) defined by $(D_{90}-D_{10})/D_{50}$. [d] The circularity degree defined by $4\pi A/L^2$, where A and L are the projected area and boundary length of a particle, respectively.

All obtained $Mg(OEt)_2$ particles were basically composed by agglomeration of plate-like structural unit. While particle morphology was rather sensitive to examined synthetic parameters, especially quantitative meanings. The morphology of Mg source has very important role for all the particle characteristics (MGE1-4). Spherical Mg sources tends to supply a larger diameter, larger particle size distributions and lower circularity compared with flake like Mg sources. The kinds of halide initiators mainly affected the

particle diameter (MGE3, 5-7). The particle diameter follows the order of $MgCl_2$ >> $MgBr_2$ > I_2 >MgI_2, while the rate of the conversion (measured by the H_2 emission rate) follows reverse the reverse order. The Mg amount is one of the most important factor on $Mg(OEt)_2$ morphology. As the Mg amount increased, the particle sizes were decreased while the size distribution became broader (MGE8,10). At the lowest Mg amount (MGE9,11), the surface texture became much rougher as the plate-like units did not lie down on surfaces. These results were plausibly explained in terms of the viscosity of the reaction slurry: A greater Mg amount increases the slurry viscosity so as to impose greater shear forces on forming particles (smaller and smoother particles), while higher viscosity reduces the uniformity of the stirring (larger RSF). The amount of the I_2 initiator hardly affected the macro particle characteristics. It seems that the amounts of the initiator added here already corresponded to the excess for initiating the reaction (MGE11,12). The stirring speed affects the particle morphology through the shear force applied during the formation of $Mg(OEt)_2$ particles (MGE14-16). In actual, we found that a higher stirring speed not only reduced the particle sizes but also narrowed the particle size distribution as a result of more uniform stirring.

In summary, various synthesis parameters such as the morphology of Mg sources, the kinds of halide initiators, the Mg amount, and the stirring speed have some effects on the

particle morphology. However, it can be concluded that strong shear force and uniform stirring are prerequisites to have spherical $Mg(OEt)_2$ particles with the smooth surface texture and narrow size distribution. In this sense, the reactor and stirrer design must be critically important.

3.3.1.2 Catalyst preparation and their characteristics

All $Mg(OEt)_2$ samples were converted into catalysts based on the same scheme showed in experimental part, where di-n-buthylphthalate (DNBP) was employed as an internal donor. Obtained catalysts are observed by SEM and their representative images are shown in Figure 3-2. Moreover, Table 3-2 summarizes the particle characteristics acquired by statistical analysis of SEM images.

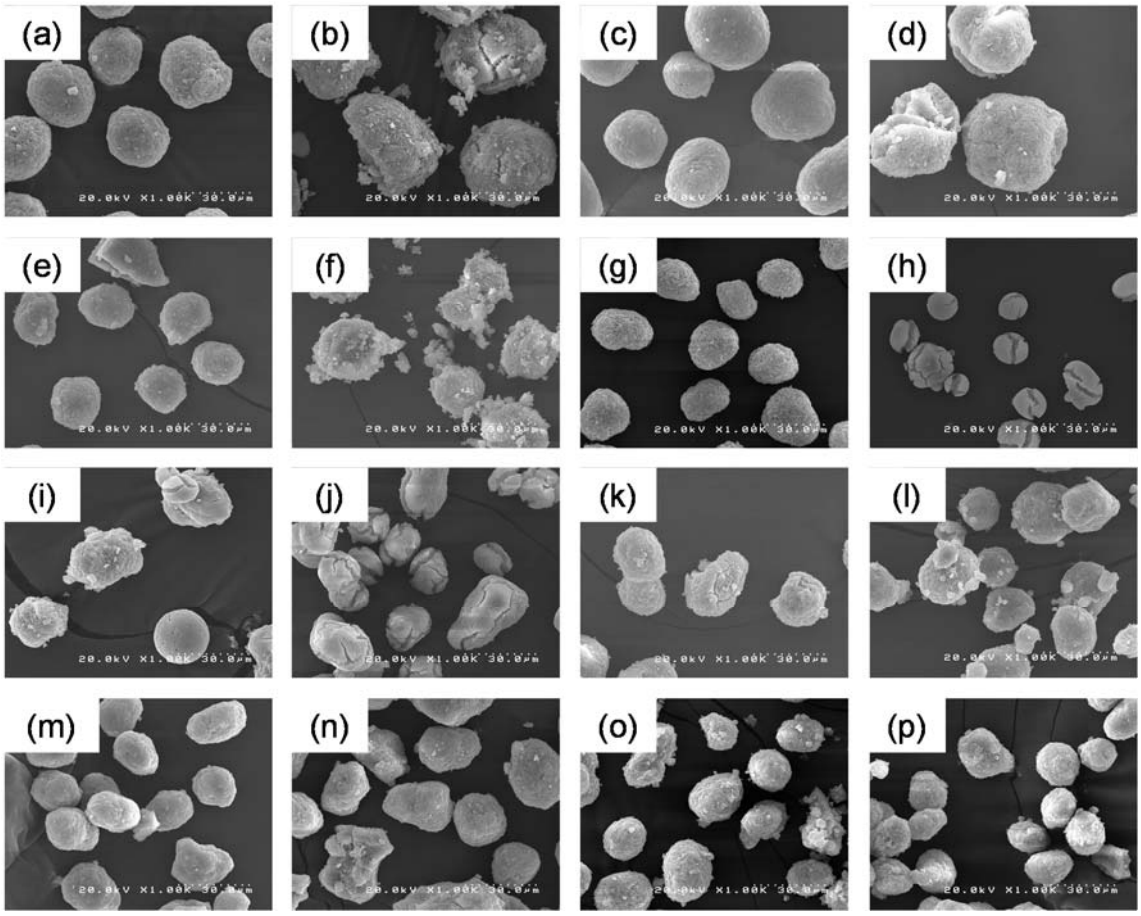

Figure 3-2. SEM images of catalyst particles

Table 3-3. Morphological characteristics of catalyst particles

Sample	SEM					Light scattering			
	D_{10} (μm)	D_{50} (μm)	D_{90} (μm)	RSF	Circularity	D_{10} (μm)	D_{50} (μm)	D_{90} (μm)	RSF
Cat1	20.2	25.7	31.0	0.42	0.84	18.5	34.4	60.3	1.22
Cat2	12.4	37.6	55.5	1.15	0.74	19.1	40.5	63.1	1.09
Cat3	27.2	32.4	44.4	0.53	0.87	29.1	40.9	62.8	0.82
Cat4	22.0	36.6	49.8	0.76	0.79	39.6	65.3	116.9	1.18
Cat5	16.1	21.9	37.2	0.96	0.82	11.1	34.5	81.5	2.04
Cat6	7.1	15.4	30.0	1.49	0.64	20.2	34.2	79.1	1.72
Cat7	17.9	21.7	29.1	0.52	0.88	20.1	31.1	75.8	1.80
Cat8	13.6	17.5	37.9	1.39	0.77	17.8	67.6	139.3	1.80[b]
Cat9	12.9	25.7	34.7	0.85	0.72	21.2	40.3	84.3	1.57
Cat10	14.1	18.3	37.2	1.26	0.77	16.6	36.9	118.9	2.77[b]
Cat11	21.1	33.6	62.4	1.23	0.82	23.2	47.9	108.8	1.79[b]
Cat12	16.9	22.2	34.2	0.78	0.83	20.4	30.5	61.5	1.35
Cat13	18.0	23.7	32.4	0.61	0.83	22.9	47.5	93.6	1.49
Cat14	22.5	28.4	41.4	0.66	0.84	26.0	56.5	129.0	1.82[b]
Cat15	15.0	22.6	35.4	0.90	0.82	17.6	34.2	72.6	1.61
Cat16	21.1	33.6	62.4	1.23	0.82	17.6	34.2	123.5	3.10[b]

[a] Modal diameter corresponding to the most frequent diameter. [b] A bimodal particle size distribution was observed.

As was already mentioned in chapter 2, the catalyst particle morphology more or less replicates the morphology of $Mg(OEt)_2$ particles. However, the catalyst conversion tended to enlarge particle sizes, broaden the particle size distribution and reduce the circularity, whose degrees were largely dependent on samples. For example, Cat8,10,11,16 experienced severe agglomeration, leading to significant increases in D_{90}

and RSF. On the other hand, Cat9 formed non-negligible particle disintegration, leading to the reduction of D_{10} as well as the expansion of RSF. Thus, it was found that $Mg(OEt)_2$ particles with the smallest sizes and/or rough surface texture tended to cause incomplete replication.

The two kinds of the particle characteristics obtained by SEM and LS has been compared. The merits and demerits for the two kinds of the methods are summarized below.

Statistical analysis of SEM images: The particle morphology can be directly observed and quantified. Especially fine particles are visible, while they are mostly neglected in the volume-based distribution. Furthermore, the number-based distribution must be more directly correlated with catalyst performances. The largest problem is the difficulty to make fair sampling, especially for samples which are not easily dispersed on a SEM grid.

Light scattering : The merits of LS are at efficient & fair sampling and at the capability to capture agglomerated particles, which are not obvious for the number-based distribution. In terms of plant operation, both fine particles for SEM and agglomerated particles for LS must be taken into consideration.

From these features, the number-based (for SEM) and volume-based (for LS) particle size distributions are not necessarily comparable unless the particle size distribution of a sample is narrow enough. On the other hand, comparison of both distributions made sample agglomeration degree clear. Those results were shown in Table 3-3. For example, the samples which possessed particle distributions are unimodal and narrow can be confirmed correlations between SEM analysis and LS. Even if particle size distribution spectrum becomes shoulder type that means agglomeration degree become little higher, correlations are remained. However, a number of particles agglomerate each other frequently and LS spectrum becomes bimodal, correlation is disappeared.

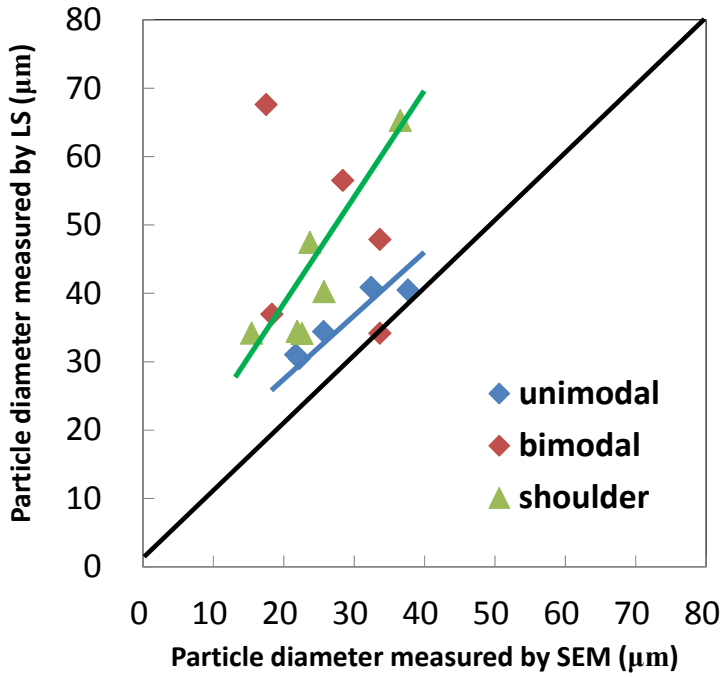

Figure 3-3. Comparison between number-based and volume-based particle size

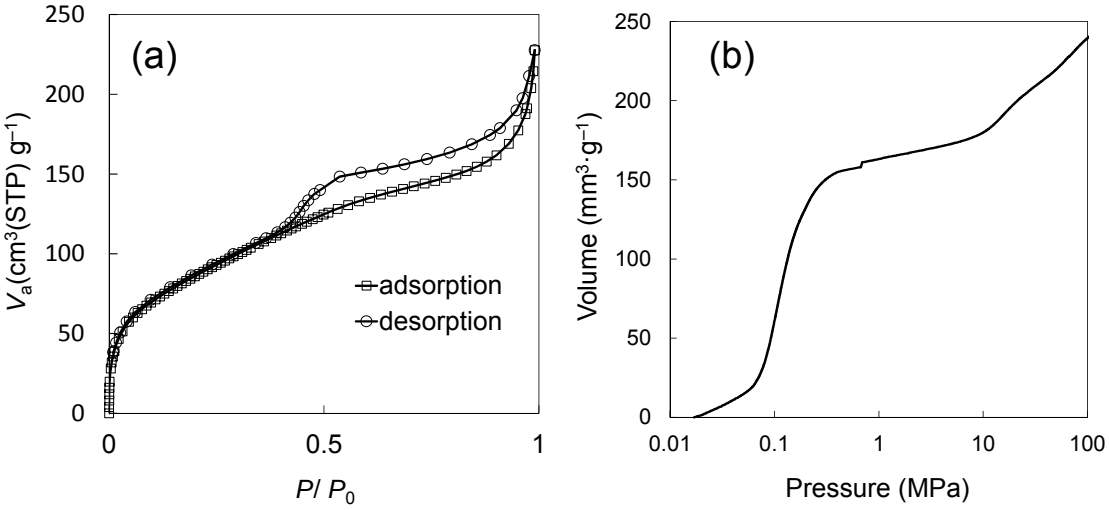

Figure 3-4. N_2 isotherm and Hg intrusion curve of Cat7

The catalyst pore structures were studied comparatively based on N_2 adsorption and Hg porosimetry. These results were shown in Table 3-4 respectively. N_2 adsorption and desorption experiments were conducted at 77 K on Belsorp-max, where the samples were preliminary outgassed at 80°C for 3 h. As was explained in chapter 2, typical Ziegler-Natta catalysts (including $Mg(OEt)_2$-based ones) contain a non-negligible volume of micropores, due to which the BET method for the specific surface area is not applicable.[1] The micropore volume is a more realistic parameter for quantifying the particle structure of Ziegler-Natta catalysts. Here, the micropore volume was calculated by the equation with the assumption that the N_2 adsorption below $p/p_0 < 0.4$ is mainly related to micropore filling. Since $Mg(OEt)_2$-based catalysts generally exhibit a hysteresis loop classified as

the type H3 for size-irregular slit-type mesopores, the mesopore size distribution was calculated based on the Innes method for slit-type mesopores. Hg intrusion were conducted and obtained data were analyzed by Washburn-Laplace equation without intrusion above 7.4 MPa (corresponding to below 200 nm) which was regarded as intraparticle pores effect. Thus calculated pore size distribution is represented only Cat7 in Figure 3-5, since the other samples shows qualitatively similar distributions.

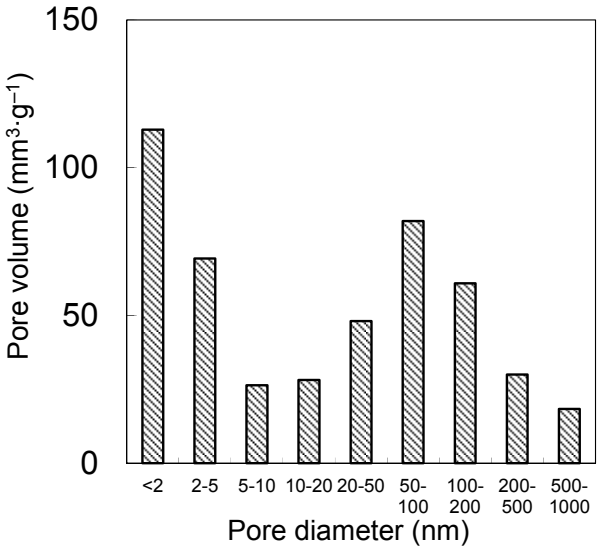

Figure 3-5. Pore size distribution of Cat7

Cat 7 possessed broad pore size distribution from micro- to meso-pores with a bimodal character centered at micropore (D<2 nm) and at macropore (50<D<100 nm). the other samples also possessed similar pore size distributions qualitatively, however the quantitatively differences among catalysts each other was confirmed. These pore volumes were shown in Table 3-4.

Table 3-4. Pore size distributions of catalysts

Sample	Pore volume (mm^3/g)							
	<2 nm[a]	2-5 nm[b]	5-10 nm[b]	10-20 nm[b]	20-50 nm[b]	50-100 nm[c]	100-200 nm[c]	200-500 nm[c]
Cat1	76.8	29.9	32.2	55.3	76.8	70.1	146.8	79.7
Cat2	81.8	27.1	28.7	49.8	81.8	72.3	100.0	49.2
Cat3	83.3	26.2	26.8	48.7	83.3	75.3	80.4	36.0
Cat4	75.5	22.5	23.5	44.1	75.5	67.4	103.5	40.5
Cat5	75.2	25.4	28.0	48.0	75.2	57.7	91.5	73.9
Cat6	78.9	28.0	27.3	48.3	78.9	69.6	51.0	29.5
Cat7	107	76.1	26.9	28.5	48.5	81.9	60.9	30.0
Cat8	101	67.4	22.0	19.4	31.7	39.5	24.2	23.0
Cat9	95	91.6	30.5	32.6	55.3	81.6	81.2	69.1
Cat10	107	78.3	25.6	19.8	32.2	34.8	18.5	17.2
Cat11	128	76.3	24.6	23.9	36.6	64.5	82.8	54.7
Cat12	112	80.5	29.8	32.9	59.0	66.5	59.4	34.4
Cat13	98	74.5	29.3	32.6	51.6	81.3	104.4	48.6
Cat14	97	84.5	27.7	30.7	58.8	78.2	65.2	42.0
Cat15	111	79.6	26.0	25.5	43.8	75.5	59.6	41.9
Cat16	104	87.3	30.7	28.7	47.4	78.2	46.3	30.6

[a] Calculated from Equation (3-3). [b] Calculated based on the Innes method. [c] calculated from Washburn-Laplace equation

Micro- and meso-pore volume and its distributions were rather insensitive to synthetic condition for $Mg(OEt)_2$ particles. However, careful analyses on the detailed pore size distributions suggested the following possible tendencies. When the largest amount of Mg source was added in the synthesis of $Mg(OEt)_2$ particles (MGE8,10), the resultant pore volume for 20-50 nm appeared to be smaller (Cat8,10). This fact could be explained in a way that high shear force applied in the formation of $Mg(OEt)_2$ particles

limited the macropore volume (*i.e.* higher bulk density), which might be replicated for the catalysts. And, a greater amount of the I_2 initiator (MGE8,13) appeared to reduce the volume of the pores below 5 nm (Cat8,13), whose mechanistic origin might high density comes from increase of precipitation amount by iodine as initiator during $Mg(OEt)_2$ synthesis but it was unclear.

Table 3-5 summarizes the results of the chemical composition analyses. The chemical composition including the Ti and DNBP contents was not significantly different among all catalyst, where the DNBP/Ti molar ratio always fell in a range of 1-1.2, typical for $Mg(OEt)_2$-based Ziegler-Natta catalysts. Thus, macroscopic structural differences in $Mg(OEt)_2$ particles did not affect microscopic chemical parameters of the resultant catalysts, which enabled us to isolate influences of structural parameters on the polymerization performances.

Table 3-5. Chemical composition of catalysts

	Ti contents (wt%)	DBP contents (wt%)
Cat1	2.4	11.3
Cat2	2.5	20.9
Cat3	2.7	18.3
Cat4	2.7	14.8
Cat5	2.6	16.4
Cat6	2.7	16.5
Cat7	2.7	15.7
Cat8	2.1	14.8
Cat9	2.6	20.2
Cat10	2.0	15.2
Cat11	2.4	13.6
Cat12	1.9	13.3
Cat13	2.5	17.0
Cat14	2.0	13.6
Cat15	2.7	11.5
Cat16	2.1	17.3

3.3.1.3 Olefin polymerization test

In order to examine the impact of particle structures on the polymerization performance, each catalyst was subjected to four kinds of polymerization tests: propylene and ethylene homopolymerization and copolymerization with 1-hexene. The results of polymerizations as well as those polymer characterization with ^{13}C-NMR are shown in Table 3-6.

Table 3-6. Polymerization results

Sample	Activity (g/g-cat·atm·h)				Bu branch (mol%)		*mmmm* (mol%
	C_3 homo	C_3 co	C_2 homo	C_2 co	C_3 co	C_2 co	C_3 homo
Cat1	155	278	122	658	5.0	6.7	96.8
Cat2	140	153	75	489	4.4	4.3	97.0
Cat3	129	155	111	401	7.2	6.9	95.0
Cat4	123	282	106	746	5.2	4.9	93.9
Cat5	101	243	135	731	3.8	4.0	96.2
Cat6	185	519	77	294	5.6	5.6	96.1
Cat7	75	230	77	307	3.5	4.6	95.3
Cat8	138	336	90	689	5.3	5.7	95.8
Cat9	154	193	104	742	5.1	4.6	92.9
Cat10	111	456	46	461	5.4	5.4	95.6
Cat11	130	260	81	463	6.3	8.0	95.3
Cat12	127	216	80	426	5.2	6.1	95.9
Cat13	100	291	89	567	5.8	6.3	95.0
Cat14	176	398	120	741	6.0	5.4	95.8
Cat15	184	280	98	554	5.1	4.5	95.5
Cat16	171	386	95	660	5.2	7.0	95.1

Compared with the catalyst structures, the polymerization activities differed greatly among the catalysts. The catalyst activity tended to follow the order of C2 co > C3 co >> C3 homo > C2 homo. The butyl branch content varied from 3.5 to 8.0 mol%, irrespective of the main monomer. On the other hand, the stereoregularity of PP was quite insensitive to the catalysts, around 95 mol% in *mmmm*.

3.3.2 Dataset evaluation based on statistics

3.3.2.1 Dataset evaluation

Evaluation of dataset is necessary operation before statistical analyses in order to obtain correct and accurate results. For example, it is possible that fake-correlation may be obtained when dataset does not possess enough statistical significance each other. Because it is not unclear that differences of parameter value are derived from experimental errors or correct correlations. Therefore, dataset evaluations are conducted generally before statistical analysis.

Dataset evaluation for all parameter which from structure to performance was conducted. In particular, difference value between maximum and minimum in dataset and standard deviation value are calculated and obtained values were divided by average for standardization. Calculated results are shown in Table 3-7 ~ 3-10.

Table 3-7. Data evaluation for particle morphology

	SEM					Light scattering			
	D_{10} (μm)	D_{50} (μm)	D_{90} (μm)	RSF	Circularity	D_{10} (μm)	D_{50} (μm)	D_{90} (μm)	RSF
Ave (x)	14.9	21.4	31.2	0.76	0.81	18.1	27.6	47.4	1.03
S_x/ Ave	0.31	0.23	0.23	0.42	0.06	0.27	0.26	0.36	0.36
(MAX-MIN) /Ave	0.99	0.88	1.07	1.37	0.26	1.05	0.90	1.29	1.23

Table 3-8. Data evaluation for particle morphology pore architectures

Sample	Pore volume (mm^3/g)							
	<2 nm	2-5 nm	5-10 nm	10-20 nm	20-50 nm	50-100 nm	100-200 nm	200-500 nm
Ave (x)	117	65.6	27.0	29.3	53.8	68.4	73.5	43.8
S_x/ Ave	0.20	0.20	0.41	0.56	0.74	0.20	0.44	0.41
(MAX-MIN) /Ave	0.76	0.71	1.39	2.03	2.96	0.69	1.75	1.43

Table 3-9. Chemical composition of catalysts

	Ti contents (wt%)	DBP contents (wt%)
Ave (x)	3.4	15.6
S_x/ Ave	0.25	0.23
(MAX-MIN) /Ave	1.01	0.86

Table 3-10. Polymerization results

Sample	Activity (g/g-cat·atm·h)				Bu branch (mol%)		*mmmm* (mol%
	C_3 homo	C_3 co	C_2 homo	C_2 co	C_3 co	C_2 co	C_3 homo
Ave (x)	144	302.5	94.5	591.5	5.4	5.7	95.5
S_x/ Ave	0.20	0.35	0.23	0.26	0.14	0.19	0.01
(MAX-MIN) /Ave	0.59	1.21	0.94	0.93	0.64	0.70	0.04

S_x/Ave value means dispersion degree of dataset and (MAX-MIN) /Ave value has information of parameter control ability. As can be seen table, the S_x/Ave values excepted *mmmm* and circularity possess higher value than 0.1 In comparison with catalysts which made by same synthesis condition, the change ratio of structural parameters were smaller than values noted above. It mentioned that not only smallness of experimental errors for structural parameters but also significant difference among prepared catalysts set.

The S_x/Ave values of parameters related to micro scales such as chemical composition and micro pore volume were about 0.1~0.2, while S_x/Ave value of macroscopic parameters such as meso-macro pore volume and particle size were about 0.3~0.4. Moreover, macroscopic parameter possessed higher (MAX-MIN) /Ave values than microscopic parameters. It is suggested that the difference of $Mg(OEt)_2$ structure have stronger effect on macro scale morphologies than micro scale.

3.3.2.2 One-to-one correlation evaluation using correlation coefficient

The correlation coefficient between structure and performance were calculated as one to one correlations, since it was confirmed that dataset possessed enough significant difference. Correlation coefficient *r* is statistical index which describes how strongly units in the same group resemble each other and calculated by variance and covariance (equal

(1)). *r* ranges from 1 to -1, ± indicates positive or negative correlation and degree of correlation became small with value closes to 0. Moreover, the summarized table which contains correlation coefficients of a number of vitiates each other is called correlation matrix. This value is very available and often used as not only statistical index but also pretreatment before multivariate analysis. However, this value is easily changed to wrong by small number of samples because of strong effect from bad leverage points. Therefore, preparation of necessary and sufficient number of samples to obtain correct value. At First, Figure 3-6 plots the variation of correlation coefficients among representative structure parameters and polymerization performances in terms of the sample number.

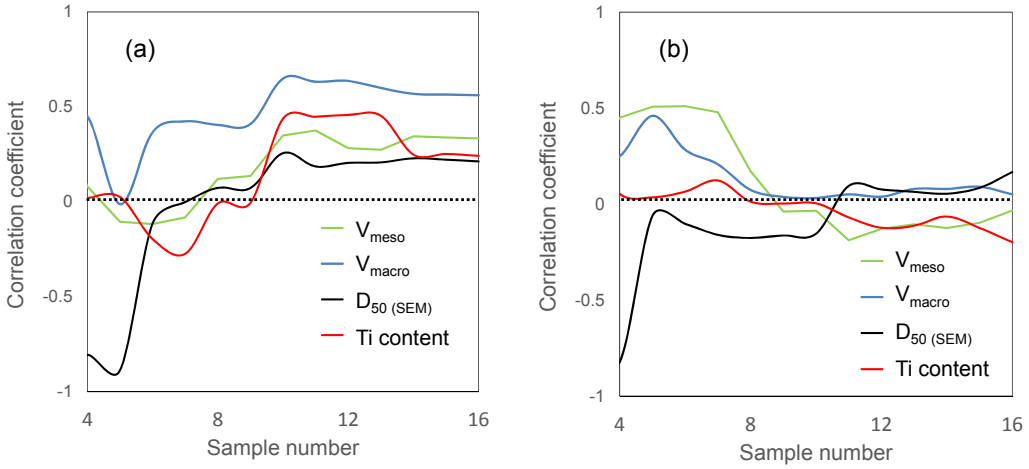

Figure 3-6. Correlation coefficients between representative structural parameters and polymerization performance; (a) ethylene polymerization activity, (b) comonomer insertion efficiency in ethylene/1-hexene coporimerization

As can been seen, correlation coefficient value become stable with increase using sample number regardless of using structural and/or performance parameters. Concretely, coefficients greatly fluctuated when the sample number was below 10. It suggests that the risk of fake correlations when the sample number was not sufficient.

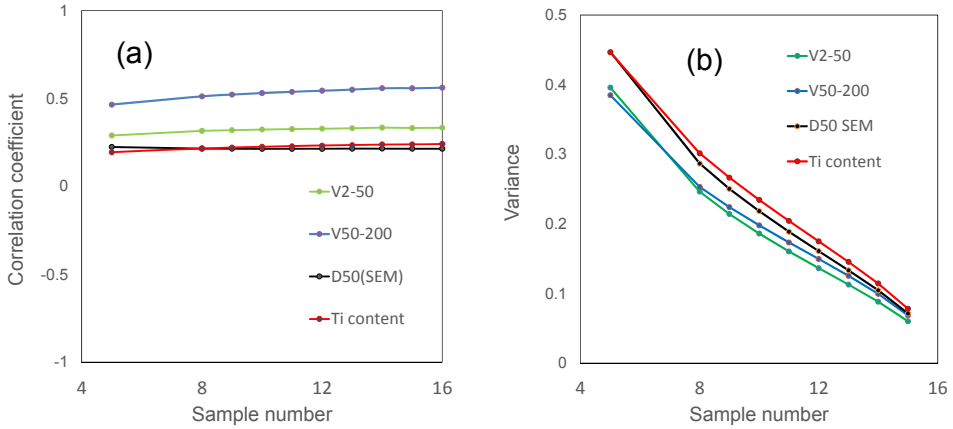

Figure 3-7. Statistical reliability of a correlation coefficient in terms of the sample number

The sample number dependence of correlation coefficient was determined by following way. The correlation coefficients were calculated by selecting arbitrary X samples among 16 samples at first. Second, average of correlation coefficient and its variances are calculated. In Figure 3-7, the average correlation coefficient between the macropore volume and the ethylene polymerization activity was stable irrespective of the sample number, while its variance monotonically decreased as the sample number increased. Concretely speaking, correlation coefficient was 0.47±0.38 when using 5 samples for determination. Error was too big to regard as statistical validity. Meanwhile, when using

15 samples, the correlation coefficient was 0.56±0.07. This tendency was confirmed by other combination between structure and performance parameters. Its result indicates that sample number makes correlation coefficient accurate enough.

3.3.2.3 Correlation matrix of structure performance relationship

Previous sections clarified that 16 samples are enough number to make one-to-one correlation stable in this study. Thus, correlation coefficient of all combinations between structure and performance were calculated and these results were shown in Table 3-11.

Table 3-11. Correlation matrix between structural parameter and polymerization performance.

	D_{10} (SEM)	D_{50} (SEM)	D_{90} (SEM)	RSF (SEM)	Circularity	D_{10} (LS)	D_{50} (LS)	D_{90} (LS)	RSF (LS)	Ti content	Donor
C3ho	-0.16	-0.10	-0.11	0.03	-0.13	-0.06	-0.23	-0.07	0.10	0.11	-0.17
C2ho	0.44	0.21	-0.07	-0.52	0.34	0.12	0.14	-0.12	-0.29	0.24	-0.13
C3co	-0.31	-0.53	-0.24	0.38	-0.28	-0.15	-0.01	0.48	0.63	-0.23	-0.27
C2co	0.23	0.09	-0.08	-0.39	0.35	0.05	0.28	0.31	0.15	0.00	-0.05
C3Bu	0.52	0.14	0.12	-0.18	0.25	0.52	0.22	0.12	-0.21	0.03	-0.06
C2Bu	0.51	0.17	0.29	-0.08	0.38	0.16	-0.03	0.11	0.09	-0.20	-0.26

	V_{micro} <2	V_{meso} 2-50	V_{macro} 50-200	V_{N2} 2-5	V_{N2} 5-10	V_{N2} 10-20	V_{N2} 20-50	V_{Hg} 7-10	V_{Hg} 10-20	V_{Hg} 20-50	V_{Hg} 50-100	V_{Hg} 100-200
C3ho	0.00	0.29	0.00	0.35	0.27	0.16	0.23	0.11	-0.05	0.33	0.45	-0.20
C2ho	-0.27	0.33	0.56	0.10	0.06	0.38	0.47	0.09	-0.01	-0.04	0.36	0.55
C3co	0.13	-0.24	-0.51	-0.18	-0.03	-0.30	-0.27	0.15	-0.03	0.24	-0.24	-0.54
C2co	-0.45	0.05	0.19	-0.04	-0.08	0.11	0.13	0.00	0.13	0.14	0.17	0.17
C3Bu	-0.02	-0.02	-0.05	0.11	-0.04	-0.10	-0.07	0.56	0.09	0.03	0.17	-0.13
C2Bu	0.19	-0.03	0.05	-0.07	0.16	0.02	-0.09	0.30	-0.18	0.18	0.10	0.02

As can been seen Table 3-11, there are no combinations which possess strong correlations ($r>0.7$ in generally). It suggested that performances of Ziegler-Natta olefin polymerization was determined the plural number of variable.

3.4 Conclusion

In this study, various data were analyzed based on statistics for the elucidation of structure performance relationship between structure and performances. Consequently, sixteen kinds of Ziegler-Natta catalyst samples were prepared from different morphological $Mg(OEt)_2$, identified by multilateral method which was established in chapter 2, and was conducted polymerization performance test. After those operations, resulted data were parameterized and evaluated following statistical way.

As results, it is identified that the dataset of sixteen catalyst samples possessed sufficiently larger significant difference to use analysis than experimental error and individual difference by evaluation of these standard deviation. And, dependence of sample numbers to the correlation coefficient values was investigated to obtain the knowledge for improvement of statistical analysis accuracy. The average of correlation coefficient was almost constant with change sample number. On the contrary, its standard deviations showed monotonic decrease with increase of sample number. It suggested that

necessary and sufficient number of sample is indispensable condition to obtain accurate correlation. After above dataset evaluations, correlation between structure and performance were calculated. However, strong correlation was not found out from all combinations. This result is normal fact, because Ziegler-Natta olefin polymerization performances were determined by the multivariate. Therefore, no correlation means proof of correct dataset evaluation.

Form those results, this study clarifies the cause of difficulty to elucidate quantitative structure performance relationship in Ziegler-Natta olefin polymerization with small number of samples and insufficient characterizations from the viewpoint of statistics. Then dataset contents such as deviation, parameter species, sample number are indispensable factor to obtain correct statistical analysis results.

Reference

[1] S. Senkan, *Angew. Chem. Int. Ed.,* 40 (2001) 312-329.

[2] S. Matsumoto, *Catal. Today*, 90 (2004) 183-190.

[3] J. Kašpar, P. Fornasiero, M. Graziani, *Catal. Today,* 50 (1999) 285-298.

[4] H.S. Gandhi, G.W. Graham, R.W. McCabe, J. Catal., 216 (2003) 433-442.

[5] R.M. Heck and R.J. Farrauto, *Appl. Catal. A: Gen.,* 221 (2001) 443-457.

[6] Y. Hiraoka, S. Y. Kim, A. Dashti, T. Taniike, M. Terano, Macromol. React. Eng., 4 (2010)

510-515

[7] T. Taniike, V. Q. Thang, N. T. Binh, Y. Hiraoka, T. Uozumi, M. Terano, Macromol. Chem. Phys., 212 (2011) 723-729

[8] K. Soga and T. Shiono, *Prog. Polym. Sci.,* 22 (1997) 1503-1546.

[9] A. Dashti, A. Ramazani, Y. Hiraoka, S.Y. Kim, T. Taniike and M. Terano, *Polym. Int.,* 58 (2009) 40-45.

[10] M. Hassan Nejad, P. Ferrari, G. Pennini and G. Cecchin, *J. Appl. Polym. Sci.*, 108 (2008) 3388–3402

[11] X. Zheng, M.S. Pimplapure, G. Weickert, J. Loos. *Macromol. Rapid Commun*., 27

(2006) 15–20

[12] T. Taniike, T. Funako, M. Terano, *J. Catal.*, 311 (2014) 33-40

[13] A. Marigo, C. Marega, R. Zannetti, G. Morini and G. Ferrara, *Euro. Polym. J.,* 36, (2000) 1921-1926

[14] P. Gall, P. Barbi, G. Guidetti, R. Zannetti, A. Martorana, A. Marigo, M. Bergozza and A. Fichera, *Eur. Polym. J.,* 19 (1983**)** 19-24

[15] P. Pokasermsong, P. Praserthdam, Eng. J., 13 (2009) 57-64

[16] L. A. Almeida, M. F. V. Marques., *Macromol. React. Eng*. 6 (2012) 57-64

[17] H. Nomura, N. Kurihara, K, Higuchi, JP Patent 1991-74341 (1991) (to COLCOAT Engineering Co., Ltd.).

[18] M. Terano, A. Murai, M. Inoue, K. Miyoshi, JP Patent 1987-158704 (1987) (to Toho Catalyst Co., Ltd.).

[19] K.S.W. Sing, D.H. Everett, R.A.W. Haul, L. Moscou R.A. Pierotti, J. Rouquérol, T. Siemieniewska, *Pure & Appl. Chem.,* 57 (1985) 603–619.

[20] T. Taniike, P. Chammingkwan, V.Q. Thang, T. Funako, M. Terano, *Appl. Catal.* A: Gen. 437–438 (2012) 24-27.

[21] P. Chammingkwan, V. Q. Thang, M. Terano, T. Taniike, *Top. Catal.*, 57 (2014) 911-917

[22] J.H. de Boer, B.G. Linsen, T. J. Osinga, *J. Catal*. 4 (1965) 643-648

[23] W.B. Innes, *Anal. Chem.* 29 (1957) 1069-1073

Chapter 4

Pore Architecture Engineering of Magnesium Alkoxide based Olefin Polymerization Catalysts

4.1 Introduction

Catalyst is a substance which can improve the reaction rate and selectivity by making new route of chemical conversion with activation energy reduction. Catalysis is used for almost chemical processes in current industrial systems, because of using catalyst for chemical reaction makes the processes efficiency such as reduction of energies for progress reaction, reaction time, reaction space and so on. Then, catalyst is one of most important substance for chemical industry, and further its performance improvements are demanded. For example, new demands such as increase production efficiency, saving cost, making lower impact on environment and so on. Therefore, catalyst researches and developments keep to be conducted aggressively.

Catalyst is classified two type of process as homogeneous catalyst and heterogeneous catalyst by existence of phase boundary between catalyst and substrate. In the case of large scale productions, heterogeneous catalyst systems are preferred because of its performance features such as multifunction, operation easiness, lifetime, and so on. Thus, various kinds of heterogeneous catalysts have been developed and investigated for improvement of performance until now [1]. From those efforts, it is well known that heterogeneous catalyst performances were determined by not only active species but also hierarchical structure [2,3]. For example, the chemical reaction efficiency and easiness

strongly depend on catalyst particle size, shape and inner structure. Specific surface area, reaction selectivity change, and crystalline structures are well known as typical structure which are able to add new functions such as increase activity, pore molecular shape selectivity [4-6]. Thus, particle architecture design from micro scale to macro is indispensable for optimization of heterogenenous catalyst performances.

Various synthesis methods were developed and used for attainment of desired catalyst morphology designs accurately. Especially, establishment of pore architecture control methods were importance for not only catalyst field but also censor [7,8], storage [9], separation [10,11] and so on. Thus, researches and developments are conducted briskly still now, and various new porous material and its synthesis methods were reported. For example, regular porous materials like a zeolite which synthesized by crystallization with structure directing agent and possesses regular micro-mesopore [12,13], metal-organic frameworks which were regular porous materials composed of an organic ligand having affinity for a metal ion and an unsaturated organic molecule [14,15] and can be coordinated at least bidentately with the metal ion and aerogel which irregular porous material synthesized by supercritical drying of solvent from gel [16] were well known as valuable porous materials. The porous materials of various substances become possible to be synthesized at present by developed synthesis methods and were used in wide field.

The heterogeneous Ziegler-Natta catalyst for olefin polymerization is a representative example of such those catalysts. It is used for polyolefin materials production in industry. Especially, 99% amount of polypropylene was produced using this catalyst. This catalyst systems get olefin polymerization performance by contacting with solid ingredients and activators. Where solid ingredients are $TiCl_4$ and lewis base compound (active spices) supported $MgCl_2$ (support), and activator are alkylaluminium and lewis base compound. This olefin polymerization performances were determined from not only chemical composition, but also hierarchical structure of solid ingredient such as particle shape, density, pore architectures, active site dispersion and so on [17]. Especially, it is well known that pore architectures affect important performances such as activity behavior, lifetime, comonomer insertion efficiency and produced polymer density [18-21]. Therefore, there are a huge variety of preparation routes empirically established in order to synthesis catalyst architectures accurately for high performance catalysts preparation. The most of industrial Ziegler-Natta catalyst is synthesized by precipitation method using alcohol [22] and chemical reaction method using $Mg(OEt)_2$ [23]at the present . Especially, latter catalyst possesses higher activity, comonomer insertion abilities and polymer morphology control ability than catalyst synthesized by other method. Furthermore, particle shape control ability is better than other type catalyst because the feature that

precursor morphologies roughly keeps up after conversion from $Mg(OEt)_2$ to $MgCl_2$ [24]. While, there are no techniques that can accurate control of $Mg(OEt)_2$ based Ziegler-Natta catalyst systematically, nevertheless its importance for industrial manufacturing. Because number of report of catalyst analysis, particle growth mechanism and control particle morphologies is less. Therefore, It becomes be demanded that elucidation of catalyst architectures and establishment of systematically morphology control method at the present.

From those backgrounds, the aim of the present study is to obtain knowledge of pore structure engineering for establishment of systematically improvement for $Mg(OEt)_2$ based Ziegler-Natta catalysts. For this purpose, Magnesium ethoxide which contains different alkoxide was synthesized. Then, these were investigated their structural characteristics and influences on pore structure of catalysts. From those results, particle morphology conversion mechanism and structure relationship between precursors and catalysts were tried to elucidate.

4.2 Experiment

4.2.1. Materials

Anhydrous $MgCl_2$, triethylaluminium (TEA), and nonporous Mg particles were donated from Toho Titanium Co., Ltd., Tosoh Finechem Corporation and Yuki Gousei Kogyo Co., Ltd., respectively.

Ethanol (purity > 99.5%), methanol, *i*-propanol (purity > 99.5%), *n*-propanol were dried over 3A molecular sieve with N_2 bubbling. Heptane (purity > 99.5%), toluene (purity > 99.5%) and di-*n*-butylphthalate (DBP) (purity > 98%) were dried over 4A molecular sieve with N_2 bubbling. Cyclohexylmethyldimethoxysilane (CMDMS) was purified by distillation under reduced pressure. Iodine (purity > 99%) and titaniumtetrachloride ($TiCl_4$) (purity > 99%) were used as received.

4.2.2. Magnesium alkoxide synthesis

$Mg(OR)_2$ was synthesized based on our recent technique [25] with adding a small amount of alcohols. 0.67 g of I_2 (as an initiator) and 32 ml of dehydrated alcohol were introduced into a 500 mL jacket-type separable flask equipped with a mechanical stirrer rotating at 180 rpm under N_2 atmosphere. After the dissolution of I_2 at 75°C, 2.5 g of Magnesium and 32 mL of alcohol were introduced repeatedly 5 times every 10 min.

Subsequently, aging at 75°C were conducted for 2 h. Finally, the temperature was decreased to 40°C, and the product was washed with alcohol. The reaction slurry was evaporated to dryness on a rotary evaporator, and white powder was obtained. In this study, $Mg(OR)_2$ particles were synthesized with different ethanol/alcohol ratios or spices under the same conditions.

4.2.3 Catalyst preparation

The preparation of Ziegler-Natta catalysts from $Mg(OR)_2$ was conducted again based on a patent [23] with several modifications. 15 g of $Mg(OR)_2$ and 150 mL of toluene were charged in a 500 mL 3-neck flask equipped with a mechanical stirrer rotating at 180 rpm under N_2 atmosphere. 30 mL of $TiCl_4$ was added slowly by dropping, while the temperature of the suspension was kept within 0-5°C. Thereafter, the temperature was first elevated to 90°C to add 4.5 mL of DBP and then it was brought to 110°C. The reaction suspension was continuously stirred at 110°C for 2 h. Subsequently, the reaction product was washed with toluene twice at 90°C and further treated with 30 mL $TiCl_4$ at 90°C for 2 h. After that, the product was washed with *n*-heptane 7 times to get the final catalyst. All Ziegler-Natta catalysts were obtained from each $Mg(OR)_2$ under the same conditions.

4.2.4 Polymerization

Ethylene homopolymerization and Propylene homopolymerization were conducted with slurry phase as catalytic performance test. Polymerization was performed in a 1 L autoclave equipped with a mechanical stirrer rotating at 350 rpm. 500 mL of *n*-heptane was introduced into the reactor. TEA ([Al] = 10 mmol/L), CMDMS (Al/ExD = 10) were introduced into the reactor, and the solution was saturated with 0.5 MPa of ethylene or propylene at 50°C. 30 mg of a catalyst was fed into the reactor by a bomb injection technique to initiate the polymerization. The polymerization was conducted for 60 min with a continuous supply of monomer gas at 0.5 MPa. The polymer was filtered by pouring the reaction slurry into funnel. The obtained polymers were dried in vacuum oven for 6 h prior to use characterization.

4.2.5. Characterization

4.2.5.1 NMR

The *i*-propanol incorporation amount, *i.e.* ratios between ethanol and *i*-propanol, in $Mg(OR)_2$ were measured by ^{13}C NMR (Bruker 400 MHz) operating at 100 MHz with proton decoupling at room temperature using 2-methoxyalcohol as a solvent and benzene-d_6 as an internal lock and reference.

2.4.5.2 Bulk density measurement

Bulk density of $Mg(OR)_2$ sample was determined by the following procedure. Sample powder was introduced to 100 ml measuring cylinder via funnel with same injection speed as same as possible, in order not to make filling rate difference. After measurement, bulk density was calculated from their mass and volume.

2.4.5.3 SEM

Particle morphological characteristics of $Mg(OR)_2$ and catalyst particles were studied with scanning electron microscopy (SEM, Hitachi S-4100) operated at an accelerating voltage of 20 kV. For the preparation of particle cross-sections, particles were cut by razor under N_2 atmosphere. Before the measurements, particles were subjected to Pt sputtering for 100 s.

2.4.5.4 XRD

The particle crystalline characteristics were measured by XRD (smart lab., RIGAKU) operated at stepwise scanning method using $CuK\alpha_1$ radiation (λ = 1.54059 Å), The optics used were a fixed divergence slit (2/3°), a fixed incident scatter slit (2/3°), a fixed receiving slit (0.3 mm). The X-ray tube worked at 40 kV and 30 mA. The spectrum data

were collected from 5° to 40° (2θ). All operations were performed under N_2, and samples were covered by mylar film for not to contact with air.

4.2.5.4 N_2 adsorption/desorption measurement

N_2 adsorption and desorption isotherms at 77 K were acquired on a BELSORP-max instrument (BEL JAPAN, INC.). *Ca*. 50-100 mg of catalyst powder in a pyrex tube with a rubber cap was outgassed at 80°C over 3 h in vacuo, prior to the measurement. Since the BET analysis is not appropriate for typical Ziegler-Natta catalysts with an abundance of micropores (pore diameter (D) < 2 nm) , the specific surface area was not determined [26]. Instead, the micropore volume (V_{micro}) was approximated with

$$V_{micro} = V_{0.4} \times \frac{V_{liquid}}{V_{gas}} - \int_2^{50} \frac{2}{D} \cdot \frac{V_{meso}(D)}{dD} dD \qquad (1),$$

where $V_{0.4}$, V_{liquid}, V_{gas}, and V_{meso}(D) are the N_2 adsorption volume at p/p_0 = 0.4, the volumes of a N_2 molecule in gaseous and liquid states, and the mesopore volume at the diameter of *D* nm determined by the method described in the next paragraph. V_{micro} was estimated by subtracting the contribution of multilayer N_2 adsorption onto mesopore surfaces from the adsorption volume at p/p_0 = 0.4 (converted to the liquid N_2 volume). Note that the thickness of the multilayer adsorption at p/p_0 = 0.4 was approximated as 2 nm, and the contribution from the multilayer adsorption onto macropore and external

surfaces was regarded as negligible. The latter is true for typical industrial Ziegler-Natta catalysts, whose pore dimensions are mainly micro and/or meso scale(s) [25].

The mesopore size distributions (2.1 nm < D < 50 nm) were analyzed by the BJH method or by the INNES method. Even though the two methods are based on the same Kelvin equation for the N_2 condensation, cylinder-type and slit-type mesopores are assumed in the BJH [27] and INNES [28] methods, respectively. Hence, the BJH method is suitable for the hysteresis types H1 and H2 respectively for uniform-size and irregular-size cylindrical-type mesopores, while the INNES method for the types H3 and H4 respectively for uniform-size and irregular-size slit-type mesopores.

4.2.5.6 Hg mercury porosimetry

The meso and macro pore size distributions (7 nm < D < 1000 nm) were measured by the mercury intrusion technique (Pascal 440 Porosimeter, Thermo Scientific). The pore size was evaluated from the intrusion pressure according to the Washburn-Laplace equation. The surface tension (γ) and contact angle (θ) were respectively set to 0.480 N / m and 141.3°.

4.3 Results and discussion

4.3.1 Screening of second alcohol for pore architecture control

Seven kinds of $Mg(OR)_2$ particles were synthesized from different alcohol mixture which consisted of ethanol and small amount of second alcohols with same reaction procedure. Following lower alcohols were used as second alcohol (methanol, *n*-propanol *i*-propanol, *n*-butanol, *i*-butanol, *s*-butanol and *t*-butanol). Their representative SEM images are shown in Figure 4-1 with pure $Mg(OEt)_2$ as standard sample.

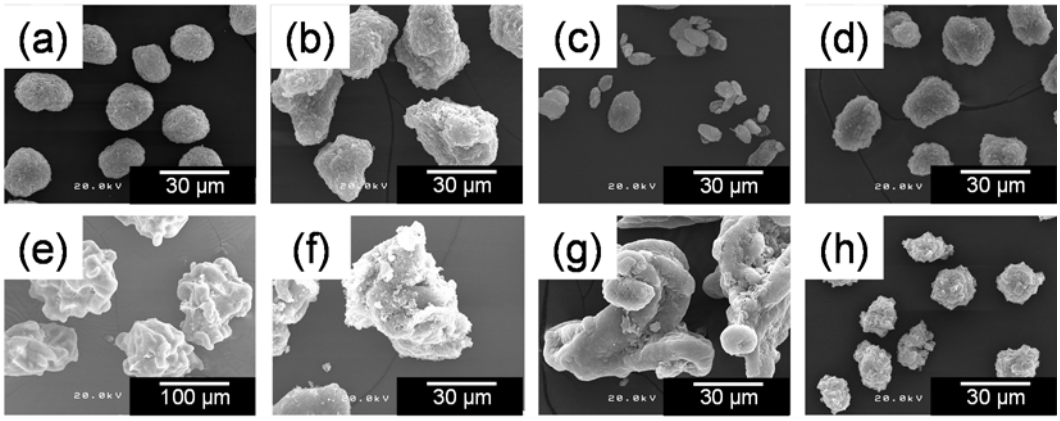

Figure 4-1. SEM images of $Mg(OR)_2$ particles made from various alcohol mixture; (a) ethanol only, (b) ethanol : methanol = 95 : 5 (mol), (c) ethanol : *n*-propanol = 95 : 5 (mol), (d) ethanol : *i*-propanol = 95 : 5 (mol), (e) ethanol : *n*-butanol = 95 : 5 (mol), (f) ethanol : *i*-butanol = 90 : 10 (mol), (g) ethanol : *s*-butanol = 90 : 10 (mol), (h) ethanol : *t*-butanol = 90 : 10 (mol)

All $Mg(OR)_2$ samples were synthesized and became white powder after drying. However, only $Mg(OR)_2$ particles which synthesized by methanol, *i*-propanol, and *t*-butanol more or less possessed spherical shape. The others particles were strongly

irregular or agglomerated. It suggested that additional second alcohols made $Mg(OEt)_2$ particle morphologies distortion even if concentration of second alcohols were low. The cause of morphology difference was considered that change the balance agglomeration and exfoliation of primary particles. It is well known that morphology of $Mg(OEt)_2$ depends various reaction condition.[25] Existences of second alcohol change the reaction condition which were reaction rate, increase boil point, soluble amount of $Mg(OR)_2$ and so on. Therefore, big morphology difference might be confirmed by small amount of mix alcohol.

All $Mg(OR)_2$ were converted to catalyst under same procedure. Obtained catalyst samples were observed by SEM and those images are shown in Figure 4-2.

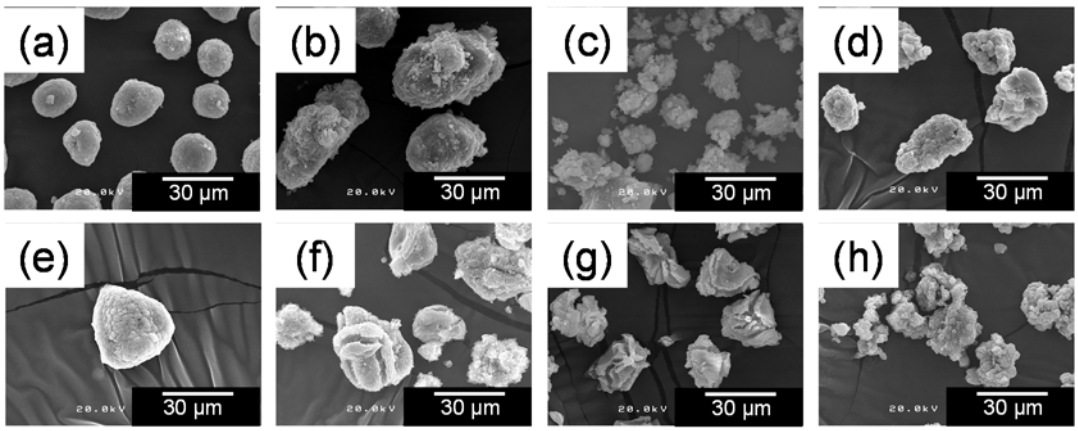

Figure 4-2. SEM images of catalyst particles made from various $Mg(OR)_2$; (a) ethanol only, (b) ethanol : methanol = 95 : 5 (mol), (c) ethanol : *n*-propanol = 95 : 5 (mol), (d) ethanol : *i*-propanol = 95 : 5 (mol), (e) ethanol : *n*-butanol = 95 : 5 (mol), (f) ethanol : *i*-butanol = 90 : 10 (mol), (g) ethanol : *s*-butanol = 90 : 10 (mol), (h) ethanol : *t*-butanol = 90 : 10 (mol)

As can been seen from Figure 4-2, almost particles morphologies were irregular shape without methanol and *i*-propanol contained samples. The reasons of those uncontrolled particle morphologies were considered that low particle strength against chlorination and/or originally bad morphologies. Those results suggested that second alcohol has large effect on catalyst macro morphologies even if concentration is low

Pore architectures of all catalyst samples were characterized by N_2 adsorption/desorption measurement in order to confirm second alcohol effects on catalyst inner structure. These results are shown in Figure 4-3.

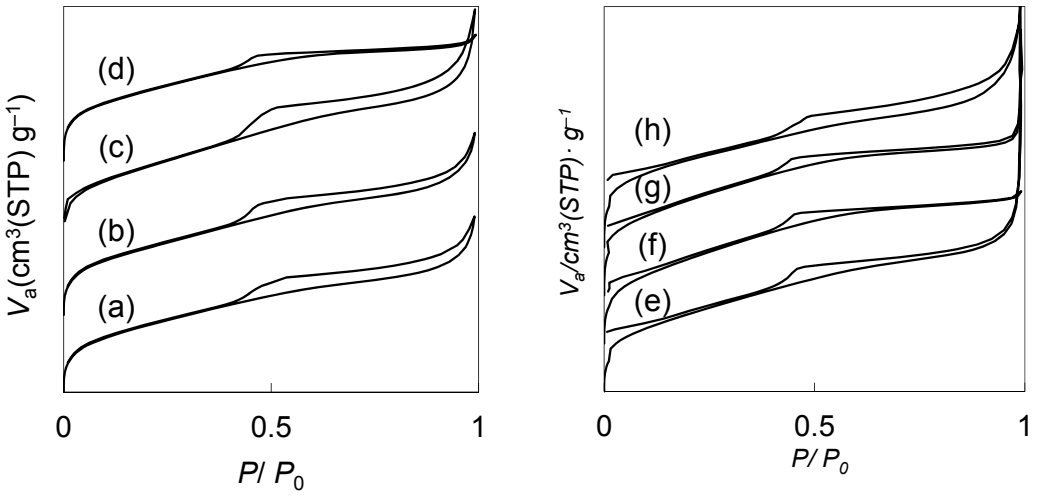

Figure 4-3. Nitrogen adsorption/desorption isotherms for catalyst made from various $Mg(OR)_2$; (a) ethanol only, (b) ethanol : methanol = 95 : 5 (mol), (c) ethanol : *n*-propanol = 95 : 5 (mol), (d) ethanol : *i*-propanol = 95 : 5 (mol), (e) ethanol : *n*-butanol = 95 : 5 (mol), (f) ethanol : *i*-butanol = 90 : 10 (mol), (g) ethanol : *s*-butanol = 90 : 10 (mol), (h) ethanol : *t*-butanol = 90 : 10 (mol),

Generally, $Mg(OEt)_2$ based Ziegler-Natta catalyst shows isotherm of type II and hysteresis loop of H3 like Figure 4-3 (a). This isotherm shape possesses the pore architecture information that existence of slit-shape mesopore with non-uniform size and macropore [29]. However, there are no techniques for change pore architectures in $Mg(OEt)_2$ based catalysts. As can be seen Figure 4-3, 4 samples possessed different shaped isotherm surprisingly. These isotherm belongs to type IV isotherm for mesoporous materials (without unrestricted sorption at relative high pressure) and H2 hysteresis loop for cylindrical pore with non-uniform shape and size. Those results suggested that the species of $Mg(OR)_2$ which consisted small amount of second alcohol changed pore shape.

Additionally, pore size distributions were calculated from obtained isotherms. The INNES method was employed to calculate mesopore size distributions of the catalysts having the H3 hysteresis, *i.e.* $Mg(OEt)_2$ based catalyst which possesses slit shaped pore, while BJH method was employed for the catalyst having the H2 hysteresis, *i.e. i*-propanol contained $Mg(OR)_2$ based catalyst which had cylindrical pore.

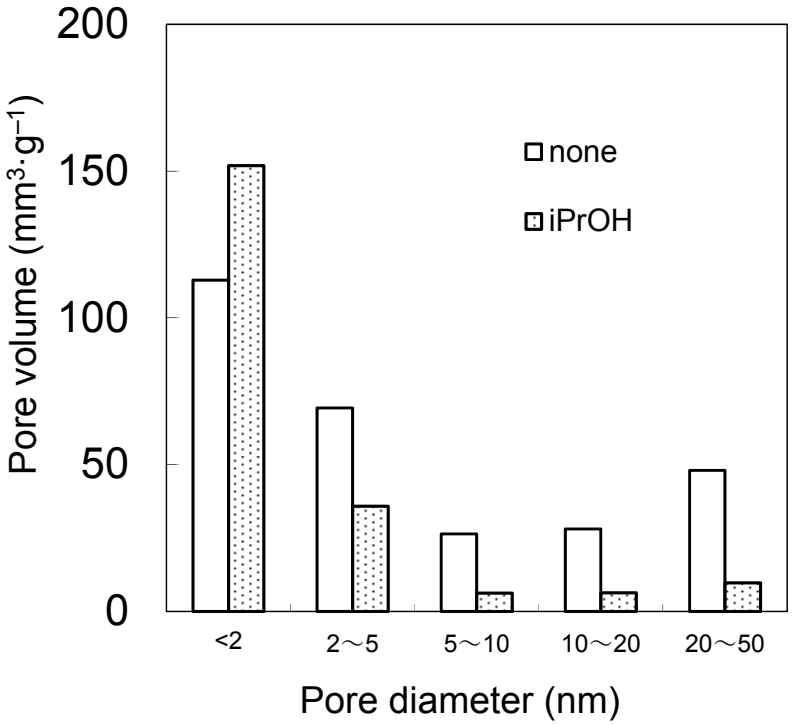

Figure 4-4. Pore volume distributions of catalyst;
(a) only ethanol, (b) i-propanol contained

$Mg(OEt)_2$ ethoxide based catalyst possessed broad pore size distribution from micro- to meso-pores with a bimodal character centered at micropore (D<2 nm) and at meso pore over 20 nm. While, catalyst made from *i*-propanol added $Mg(OR)_2$ possessed unimodal pore size distribution centered at micropore.

As mentions above, It is succeeded that change of pore architectures such as distribution and shape which has been too difficult to change. However, the uncontrolled shape catalyst can not be used from the viewpoint of industrial operation in order to manage process efficiency. Therefore, the catalyst systems which made from *i*-propanol

contained $Mg(OR)_2$ were investigated in detail because samples which possesses controllability of catalyst shape is only this catalyst.

4.3.2 i-Propanol incorporation effect on particle structure

4.3.2.1 $Mg(OR)_2$ including i-propanol

Table 4-1. The characterization results for synthesized $Mg(OR)_2$ including i-propanol

Sample	*i*-Propanol composition(mol%)		Bulk density ($g \cdot ml^{-1}$)
	Solution	Particle	
MGE7	0	0.0	0.300
MGR1%	1	1.1	0.309
MGR3%	3	2.2	0.323
MGR5%	5	5.9	0.425
MGR7%	7	7.5	0.434
MGR9%	9	9.5	0.437

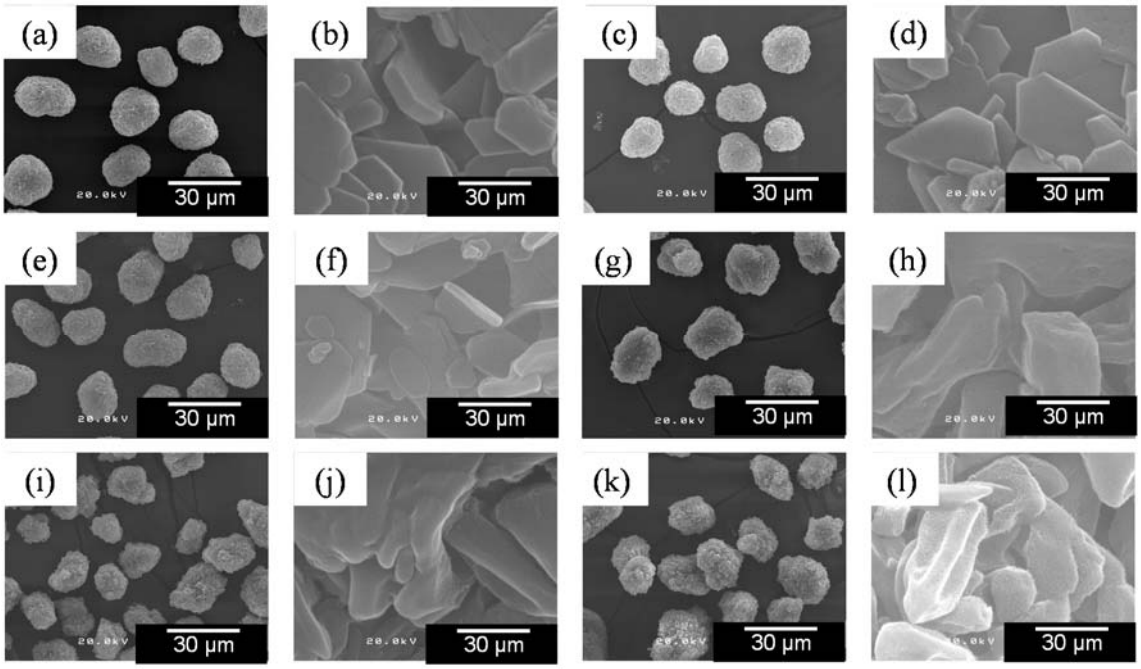

Figure 4-4. SEM images of Magnesium ethoxide including i-propanol. (a,b) MGE0% (x1000, x50000), (c,d) MGE-1% (x1000, x50000), (e,f) MGE-3%(x1000, x50000), (g,h) MGE-5% (x1000, x50000), (i,j) MGE-7%(x1000, x50000), (k,l) MGE-9% (x1000, x50000)

Figure 4-4 shows SEM images of $Mg(OR)_2$ particles which were synthesized by various ratio of ethanol and *i*-propanol. $Mg(OR)_2$ particles containing below 3 mol% of *i*-propoxide possessed more or less spherical shapes. Magnified images revealed that the particles composed by aggregation of thin plate-like building blocks, whose dimension of the building blocks varied in the range of 100-700 nm, and whose thickness was about 10 nm. These architectures were the same as pure $Mg(OEt)_2$ particles in our previous report. [25]. On the other hand, the addition of *i*-propanol up to over 5 mol% hardy affected the particle architectures. These particle shapes were less spherical than pure

$Mg(OEt)_2$, though particle diameters and particle size distributions mostly same as other. The particles consisted of agglomeration of building blocks too, however, whose shapes were different with plate-like. The building blocks had distorted lod-like shapes whose dimension varied in the range of 100-500 nm, and whose thickness were about 100 nm. Because of its thickness, the surface of particles were rougher than pure $Mg(OEt)_2$. The drastically change of shape was synchronized with change of bulk density. Thus, the particle architectures were drastically changed by the addition of *i*-propanol over the critical amount.

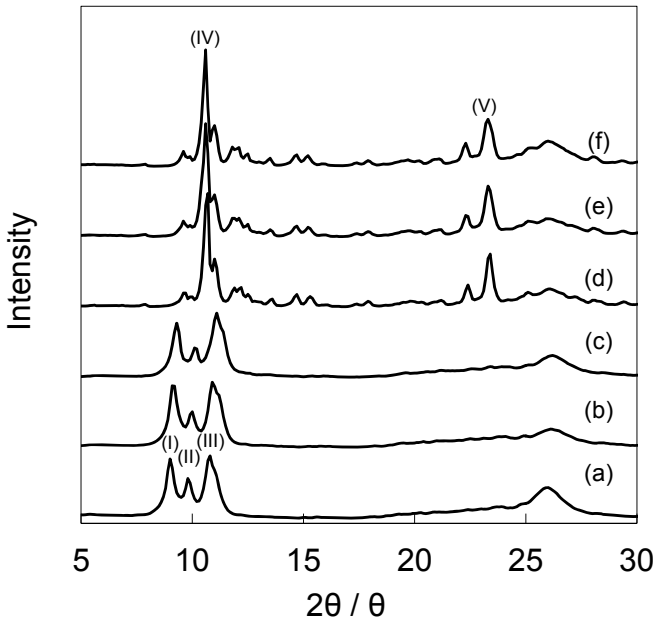

Figure 4-5. XRD patterns for magnesium ethoxide samples; (a) MGE7, (b) MGR1%, (c)MGE3%, (d)MGR5%, (e)MGR7%, (f)MGR9%

Building block shapes were hardly changed by changing the synthetic conditions when pure ethanol reacted with magnesium, in contract, the addition of *i*-propanol drastically changed it. It was possible that formation of building blocks shapes was attributed to change of crystalline growth process. Therefore, crystalline structures were measured by XRD, in order to clarify the cause of the morphological changes. These results are shown in Figure 2. The XRD spectra of MGR-0% possessed almost same characteristics as MGE1% and MGE3%, which were exhibited three peaks at 9.0˚, 9.8˚, 10.7˚ . In contrast, $Mg(OR)_2$ particles containing over 5 mol% of *i*-propoxide (MGE5%, MGE7% and MGE9%) had almost same spectral characteristics whose high intensity peaks located at 10.6˚ and 23.3˚ and which were existences of a number of low intensity peaks in the ranges of 5-30˚. Thus, crystalline structure of $Mg(OR)_2$ samples had two types, according to composition of alcohol ratios. It is a considered that the cause of crystalline structure changes were because incorporation of *i*-propanol. However, the reasons were not determined because of complex architectures prevented accurate characterization. In addition, the change of crystal structure was synchronized with the change of building block shape. This result leads us to presume that change of the building blocks shape is attribute to change of crystalline structure.

Representative spectrum peaks were accurately analyzed, whose peak tops and full width at half maximum (FWHM) were shown in Table 4-2 and Table 4-3 in order to obtain the additional information on the crystalline structure. In the cases of MGR0%, the spectral peak position shifted toward higher angles and FWHM had no changes with increasing incorporation of *i*-propanol, as can be seen in Table 4-2. It means that the addition of *i*-propanol distorts $Mg(OEt)_2$ crystal structure a little before the drastic change with a critical amount of *i*-propanol. On the other hands, Table 4-3 shows changing spectrum characteristics of $Mg(OR)_2$ particles containing over 5 mol% of *i*-propoxide, whose peak positions were same and FWHM became broader as increase incorporation of *i*-propanol. It suggested that growth of crystal diameter became slow by incorporation of *i*-propanol without any crystal structure changing after the drastic crystal change. In comparison with magnified SEM images which can observe shape of building blocks, correlation between crystal size and building block shapes were not founded. It is suggested that fundamental crystalline structure affects building block shape, however crystal size has too small effect to change building block shapes.

Table 4-2. The summary of XRD peak positions and FWHM for MGE7, MGR1%, MGR3%

Sample	Peak (I)		Peak (II)		Peak (III)	
	Position (deg)	FWHM (deg)	Position (deg)	FWHM (deg)	Position (deg)	FWHM (deg)
MGE7	8.96	0.40	9.80	0.41	10.73	0.65
MGR1%	9.09	0.44	9.95	0.42	10.90	0.67
MGR3%	9.36	0.34	10.12	0.38	11.09	0.45

Table 4-3. The summary of XRD peak positions and FWHM for MGR5%, MGR7%, MGR9%

Sample	Peak (IV)		Peak (V)	
	Position (deg)	FWHM (deg)	Position (deg)	FWHM (deg)
MGR5%	10.67	0.27	23.38	0.34
MGR7%	10.66	0.28	23.28	0.40
MGR9%	10.58	0.34	23.29	0.45

From above results, one interpretation of *i*-propanol effects on $Mg(OEt)_2$ crystal changing behaviors is proposed. It is considered that the change of crystal structure depends on stableness of the crystal. $Mg(OEt)_2$ crystal can take in *i*-propanol with a little distortion of original crystal structure until over capacity which is energetically stable. While, in the case of filling over the capacity, $Mg(OEt)_2$ greatly change its crystal structure, because structural change make it more stable. In addition, these crystal structure changes effect on the shape of building blocks. Therefore, the addition over the critical amount of *i*-propanol changes particle architectures drastically from

micro to macro scales.

4.3.2.2. Catalyst made from $Mg(OR)_2$ including i-propanol

All $Mg(OR)_2$ samples were converted into catalysts under the same conditions, to bear the corresponding catalysts respectively termed as Cat7, Cat1%, Cat3%, Cat5%, Cat7% and Cat9%. Their SEM images are shown in Figure 4-6. As can be seen in Figure 4-6, the catalyst shape more or less replicated the shape of the original $Mg(OEt)_2$ particles. The catalyzation greatly smoothened the building block in a way to reduce the differences in the shape of building blocks among the different samples.

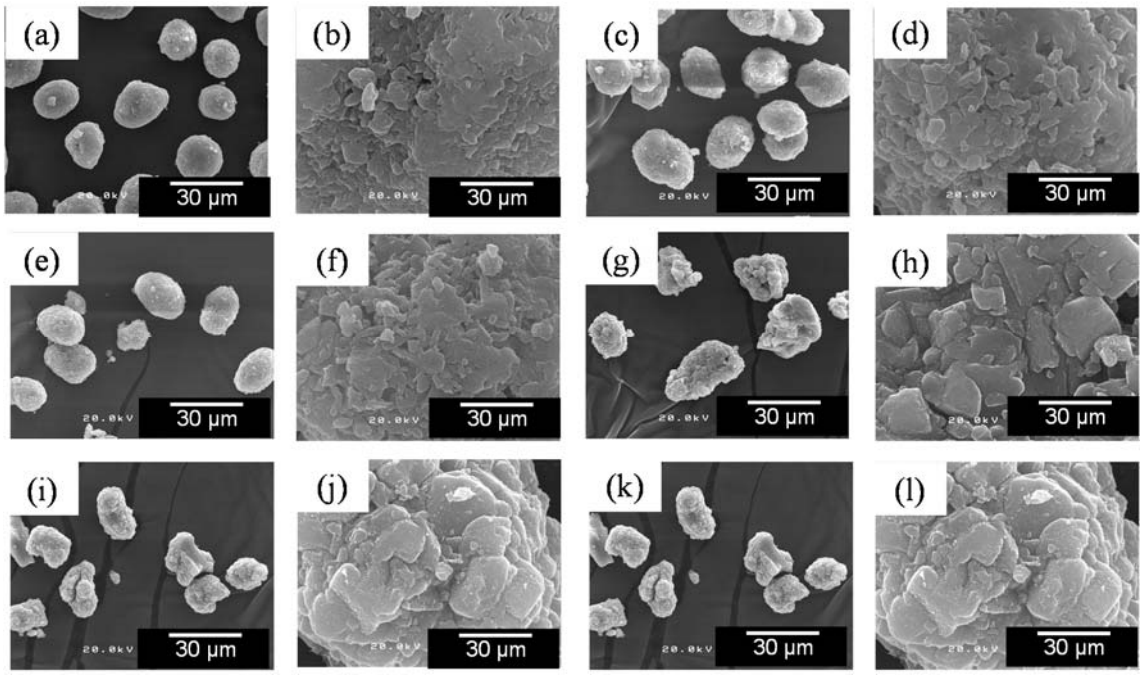

Figure 4-6. SEM images of catalyst samples; (a,b) Cat7 (x1000, x10000), (c,d) Cat1% (x1000, x10000), (e,f) Cat3% (x1000, x10000), (g,h) Cat5% (x1000, x10000), (i,j) Cat7% (x1000, x10000), (k,l) Cat9% (x1000, x10000)

The catalyst pore structures were studied based on N_2 adsorption measurement and Hg porosimetry. Hg intrusion curves had little differences among these samples, however N_2 isotherms and hysteresis showed obvious difference. Representative N_2 adsorption / desporption measurement isotherms for Catalysts are shown in Figure 4-7. The adsorption isotherms for Cat0%, Cat1% and Cat3% belong to the type II of IUPAC classification for macroporous materials and the hysteresis loops to the type H3 for slit-shaped mesopore with non-uniform sizes and shapes. Meanwhile, the addition of over 5 mol% of *i*-propanol totally altered the types of adsorption isotherms and hysteresis loops respectively to the

type IV for mesoporous materials and to the type H2 for cylindrical mesopores with non-uniform sizes and shapes.

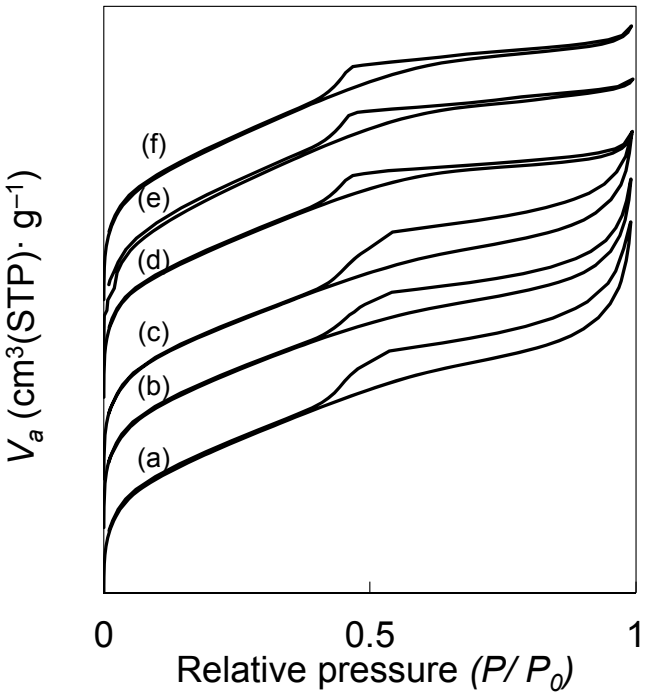

Figure 4-7. N_2 isotherm for catalyst samples;
(a) Cat7, (b) Cat1%, (c) Cat3%, (d) Cat5%, (e) Cat7%, (d) Cat9%

Pore size distribution were calculated from the obtained N_2 isotherms and Hg intrusion curves. The results are summarized in Figure 4-7. The micropore volume was calculated from equation (1). The INNES method was employed to calculate the mesopore size distribution of catalysts having the H3 hysteresis, *i.e.* slit-shaped mesopore such as Cat0%, Cat1% and Ca3%. While the BJH method was employed for the catalysts having the H2 hysteresis, *i.e.* cylindrical pore such as Cat5%, Cat7% and Cat9%. The macropore volume

was calculated by Washburn-Laplace equation from the Hg intrusion curve. It can be seen in Figure 4-8, these catalysts showed two types of pore size distribution. Cat0%, Cat1% and Cat3% possessed a wide range porosity from micro to macro with bimodal character centered at micropore (D < 2 nm) and at macropore from 50 to 100 nm. In contrast, Cat5%, Cat7% and Cat9% possessed a narrow range porosity with monomodal character centered at micropore. Micropores occupied the largest volume and the pore volume greatly decreases as the pore size increases. The mesopore and macropore volumes of its catalysts were low. In compared with two types of pore size distributions, big difference of these two type is existence of mesopore and macropore.

Thus, these result imply that catalysts made from $Mg(OR)_2$ whose crystal structure was changed by incorporation of *i*-propanol changed not only shapes of mesopore but also pore size distributions from micropore to macropore.

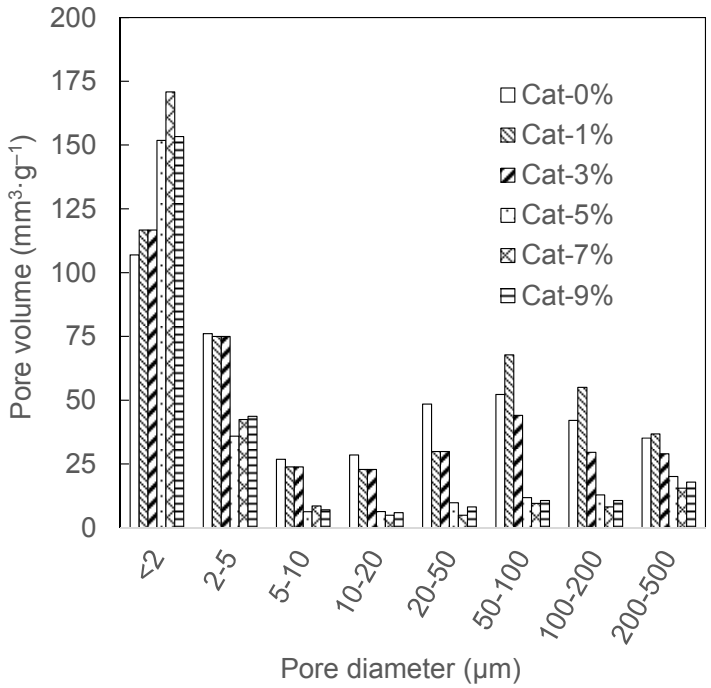

Figure 4-8. N_2 isotherm for catalyst samples;
(a) Cat7, (b) Cat1%, (c) Cat3%, (d) Cat5%, (e) Cat7%, (d) Cat9%

From the above, it seems that crystalline structure of $Mg(OEt)_2$ has strong effects on pore structure of catalyst. In particular, the change of pore structure in the range of meso to macro scales were greater than micro scales. However, it is considered that crystal structure has indirectly effects on pore structure of catalyst particles, because size difference between crystalline structure and macropore structure is too big to compare. Therefore, it was seemed that the cause of micropore change and of meso-macropore change were different. The mechanism of influences to catalyst pore structure frrom $Mg(OR)_2$ architectures were proposed with separating structural scales.

The generation mechanisms of micropore in catalysts were considered at first. To begin with, the synthesis conditions of $Mg(OEt)_2$ had little effect for micropore of catalyst. Originally, micropore exists little in $Mg(OEt)_2$ structure, it is generated by conversion to catalyst. It is considered that micropore comprised void which was generated by chlorination of $Mg(OR)_2$. Chlorination progress ligand exchange between ethoxy group and chrolide made some voids because of difference of ligand size and crystalline structure distortion between $Mg(OR)_2$ and catalyst. From the results, the changes of $Mg(OR)_2$ crystal structure had effects to structural difference of catalyst micropore. On the other hand, composition of *i*-propanol had little effects, nevertheless the sizes of ethanol and *i*-propanol were different. It is considered that distortion of crystalline structure has big effect, however chemical effects of *i*-propanol were not important cause of changing micropore structures.

The meso-macropore in the catalysts depended on $Mg(OEt)_2$ architectures because of the phenomenon that $Mg(OEt)_2$ kept its architectures after conversion to catalyst. Therefore, agglomerations degree of building block strongly effects on pore structure. The shape of building block strongly affects void of inner particles and bulk density. When $Mg(OEt)_2$ converts to catalyst, agglomerated particle shape and building block

shape mostly keep those shapes, though building blocks slightly melt and adhere each other. Therefore, agglomeration degree of building blocks may affect the catalyst pore volume. In fact, Cat5% which has a small amount of meso-macropore was prepared by MGE5% whose bulk density value was high. It is difficult to reveal the progress of pore generation, because reaction is too fast to detect the structure change. However, It is revealed that inner structure of $Mg(OR)_2$ is most important factors to control catalyst meso-macropore.

4.3.3 Polymerization test

The polymerization performance tests for prepared catalysts were conducted. Propylene and ethylene homopolymerization and their copolymerization with 1-hexene were conducted as performance test. All catalysts were object samples however catalyst prepared from $Mg(OR)_2$ including butanol spies because of their terrible particle morphologies. The polymerization results and obtained polymer characteristics were shown in Table 4-8. Moreover, activity profile was recorded by consumption amount of monomer during polymerization and represent data was shown in Figure 4-9.

Table 4-8. Result of polymerization

Sample	Activity (g/g-cat·atm·h)				Bu branch (mol%)		*mmmm* (mol%)
	C_3 homo	C_3 co	C_2 homo	C_2 co	C_3 co	C_2 co	C_3 homo
Cat7	183	394	83	843	5.3	6.0	95.3
Cat-methanol	89	115	37	189	4.2	4.8	95.0
Cat-*n*-propanol	154	193	233	423	3.9	3.4	95.5
Cat1%	175	315	138	868	5.0	4.7	95.2
Cat3%	238	357	148	684	4.5	7.3	95.2
Cat5%	253	354	93	903	5.0	4.3	95.1
Cat7%	193	353	70	918	4.6	4.4	96.0
Cat9%	225	435	83	1084	4.9	5.3	94.6

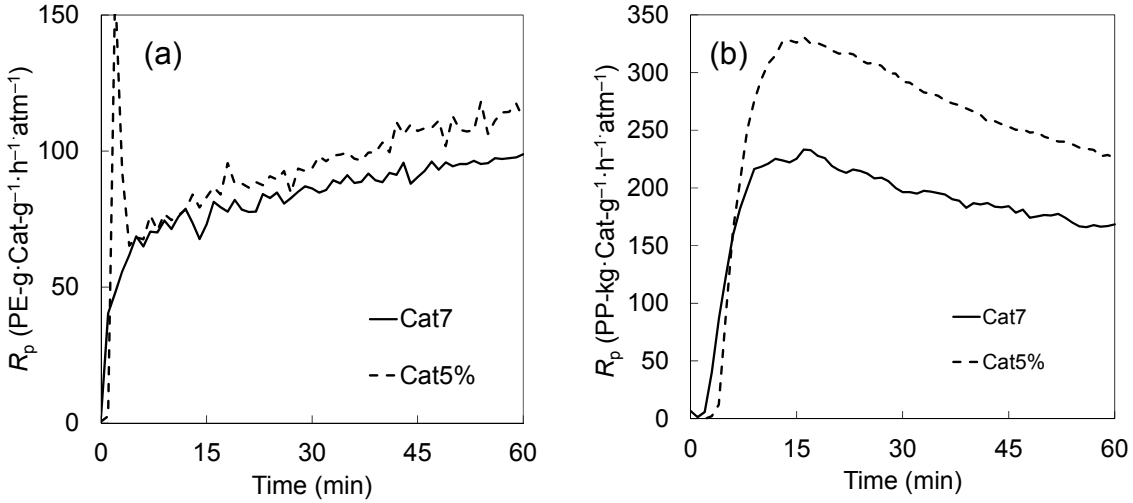

Figure 4-9. Activity profile of homopolymerization; (a) ethylene polymerization, (b) propylene polymerization

In Figure 4-9, propylene polymerization activity profile belonged to decay type and ethylene polymerization activity profile belonged to build-up type, even if using catalyst were changed. In Table 4-8, propylene polymerization activity was synchronized with *i*-propanol composition of converted $Mg(OR)_2$. Ethylene polymerization activity was increased with increased composition

of used $Mg(OR)_2$ until over 5 mol% and decreased rapidly after structural change. Moreover, the morphology of obtained polymers were irregular (not replicated catalyst morphology) when catalyst prepared *i*-propanol contained $Mg(OR)_2$ was used. Those results suggests possibility that catalyst structure changes not only pore architectures but also stiffness of particles by using prepared catalyst from *i*-propanol containing $Mg(OR)_2$. The cause of activity enhancement effect may be derived from increase rate of generate new active site by fragmentation. Fragmentation rate might become higher by lower stiffness of particle. On the contrast, it is considered that diffusion limitation make activity low. The diffusion limitation derived from small pore might possess greater effect to activity than increase of fragmentation rate derived from low particle stiffness in the strong diffusion limitation situations.

4.4 Conclusion

In this study, several $Mg(OR)_2$ particles with various chemical composition were synthesized as precursor using small amount of second alcohols in order to synthesis novel pore architectures in Ziegler-Natta catalyst. First of all, six kinds $Mg(OR)_2$ were synthesized with different *i*-propanol/ethanol ratio range from 0-9 mol%. It is conformed that synthesized particles possessed more or less spherical shape under any alcohol ratio. On another front, the ratio of *i*-propanol up to 5 mol% hardly affected its building block shapes and crystalline structure. Catalyst preparation was conducted to convert catalyst from the $Mg(OR)_2$ which structure was changed. As a results, catalysts, whose pore size distribution was unimodally centered at the micropore with maintaining its particle shape, was prepared. It is considered that the cause of its change derived from the behavior of conversion from different particle inner architectures such as crystalline structure, building bloke shape, agglomeration degree and so on. The pore structure of traditional Ziegler-Natta catalyst prepared by chemical reaction method is not able to control systematically and range of structure is strongly limited. However, this study succeeded to prepare novel pore structure in Ziegler-Natta catalyst by conversion from *i*-propanol containing $Mg(OR)_2$. This knowledge will contribute development of new type Ziegler-Natta catalysts and elucidation of structure performance relationship.

Reference

[1] S. Senkan, *Angew. Chem. Int. Ed*., 40 (2001) 312-329

[2] H. S. Gandhi, G. W. Graham, and R. W. McCabe, *J. Catal.* 216 (2003) 433–442.

[3] R. M. Heck, R. J. Farrauto, *Appl. Catal. A: General* 221 (2001) 443–457

[4] N. van der Puil, F.M. Dautzenberg,H. van Bekkum, J.C. Jansen. *Microporous Mesoporous Mater*. 27, (1999) 95-106

[5] S. M. Csicsery, *Zeolites*, 4, (1984) 202-213

[6] M. Andersson, L. Österlund, S. Ljungström, A. Palmqvist, *J. Phys. Chem. B,106 (*2002) 10674-10679

[7] D. N. Dybtsev, H. Chun, S. H. Yoon, D. Kim, K. Kim, *J. Am. Chem. Soc.,* 126 (2004) 32-33

[8] G. Sakai, N. Matsunaga, K. Shimanoe, N. Yamazoe, *Sens. Actuators, B*, 80 (2001)125-131

[9] D. W. Wang, F. Li, M. Liu, G. Q. Lu, H. M. Cheng, *Angew. Chem. Int.* 47 (2008) 373-376

[10] M. E. Davis, *Nature*, 417 (2002) 813-821

[11] P. Gibson, H. S. Gibson, D. Rivin, *Colloids Surf., A*, 187–188 (2001) 469–481

[12] C. S. Cundy, P. A. Cox, *Chem. Rev*. 103, (2003) 663-701

[13] M. E. Davis, *Nature*, 417, (2002) 813-821

[14] H. Furukawa, N. Ko, Y. B. Go, N. Aratani, S. B. Choi, E. Choi, A. Ö. Yazaydin, R. Q. Snurr, M. O'Keeffe, J. Kim, O. M. Yaghi, *Science*, 329, (2010) 424-428

[15] H. Li, M. Eddaoudi, M. O'Keeffe, O. M. Yaghi, *Nature*, 402, (1999) 276-279

[16] V. Bock, A. Emmerling, R. Saliger, J. Fricke, *J. Porous Mater.,* 4 (1997) 287-294

[17] N. Pasquini Ed, "Polypropylene handbook"(ポリプロピレンハンドブック) Nikkankougyoushinbunsha (日刊工業新聞社) Japan (2012)

[18] A. Dashti, A. Ramazani SA., Y. Hiraoka, S. Y. Kim, T. Taniike and M. Terano, Polym. Int. 58 (2009) 40–45.

[19] M. Hassan Nejad, P. Ferrari, G. Pennini, G. Cecchin, *J. Appl. Polym. Sci*., *108* (2008) 3388-3402

[20] Y.S. Ko, S.I. Woo, J. *Polym. Sci. Part A: Polym. Chem*. 41 (2003) 2171–2179

[21] X. Zheng, M.S. Pimplapure, G. Weickert, *J. Loos. Macromol. Rapid Commun.* 27 (2006) 15–20.

[22] JP1981011908 (1981) Mitsui Petrochemical Industries,Ltd.

[23] JP Patent 1987158704 (1987) Toho Catalyst Co. Ltd.

[24] S. Tanase, K. Katayama, S. Inasawa, F. Okada, Y. Yamaguchi, T. Sadashima, T. Konakazawa, T. Junke, N. Ishihara, *Macromol. React. Eng.,* 2*,* (2008), 233-239

[25] T. Taniike, T. Funako, M. Terano, *J. Catal*., 311 (2014) 33-40

[26] T. Taniike, P. Chammingkwan, V. Q. Thang, T. Funako, M. Terano, *Appl. Catal. A* 437– 438 (2012) 24– 27.

[27] J.H. de Boer, B.G. Linsen, T. J. Osinga, *J. Catal*. 4 (1965) 643–648.

[28] W.B. Innes, *Anal. Chem.* 29 (1957) 1069–1073.

[29] K.S.W. Sing, *Pure & Appl. Chem*. 54 (1982) 2201–2218

Chapter 5

Multivariate analysis of structure-performance relationships in heterogeneous Ziegler-Natta olefin polymerization

5.1 Introduction

Catalyst is a genetic name of substance which can improve the reaction rate and chemical selectivity by making new route of chemical conversion with activation energy reduction. Because of these merit, catalyst keeps growing continually with industrial growth. Catalysts are used in the industrial production of over 7000 compounds worth over $3 trillion globally. Catalyst-based manufacturing accounts for about 60% of chemicals production and 90% of processes [1]. In recently, catalysts were focused on not only economic importance from increase efficiency of industrial processes but also environmental importance from reduction of materials emission which possesses adverse impacts on environment. Therefore, catalysts are desired that further performance improvement and new function addition.

From these backgrounds, great variety of catalyst investigation has been conducting briskly and high performance catalyst has been reported continually. In recently, industrial processes becomes to demand that catalyst has multifunction as one of improvement way in the viewpoint from economics and environments. Multifunctional catalyst possesses complex structure from active species to particle because multifunctional catalyst performances is demonstrated by diversification of active species and/or formation of hierarchy structures. Therefore, “elucidation of precise structure-performance

relationship" to design catalyst architecture and "establishment of control particle structure way" to synthesis desired catalyst are indispensable for development of multifunctional catalyst.

Enormous studies are tired and reported "elucidation of precise structure-performance relationship" and "establishment of control particle structure way" for catalyst development because of its importance. There are many reports about structure-performance relationship. For example, catalyst performances depend on not only active species and structures but also condition of active site neighborhood such as dispersion state and interaction between support substances. Catalyst particle morphology such as specific surface area, pore architecture and particle shape also affect performances to improve activity, selectivity, operation easiness and so on, because of these change diffusion efficiency of substrates. In the lately reports, the substance which were constructed great architectures of biomaterial by artificial way demonstrated excellent performances [2]. From using these knowledge, multifunctional catalyst will be designed. On the other hand, reports about establishment of control particle structure way are also reported with enormous number. The control of active site structures and dispersion state are used coprecipitation method and impregnation method, and control particle shape, size, pore architectures are controlled by sol-gel methods and hydrothermal synthesis

method as traditional ways [4,5]. The resent reports describe establishment of new method and synthesis novel material structures. For example, precise morphology and size control methods for nanoparticle [6-8], synthesis method for self-assembling materials [9] and synthesis methods of 3DOM [10,11] were established and various kinds of materials can be controlled particles structure from micro scale to macro. In recently, the pilling up of these available knowledge can conduct precise designing and control of catalyst architectures and great performance multifunctional catalysts are prepared and used. However, it is difficult that systematic developments of all present multifunctional catalyst because systematic development demands clear structure performance relationship and establishment of control particle structure. Thus, development way of these catalyst is to follow an empirical try-and-error manner only.

Industrial Ziegler-Natta catalyst is one of the example of multifunctional catalyst which can not be conducted systematic development. This catalyst composed of simple combination between $TiCl_3$ (active species) and alkylaluminium (activator) at early development stage. However, this simple systems possessed too low polymerization performances to produce good property polyolefin with efficiently. Since then, enormous researches and developments were conducted to improve olefin polymerization performances following importance of polyolefin. Those investigations established new

multicomponent system which is $TiCl_4$ (active species) and donor (active site modifier) supported $MgCl_2$ (support) and new preparation method for control hierarchical structures [11,12]. Those developments made catalytic performances greatly high and expanded polyolefin industry. After 1990s, catalyst possessed enough activity and stereospecificity to fulfill industrial demands, and addition of new functions become to be desired. As industrial demands, polymer morphology control ability, copolymerization performance, hydrogen responsibility and stable activity were newly desired to add catalyst performance with maintenance high activity and stereospecificity. Therefore further investigations were conducted about elucidation of structure performance relationship to obtain development guideline. Thus various combinations of correlation were investigated. For example, correlation between active site structure-activity [14,15], chemical component – activity [16], specific area – activity [17,18], pore architecture – copolymerization ability [19], particle morphology – polymer morphology [20] and so on. However, present catalyst development is not systematic designing and preparation of ideal catalyst but optimization of catalyst performance following an empirical try-and-error manner. Because greatly complex structure performance relationship in Ziegler-Natta olefin polymerization and imperfect establishment of precise particle morphology control method. Therefore, increase of catalytic performance tends to be slumber.

Statistical analysis is one of powerful tools for elucidation of complex correlation like this. Statistical analysis is data treatment method based on statistical concept which aims to understand characteristics and regularity of dataset from small number of variable using mathematics techniques. In recently, statistical analysis becomes to get attentions with development of information technology and to be used widely field. In the material science field, this method has been used as screening of candidate materials of new medicine in organic synthesis field since long time ago [21,22]. Then, it becomes to be counted on further usages in material science field because of tightening registration of chemicals usage in the world. As the example of statistical analysis usage in catalyst chemistry, several investigations which used were reported as performance prediction in homogeneous catalyst [23,24]. However, there are no example which applied heterogeneous catalyst systems with high validity results. Because heterogeneous catalyst systems possess many difficulties such as large number of structure parameters which affects performance, difficulty of full characterization, difficulty of selection correct statistical analysis method and difficulty of preparation dataset which has significant difference. It is necessary that not only knowledge of chemistry but also statistics and mathematics to solve these problems [1]. Therefore, application of heterogeneous reaction system becomes difficult and number of reports are too less and precise structure

performance relationship has not been established.

From these backgrounds, this study aims to elucidate quantitative structure performance relationship in industrial Ziegler-Natta olefin polymerization by statistical analysis. $Mg(OEt)_2$ based Ziegler-Natta catalyst was used for this study because easiness of catalyst morphology control and possession of high performance. Concretely, all $Mg(OEt)_2$ and catalyst samples were characterized structures by multilateral characterization methods which established in chapter2 [25], and performed olefin polymerization test. Then obtained data were parameterized to apply statistical analysis. Subsequently, dataset was analyzed based on statistics to elucidate relationship between catalyst structures and polymerization performances. Finally, obtained equations were evaluated to confirm validity.

5.2 Experiment

5.2.1 Materials

Anhydrous $MgCl_2$, triethylaluminium (TEA), and four kinds of poreless Mg particles (termed Mg A-E) were donated from Toho Titanium Co., Ltd., Tosoh Finechem Corporation and Yuki Gousei Kogyo Co., Ltd., respectively. The morphologies of Mg A , C and E are flake-like, while those of Mg B and D are spherical. Characterization results

of the Mg particles are shown in Table 1. The size of Mg particles becomes smaller in the order of A→C=E→B→D.

Ethanol (purity > 99.5%) was dried over 3A molecular sieve with N_2 bubbling. Heptane (purity > 99.5%), toluene (purity > 99.5%) and di-*n*-butylphthalate (DBP) (purity > 98%) were dried over 4A molecular sieve with N_2 bubbling. Cyclohexylmethyldimethoxysilane (CMDMS) was purified by distillation under reduced pressure. Ethylene of research grade donated by Sumitomo Chemical Co., Ltd. was used as delivered.

5.2.2 $Mg(OEt)_2$ synthesis

$Mg(OEt)_2$ was synthesized based on a patent [26] with several modifications. 0.67 g of I_2 (as an initiator) and 31.7 mL of dehydrated ethanol were introduced into a 500 mL jacket-type separable flask equipped with a mechanical stirrer rotating at 180 rpm under N_2 atmosphere. After the dissolution of I_2 at 75°C, 2.5 g of Mg and 31.7 mL of ethanol were introduced. 2.5 g of Mg and 31.7 mL of ethanol were again added 10 min after the reaction was initiated by I_2. Thereafter, 2.5 g of Mg and 31.7 mL of ethanol were added repeatedly 4 times every 10 min, followed by aging at 75°C for 2 h. Finally, the temperature was decreased to 40°C, and the product was washed with ethanol. In this study, 39 kinds of $Mg(OEt)_2$ particles were synthesized from various conditions but basic

operations were shown in below (as MGE7). $Mg(OEt)_2$ synthesis conditions were shown in Table 1. MGE1-23 is same sample which synthesized in previous chaptors. A set of synthetic conditions for $Mg(OEt)_2$ were simultaneously varied to fill multidimensional parametric spaces.

Table 5-1. $Mg(OEt)_2$ synthesis conditions

Sample name	Mg type shape	Stirring speed (rpm)	Injection frequency (times)	Injection amount of Mg at one time (g)	amount of Iodine (g)	Third component (mol%)	Amount of third component (mol%)
MGE1	A	180	5	2.5	0.67	-	-
MGE2	B	180	5	2.5	0.67	-	-
MGE3	C	180	5	2.5	0.67	-	-
MGE4	D	180	5	2.5	0.67	-	-
MGE5	C	180	5	2.5	0.67	-	-
MGE6	C	180	5	2.50	0.67	-	-
MGE7	C	180	5	2.50	0.67	-	-
MGE8	C	180	5	3.33	0.89	-	-
MGE9	C	180	5	2.00	0.53	-	-
MGE10	C	180	5	3.33	0.67	-	-
MGE11	C	180	5	2.00	0.67	-	-
MGE12	C	180	5	2.50	0.51	-	-
MGE13	C	180	5	2.50	0.84	-	-
MGE14	C	120	5	2.50	0.67	-	-
MGE15	C	240	5	2.50	0.67	-	-
MGE16	C	300	5	2.50	0.67	-	-
MGE17	C	180	5	2.50	0.67	methanol	5
MGE18	C	180	5	2.50	0.67	*n*-propanol	5
MGE19	C	180	5	2.50	0.67	*i*-propanol	1
MGE20	C	180	5	2.50	0.67	*i*-propanol	3
MGE21	C	180	5	2.50	0.67	*i*-propanol	5
MGE22	C	180	5	2.50	0.67	*i*-propanol	7
MGE23	C	180	5	2.50	0.67	*i*-propanol	9
MGE24	E	180	5	2.50	0.67	-	-
MGE25	E	120	5	2.00	0.27	-	-
MGE26	E	300	5	3.00	0.68	-	-
MGE27	E	270	5	2.00	0.13	-	-
MGE28	E	210	5	2.25	0.80	-	-
MGE29	E	240	5	1.50	0.56	-	-
MGE30	E	180	7	2.50	0.68	-	-
MGE31	E	180	9	2.50	0.68	-	-
MGE32	E	150	9	3.25	1.00	-	-
MGE33	E	240	9	2.00	0.67	-	-
MGE34	E	300	7	3.00	0.14	-	-
MGE35	E	270	3	2.50	0.54	-	-
MGE36	E	210	3	2.00	0.99	-	-
MGE37	E	150	7	1.75	0.80	-	-
MGE38	E	210	5	3.00	0.40	-	-
MGE39	E	180	3	3.00	0.27	-	-

5.2.3 Catalyst preparation

The preparation of Ziegler-Natta catalysts from $Mg(OEt)_2$ was conducted again based on a patent [27] with several modifications. 15 g of $Mg(OEt)_2$ and 140 mL of toluene were charged in a 500 mL 3-neck flask equipped with a mechanical stirrer rotating at 180 rpm under N_2 atmosphere. 30 mL of $TiCl_4$ was dropwisely added, where the temperature of the suspension was kept within 0-5°C. Thereafter, the temperature was once elevated to 90°C to add 4.5 mL of DBP and then brought to 110°C. The reaction slurry was continuously stirred at 110°C for 2 h. Subsequently, the reaction product was washed with toluene twice at 90°C and further treated with 30 mL $TiCl_4$ at 90°C for 2 h. After that, the product was washed with *n*-heptane 7 times to get the final catalyst. 39 kinds of Ziegler-Natta catalysts (Cat 1-39) were obtained from MGE 1-39 under the same conditions.

5.2.4 Polymerization test

Propylene and ethylene homopolymerization and copolymerization with 1-hexene. Homopolymerization was performed in a 1 L autoclave equipped with a mechanical stirrer rotating at 350 rpm. 500 ml of *n*-heptane was introduced into the reactor. TEA ([Al] = 10 mmol/L) and CMDMS (Al/ExD = 10) were introduced into the reactor, and the solution was saturated with 0.5 MPa of monomer at 50°C. 30 mg of a catalyst was fed

into the reactor by a bomb injection technique to initiate the polymerization. The polymerization was conducted for 60 min with a continuous supply of monomer gas at 0.5 MPa. At the end of the reaction, monomer was vented and the polymer slurry was filtered immediately. In the case of copolymerization with 1-hexene, 500 ml mixture of *n*-heptane (407 ml) and 1-hexene (93 ml, corresponding to 0.75 mol) were used instead of 500 ml of *n*-heptane. The polymerization was conducted for 30 min with 15 mg of a catalyst. The other conditions were the same as those for the homopolymerization.

5.2.5 Characterization

• Scanning electron microscopy

Particle morphological characteristics of $Mg(OEt)_2$ and catalyst particles were studied with scanning electron microscopy (SEM, Hitachi S-4100) operated at an accelerating voltage of 20 kV. Before the measurements, particles were subjected to Pt sputtering for 100 s. To quantify observed particle morphology, SEM images (> 500 particles) were analyzed by a software (Image J software, NIH). D_{10}, D_{50} and D_{90} were defined as the particle diameters at 10%, 50% and 90% in the cumulative number-base particle size distribution. The relative span factor (RSF) and the circularity degree were respectively calculated based on Eqs. (5-1) and (5-2),

$$relative\ span\ factor\ (RSF) = \frac{D_{90} - D_{10}}{D_{50}} \qquad (5-1)$$,

$$circularity\ \ degree = \frac{4 \times \pi \times area}{(boundary\ \ length)^2} \qquad (5-2)$$

where the area and boundary length for a two-dimensionally projected particle were determined over 500 particles.

• N_2 adsorption/desorption measurement

N_2 adsorption and desorption isotherms at 77 K were acquired on BELSORP-max (BEL JAPAN, INC.). *Ca*. 50-100 mg of catalyst powder in a pyrex tube with a rubber cap was outgassed at 80°C over 3 h in vacuo, prior to the measurement. Since the BET analysis does not work properly for typical Ziegler-Natta catalysts with a plenty of micropores (pore diameter (D) < 2 nm) [28,29], the specific surface area was not determined. Instead, the micropore volume (V_{micro}) was approximated with

$$V_{micro} = V_{0.4} \times \frac{V_{liquid}}{V_{gas}} - \int_2^{50} \frac{2}{D} \cdot \frac{V_{meso}(D)}{dD} dD \qquad (5-3)$$

where $V_{0.4}$, V_{liquid}, V_{gas}, and $V_{meso}(D)$ are the N_2 adsorption volume at $p/p_0 = 0.4$, the volumes of a N_2 molecule in gaseous and liquid states, and the mesopore volume at the diameter of *D* nm determined by the method described in the next paragraph. V_{micro} was estimated by subtracting the contribution of multilayer N_2 adsorption onto mesopore surfaces from the adsorption volume at $p/p_0 = 0.4$ (converted to the liquid N_2 volume).

Note that the thickness of the multilayer adsorption at $p/p_0 = 0.4$ was approximated as 2 nm, and the contribution from the multilayer adsorption onto macropore and external surfaces was regarded as negligible. The latter is true for typical industrial Ziegler-Natta catalysts, whose pore dimensions are mainly micro and/or meso scale(s) [30].

The mesopore size distributions (2.1 nm < D < 50 nm) were analyzed by the BJH method or by the INNES method. Even though the two methods are based on the same Kelvin equation for the N_2 condensation, cylinder-type and slit-type mesopores are assumed in the BJH [31] and INNES [32] methods, respectively. Hence, the BJH method is suitable for the hysteresis types H1 and H2 respectively for size-uniform and size-irregular cylindrical-type mesopores, while the INNES method for the types H3 and H4 respectively for size-uniform and size-irregular slit-type mesopores .

• Mercury intrusion measurement

The meso and macro pore size distributions (7 nm < diameter < 1000 nm) were measured with the mercury intrusion technique (Pascal 440 Porosimeter, Thermo Scientific). The pore size was evaluated from the intrusion pressure according to the Washburn-Laplace equation which was shown in equation (5-4). The surface tension (γ) and contact angle (θ) were respectively set to 0.480 N / m and 141.3°.

$$D = \frac{2\gamma \cos\theta}{P} \qquad (5-4)$$

• Chemical analysis

The Ti content was determined with UV-vis spectroscopy (V-670 JASCO), where a measured amount of a catalyst sample was dissolved in $HCl/H_2SO_4/H_2O_2$ solution and the intensity of a ligand metal charge transfer band at 410 nm was measured. The DNBP content was determined by IR spectroscopy (FT/IR-4100, JASCO): A measured amount of a catalyst sample was once dissolved in HCl solution, then DNBP was fully phase transferred to *n*-heptane, and finally the carbonyl absorption band was integrated to determine the DNBP content.

• ^{13}C NMR

The 1-hexene incorporation amount, *i.e. n*-Bu branch content, in ethylene/1-hexene copolymer and isotacticity in polypropylene were measured by ^{13}C NMR (Bruker 400 MHz) operating at 100 MHz with proton decoupling at 120°C using 1,2,4-trichlorobenzene as a diluent and 1,1,2,2-tetrachloroethane-d_2 as an internal lock and reference.

5.2.6 Statistical analysis

• Correlation coefficient

The correlation coefficient is one of statistical index and directly expresses the correlation extent between the two variables. As the *r* value approaches +1 or –1, the correlation extent becomes higher in a positive or negative direction, respectively. In general, the correlation coefficient, *r*, between two variables (*x* and *y*) is defined as

$$r = \frac{C_{(x,y)}}{\sqrt{V_x \times V_y}} \qquad (5.5)$$

$C_{(x,y)}$, V_x and V_y are the covariance and the variances for *x* and *y*, respectively. They are defined as

$$C_{(x,y)} = \sum_{i=1}^{n} \frac{\left(x_i - \bar{x}\right)\left(y_i - \bar{y}\right)}{n} \qquad (5.6)$$

$$V_x = \sum_{i=1}^{n} \frac{\left(x_i - \bar{x}\right)^2}{n} \qquad (5.7)$$

$$V_y = \sum_{i=1}^{n} \frac{\left(y_i - \bar{y}\right)^2}{n} \qquad (5.8),$$

where *n* is the number of data.

In this study, correlation coefficient of various parameters combinations were calculated by software (material studio 6.0, accelrys) and used for removing collinearity parameters as pretreatment of dataset before principal component analysis.

• Principal Component Analysis

Principal component analysis (PCA) is one of multivariate analysis which can reduce large number of variables to smaller number without any information losses. In this study, PCA were calculated by software (SIMCA, Umetrics) to classify samples and used for removing outlier as pretreatment of dataset.

• Genetic function approximation

Genetic function approximation (GFA) is one of multivariate analysis which can construct quantitative structure-performance relationship with genetic algorithm. In this study, GFA were calculated by software (material studio 6.0, accelrys) to construct the structure performance relationship model equations.

5.3 Results and discussion

5.3.1 Sample preparation and parameterization

5.3.1.1 Catalyst structure characterizations

Thirty nine kinds of Zigler-Natta catalyst were prepared and characterize with multirateral characterizations. Cat1-23 corresponds to samples which appeared in previous chapter and Cat24-39 are newly synthesized samples. The particle shape characteristics were characterized by statistical analysis of SEM images and light scattering measurement and these results were shown in Table 5-2. And, particle characteristics (D<50 nm) were measured by N_2 adsorption measurement and chemical compositions were determined by applied spectroscopies. These results were shown in Table 5-3.

As can be seen, characterization and parameterization were conducted without any problems. From the viewpoints of dataset evaluation, dataset was improved in comparison with previous dataset (16 samples) because sample number and standard deviations were increase. It means that validity of dataset were imporved.

Table 5-2. Catalyst particle size characteristics

	SEM					LS			
	D_{10} (μm)	D_{50} (μm)	D_{90} (μm)	RSF	Circularity	D_{10} (μm)	D_{50} (μm)	D_{90} (μm)	RSF
Cat1	20.2	25.7	31.0	0.42	0.84	18.5	34.4	60.3	1.22
Cat2	12.4	37.6	55.5	1.15	0.74	19.1	40.5	63.1	1.09
Cat3	27.2	32.4	44.4	0.53	0.87	29.1	40.9	62.8	0.82
Cat4	22.0	36.6	49.8	0.76	0.79	39.6	65.3	116.9	1.18
Cat5	16.1	21.9	37.2	0.96	0.82	11.1	34.5	81.5	2.04
Cat6	7.1	15.4	30.0	1.49	0.64	20.2	34.2	79.1	1.72
Cat7	17.9	21.7	29.1	0.52	0.88	20.1	31.1	75.8	1.80
Cat8	13.6	17.5	37.9	1.39	0.77	17.8	67.6	139.3	1.80
Cat9	12.9	25.7	34.7	0.85	0.72	21.2	40.3	84.3	1.57
Cat10	14.1	18.3	37.2	1.26	0.77	16.6	36.9	118.9	2.77
Cat11	21.1	33.6	62.4	1.23	0.82	23.2	47.9	108.8	1.79
Cat12	16.9	22.2	34.2	0.78	0.83	20.4	30.5	61.5	1.35
Cat13	18.0	23.7	32.4	0.61	0.83	22.9	47.5	93.6	1.49
Cat14	22.5	28.4	41.4	0.66	0.84	26.0	56.5	129.0	1.82
Cat15	15.0	22.6	35.4	0.90	0.82	17.6	34.2	72.6	1.61
Cat16	21.1	33.6	62.4	1.23	0.82	17.6	34.2	123.5	3.10
Cat17	8.1	31.8	46.7	1.21	0.78	20.6	38.0	57.7	0.98
Cat18	7.5	14.4	35.7	1.96	0.57	8.8	16.0	38.4	1.85
Cat19	10.2	22.0	38.7	1.30	0.76	26.4	35.0	49.1	0.65
Cat20	14.6	23.6	53.5	1.65	0.78	20.3	34.1	65.5	1.33
Cat21	11.1	17.0	27.8	0.98	0.82	12.4	20.8	39.7	1.32
Cat22	13.7	19.4	36.6	1.17	0.78	15.1	22.5	33.5	0.81
Cat23	17.9	22.0	30.7	0.58	0.80	17.1	25.0	36.2	0.76
Cat24	15.6	19.6	26.9	0.57	0.85	18.0	32.6	69.0	1.56
Cat25	16.2	21.9	31.3	0.69	0.78	21.4	33.4	63.2	1.25
Cat26	11.3	16.5	29.7	1.11	0.83	19.6	19.6	28.2	0.44
Cat27	9.9	18.0	29.1	1.06	0.66	14.1	22.2	34.2	0.90
Cat28	10.0	26.1	46.0	1.38	0.80	22.3	35.7	81.3	1.65
Cat29	20.6	24.9	32.1	0.46	0.85	22.8	33.0	51.1	0.86
Cat30	16.0	25.8	34.4	0.71	0.86	21.0	29.3	43.0	0.75
Cat31	21.8	26.0	33.4	0.45	0.87	26.8	31.4	39.0	0.39
Cat32	18.4	23.2	29.7	0.49	0.84	17.3	31.9	61.2	1.38
Cat33	23.9	29.3	37.5	0.46	0.84	24.0	37.4	62.1	1.02
Cat34	9.1	10.6	12.7	0.34	0.78	7.8	12.6	20.0	0.97
Cat35	13.0	16.4	23.6	0.64	0.86	13.4	20.7	34.2	1.01
Cat36	10.4	25.8	38.0	1.07	0.81	16.8	33.8	62.8	1.36
Cat37	29.5	38.0	52.4	0.60	0.84	36.7	63.6	135.3	1.55
Cat38	10.8	16.0	24.0	0.83	0.83	14.0	21.3	35.1	0.99
Cat39	11.1	14.4	22.0	0.75	0.84	10.9	18.1	37.3	1.46
AVE	15.6	23.6	36.6	0.90	0.80	19.7	34.5	67.9	1.3
STDEV/AVE	0.35	0.29	0.29	0.42	0.08	0.33	0.37	0.47	0.41

Table 5-3. Catalyst pore characteristics and chemical component.

	N_2 adsorption ($mm^3 \cdot g^{-1}$)					Chemical component analysis	
	2<D (nm)	2<D<5 (nm)	5<D<10 (nm)	10<D<20 (nm)	20<D<50 (nm)	Ti cont. (wt%)	Donor cont. (wt%)
Cat1	111.4	76.8	29.9	106.7	55.3	2.4	11.3
Cat2	113.9	81.8	27.1	108.9	49.8	2.5	20.9
Cat3	103.2	83.3	26.2	109.5	48.7	2.7	18.3
Cat4	120.4	75.5	22.5	98.1	44.1	2.7	14.8
Cat5	108.5	75.2	25.4	100.6	48.0	2.6	16.4
Cat6	124.6	78.9	28.0	106.9	48.3	2.7	16.5
Cat7	107.2	76.1	26.9	103.0	48.5	2.7	15.7
Cat8	101.2	67.4	22.0	89.4	31.7	2.1	14.8
Cat9	94.8	91.6	30.5	122.1	55.3	2.6	20.2
Cat10	107.5	78.3	25.6	103.9	32.2	2.0	15.2
Cat11	128.1	76.3	24.6	100.9	36.6	2.4	13.6
Cat12	112.1	74.5	29.3	103.8	51.6	1.9	13.3
Cat13	98.2	80.5	29.8	110.3	59.0	2.5	17.0
Cat14	97.0	84.5	27.7	112.2	58.8	2.0	13.6
Cat15	110.7	79.6	26.0	105.6	43.8	2.7	11.5
Cat16	103.9	87.3	30.7	118.0	47.4	2.1	17.3
Cat17	100.9	88.9	28.4	117.3	47.9	3.5	13.0
Cat18	100.4	106.9	32.5	139.4	70.6	2.2	13.7
Cat19	119.6	65.7	22.9	88.6	40.1	2.4	18.9
Cat20	116.7	71.2	23.2	94.4	34.4	3.7	18.2
Cat21	128.5	67.0	8.2	75.2	11.2	4.3	19.7
Cat22	144.8	76.9	11.6	88.4	5.8	4.6	18.6
Cat23	128.3	76.7	10.4	87.1	9.5	5.2	17.6
Cat24	118.2	70.4	34.9	105.3	60.9	3.4	10.3
Cat25	104.8	72.9	33.7	106.6	60.4	3.8	10.8
Cat26	110.0	68.2	27.7	95.9	56.2	2.3	12.1
Cat27	101.5	74.3	40.7	115.0	164.1	1.8	17.5
Cat28	120.7	66.0	26.8	92.8	48.9	3.2	12.3
Cat29	108.2	69.3	27.0	96.3	42.9	3.2	15.2
Cat30	104.2	75.9	31.2	107.1	44.7	3.0	17.9
Cat31	106.0	82.6	31.6	114.2	61.3	2.8	16.6
Cat32	115.8	65.7	23.1	88.8	31.6	2.7	14.4
Cat33	108.6	68.6	28.1	96.7	68.3	3.1	23.8
Cat34	111.3	74.2	26.6	100.8	23.8	3.2	12.6
Cat35	101.2	67.3	35.3	102.6	63.5	3.7	16.2
Cat36	82.5	72.6	43.9	116.5	111.2	3.7	14.4
Cat37	95.4	70.1	32.9	103.0	80.9	3.6	11.7
Cat38	94.4	76.3	38.8	115.1	149.8	3.3	16.2
Cat39	91.4	73.1	37.6	110.7	139.1	3.9	13.3
AVE	111	73	28	30	56	3.0	15.5
STDEV/AVE	0.15	0.16	0.28	0.40	0.61	0.26	0.20

5.3.1.2 Polymerization performances

Polymerization test for 39 samples were conducted. Propylene and ethylene homopolymerization and copolymerization with 1-hexene were conducted as polymerization test. Stereoselectivity and 1-hexene incorporation amount was determined by ^{13}C-NMR. NMR results and polymerization activities were shown in Table 5-4.

As a results, polymerization and parameterization were conducted without any problems and dataset become to be improved as same as structural dataset.

Table 5-4. Results of polymerization performances

	Activity ($Kg\text{-}polymer \cdot g^{-1}\text{-}cat \cdot atm^{-1} \cdot h^{-1}$)				Bu-content (mol%)		*mmmm* (mol%)
	C2 homo	C3 homo	C2 co	C3 co	C2 co	C3 co	C3 homo
Cat1	122	155	658	278	6.7	5.0	96.8
Cat2	75	140	489	153	4.3	4.4	97.0
Cat3	111	129	401	155	6.9	7.2	95.0
Cat4	106	123	746	282	4.9	5.2	93.9
Cat5	135	101	731	243	4.0	3.8	96.2
Cat6	77	185	294	519	5.6	5.6	96.1
Cat7	83	183	843	394	6.0	5.3	95.3
Cat8	90	138	689	336	5.7	5.3	95.8
Cat9	104	154	742	193	4.6	5.1	92.9
Cat10	46	111	461	456	5.4	5.4	95.6
Cat11	81	130	463	260	8.0	6.3	95.3
Cat12	80	127	426	216	6.1	5.2	95.9
Cat13	89	100	567	291	6.3	5.8	95.0
Cat14	120	176	741	398	5.4	6.0	95.8
Cat15	98	184	554	280	4.5	5.1	95.5
Cat16	95	171	660	386	7.0	5.2	95.1
Cat17	37	89	189	115	4.8	4.2	95.0
Cat18	232	154	422	193	3.4	3.9	95.5
Cat19	138	175	868	315	4.7	5.0	95.2
Cat20	148	238	684	357	7.3	4.5	95.2
Cat21	93	253	903	354	4.3	5.0	95.1
Cat22	70	193	918	353	4.4	4.6	96.0
Cat23	83	225	1084	435	5.3	4.9	94.6
Cat24	144	141	409	82	3.6	4.2	95.7
Cat25	131	104	698	247	3.2	4.8	95.5
Cat26	77	141	798	147	3.7	4.3	92.7
Cat27	226	158	1294	233	2.6	4.3	95.1
Cat28	129	160	947	207	4.3	4.8	93.9
Cat29	147	184	897	275	5.4	5.4	93.9
Cat30	91	205	779	221	4.5	4.4	94.0
Cat31	114	170	641	157	5.9	4.7	93.6
Cat32	78	180	602	176	4.8	5.2	94.0
Cat33	129	149	809	168	4.4	4.6	95.3
Cat34	69	182	360	343	2.4	4.0	94.4
Cat35	234	195	722	256	2.4	4.3	93.7
Cat36	167	121	487	140	2.3	3.5	94.3
Cat37	91	132	399	201	4.2	4.2	93.7
Cat38	170	153	298	551	3.6	3.8	93.7
Cat39	136	100	516	140	2.2	4.1	93.7
AVE	114	157	646	269	4.75	4.84	95.0
STDEV/AVE	0.40	0.25	0.36	0.42	0.30	0.15	0.01

5.3.2 Statistical analysis to elucidate structure performance relationship

5.5.2.1 Outlier removal

Prior to multivariate analyses, the pretreatment of dataset is necessary in order to remove samples as outliers, which would strongly distort regression results through leverage. Therefore dataset was analyzed based on the principle component analysis (PCA) which can visualized dataset information without any information loss by reduction of the dimensions of dataset.

Inclusion of similar parameters with strong colinearity in PCA leads to overestimated impacts of the parameters on the resultant model. Consequently, descriptors for PCA were selected based on correlation matrix analyses as well as physical consideration. The way of selection parameters were explained using catalyst particle characteristics as follows. There were 9 parameters for catalyst particle characteristics. These parameters were used to calculate correlation matrix in order to check collinearity and these results shown in Table 5-5 (when absolute value of correlation coefficient is over 0.7 or 0.6, cell is turned yellow or orange respectively). As can be seen table, D_{50} possessed strong collinearity with D_{10} and D_{90} for both SEM and LS, while D_{50} for SEM and that for LS were also collinear with each other. Thus, it would be reasonable to select D_{50}(SEM) (or D_{50}(LS)) to represent the particle size. Subsequently, all parameters including performances were

checked by this way and selected parameters as descriptors for PCA. Selected descriptors were shown in Table 5-6.

Table 5-5. Correlation matrix for catalytst particle characteristics

	D_{10}(SEM)	D_{50}(SEM)	D_{90}(SEM)	RSF(SEM)	Circularity	D_{10}(LS)	D_{50}(LS)	D_{90}(LS)	RSF(LS)
D_{10}(SEM)		0.65	0.38	-0.55	0.58	0.71	0.54	0.42	0.03
D_{50}(SEM)	0.65		0.81	-0.12	0.26	0.74	0.63	0.50	0.10
D_{90}(SEM)	0.38	0.81		0.41	-0.04	0.55	0.64	0.67	0.40
RSF(SEM)	-0.55	-0.12	0.41		-0.69	-0.15	0.17	0.36	0.46
Circularity	0.58	0.26	-0.04	-0.69		0.16	-0.03	-0.09	-0.15
D_{10}(LS)	0.71	0.74	0.55	-0.15	0.16		0.72	0.48	-0.13
D_{50}(LS)	0.54	0.63	0.64	0.17	-0.03	0.72		0.87	0.30
D_{90}(LS)	0.42	0.50	0.67	0.36	-0.09	0.48	0.87		0.72
RSF(LS)	0.03	0.10	0.40	0.46	-0.15	-0.13	0.30	0.72	

Table 5-6. Selected descriptors for PCA

	Number of descriptor	Descriptor
Structural descriptor	7	D_{50}(SEM), RSF(SEM), Circularity, $V_{<2}$, $V_{2\text{-}50}$, Ti cont., Donor cont.
Performance descriptors	7	Activity (C3 homo), Activity (C3 co), Activity (C2 homo), Activity (C2 co), *mmmm*, Bu cont. (C3 co), Bu cont. (C2 co)

After selection of descriptors to use, PCA was conducted to find out outliers. These results were shown in Figure 5-1.

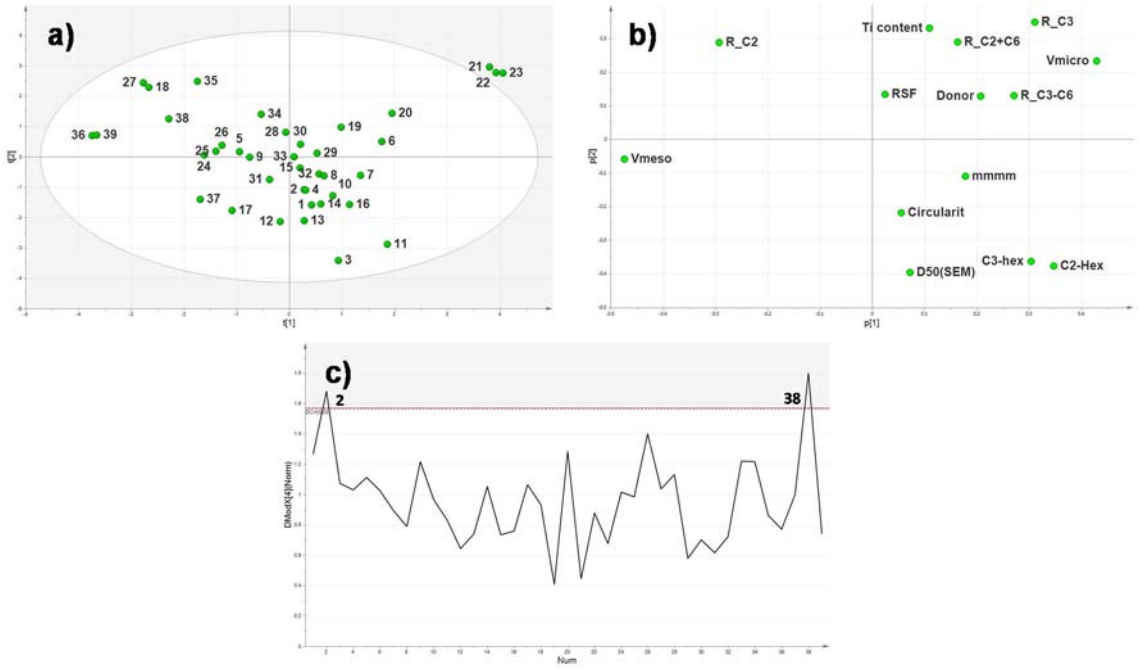

Figure 5-1. Results of first PCA: a) Score plot with Hotelling's T^2 at 95% confidence, b) loading plot and c) DModX plot

Figure 5-1 (a) and (b) show the score and loading plots for the first two principle components (i.e. t_1 and t_2). Score plot showed sample characteristics and similarity. For example, samples plots neighbor in the score plot means sample characteristics are similar and vise versa. Loading plot means parameter contribution degree of new axis. While Figure 5-1 (c) shows a so-called DModX plot, which represents the residual distance for each sample.

Cat21-23 were found to be strong outliers, being out of Hotelling's T^2 at 95%

confidence. This was because these samples prepared using *i*-propanol over 5 mol% were greatly microporous without mesopores (as can be judged from the loading plot). On the other hand, the DModX plot shows that Cat2,38 were beyond the critical distance at the 0.05 level: These samples were not sufficiently explained by the PCA model and therefore removed as moderate outliers. Cat2 showed unacceptably low activities compared with its large particle size and donor content, while Cat38 possessed a high copolymerization activity for propylene in spite of a low copolymerization activity for ethylene.

In summary, 5 catalyst samples were removed as outliers in the first PCA. The model was then updated using the remaining 34 samples (second PCA, not shown), leading to the removal of Cat18 and Cat27 as strong outliers due to their extremely high activities for ethylene copolymerization with 1-hexene. The third PCA using the remaining 32 samples finally led to the absence of outliers, as shown in Figure 5-2.

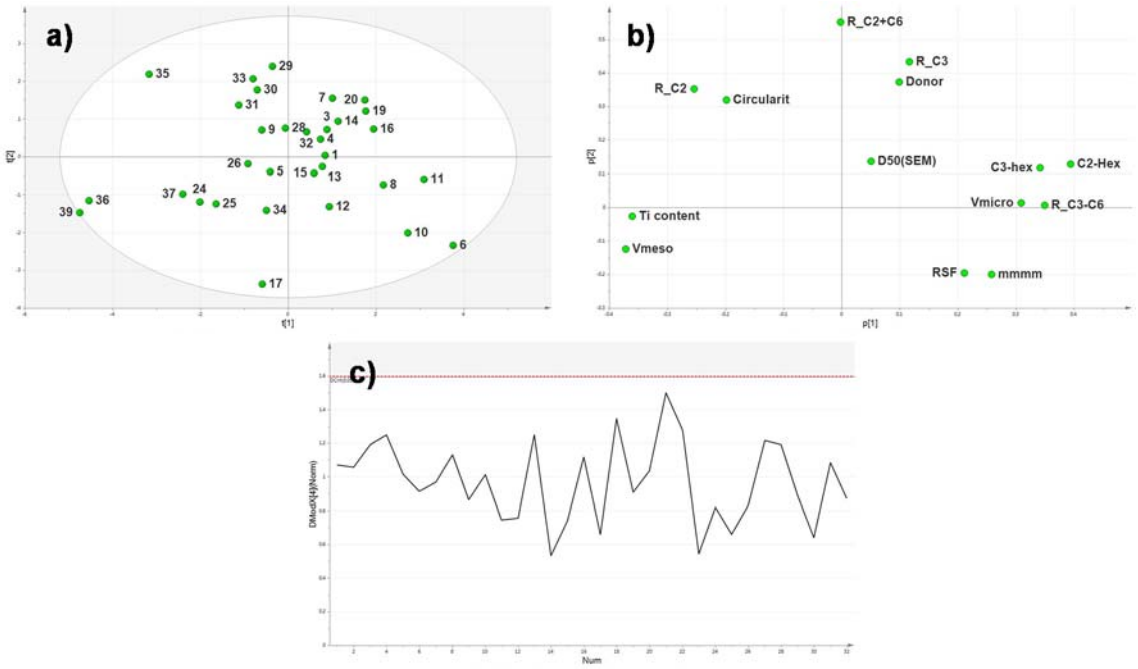

Figure 5-2. Results of 3rd PCA: a) Score plot with Hotelling's T^2 at 95% confidence, b) loading plot and c) DModX plot

Samples were relatively were relatively evenly dispersed in the score plot. It indicates that various catalysts were synthesized with different structures. The loading plot (Figure 5-2 (b)) indicated interesting collinearly relationships: Samples with large $V_{<2}$ tend to have small $V_{2\text{-}50}$ and a small Ti content as well as large Bu contents, samples with a large donor content tend to have a high activity for propylene homopolymerization, and so on.

From above operations, outliers which stayed in dataset were removed based on statistical manner. Multivariate analysis would be conducted this dataset (32 sample)

5.3.2.2 Multivariate analysis

Multivariate analysis was implemented based on Genetic function approximation (GFA) was used as in order to establish correlation between structure and performance in Ziegler-Natta olefin polymerization. Fundamental analysis conditions were shown in Table 5-7, where N_{pop} and $P_{mutation}$ were respectively set to 200 and 0.1% and the 1-leave-out method was employed for cross validation (cf. R^2_{CV}).

At First, multivariate analysis was conducted only butyl contents in ethylene/1-hexene copolymerization in order to examine GFA condition.

Table 5-7. Conditions for GFA analysis

condition		
Dataset	samples	Cat1, 3-17, 19, 20, 24-26, 28-37,39
	sample number	32
GFA analysis	population	200
	mutation	0.1 %
	maximum generation	10000
	equation form	liner

GFA was implemented with changing equation length in order to confirm multivariate of catalyst structure-performance relationship and explore necessary and sufficient equation length for establishment of precise model equations.

The GFA results which the most precise equation with different equation length were summarized in Table 5-8. The Comparison between regression model which obtained by

multivariate analysis and experimental values were shown in Figure 5-3. Moreover, the changing behavior of precision and validity of calculated regression model with different equation length were shown in Figure 5-4.

Table 5-8. Equation length effect on regression models for 1-hexene incorporation efficiency in ethylene copolymerization

length	Best equation	Friedman LOF	R^2	R^2_{cv}
1	+ 0.59D_{90}(SEM)	2.64	0.35	0.31
2	+ 0.50 D_{90}(SEM) – 0.47 Ti cont.	1.88	0.56	0.49
3	+ 0.68 D_{10}(SEM) + 0.49 RSF(SEM) – 0.40 $V_{20\text{-}50}$	1.82	0.61	0.49
4	+ 0.61 D_{10}(SEM) + 0.44 RSF(SEM) + 0.37 $V_{2\text{-}5}$ – 0.40 $V_{2\text{-}50}$	1.55	0.69	0.59
5	+ 0.61 D_{10}(SEM) + 0.40 RSF(SEM) + 0.23 $V_{<2}$ + 0.39 $V_{2\text{-}5}$ – 0.25 $V_{2\text{-}50}$	1.47	0.71	0.61

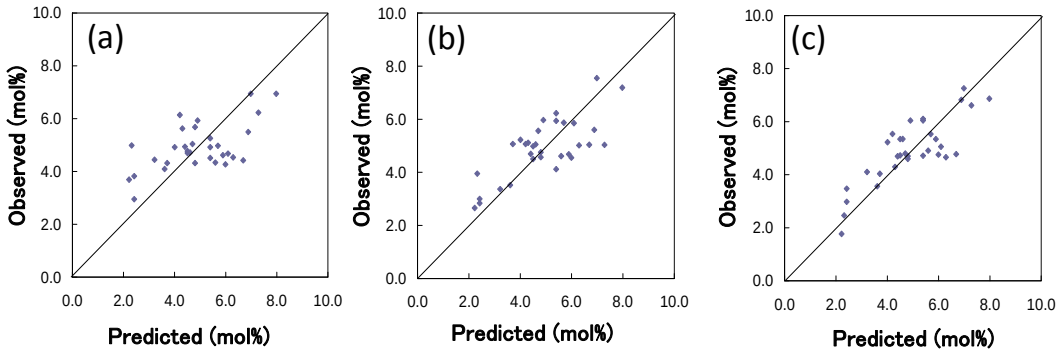

Figure 5-3. Equation length effect on regression models for 1-hexene incorporation efficiency in ethylene copolymerization; (a) equation length : 1, (b) equation length : 2, (c) equation length : 4

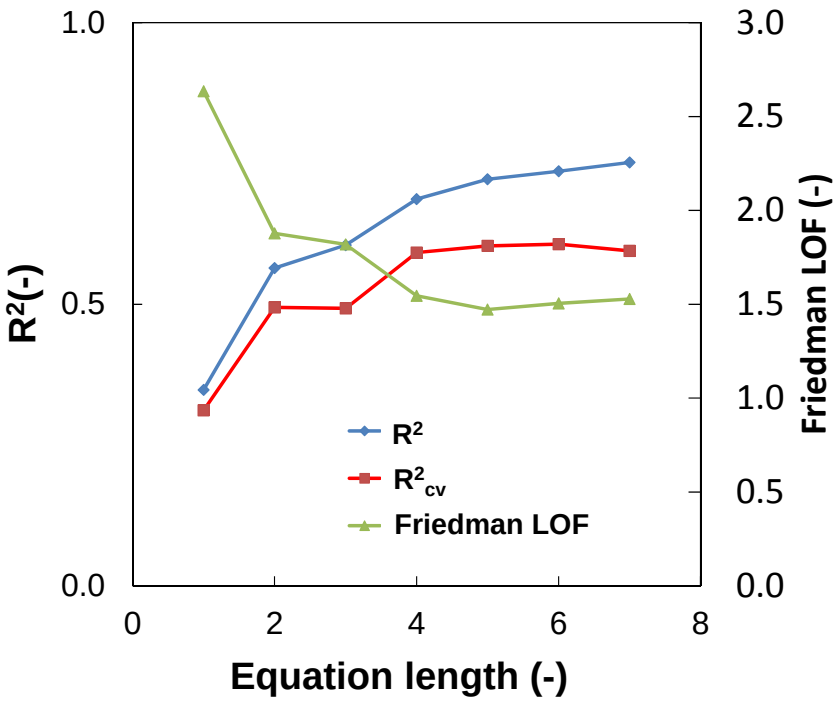

Figure 5-4. Correlation among equation length and validation factors

As can be seen regression equation in table 5-8, the contents of equation changed with appeared same descriptors consistently, after equation length set over three. It suggests that identification of important descriptor might be able to determine. And, Table 5-8 and Figure 5-3 shows increase of equation precision with increase equation length. It suggested that catalyst performances were multivariate factor. Moreover, Figure 4 shows monotonic increase R^2 and R^2_{cv} and monotonic decrease Friedman LOF during regression equation length increase from 1 to 4. Where, Friedman LOF is statistical index of equation validity for regression equation with penalty of over fitting by increase equation length (lower value means good validity). However, even if equation length become over 5,

values does not change. This results suggests that usage of over five descriptors make equation over fitting. From above results, it is concluded that equation length possess adequate number and it has to use adequate value to obtain precise regression equations. In this study, adequate equation length are determined 3 or 4 by Figure 5-4.

In the viewpoint from catalyst chemistry, amount of small particle and micro pore volume are important factor for 1-hexene incorporation efficiency in ethylene/1-hexene copolymerization from results of Table 5-8. It is considered that 1-hexene incorporation efficiency may be determined by particle surface amount rather than substrate diffusion limitation in pore in ethylene/1-hexene copolymerization.

Secondly, effect of sample number and removal outlier on precise and validity of regression models was investigated. The following three datasets were employed (Table 5-9) for multivariate analysis. Where dataset 1 is 15 samples that had been used in chapter 3 except Cat2 as an outlier. And dataset 2 is all of the samples including the outliers. GFA were implemented with each dataset respectively and obtained regression models with highest R^2 and R^2_{CV} values are summarized in Table 5-10 for each dataset and each equation length. The best-fit results are also given in Figure 5-5.

Table 5-9. Contents of dataset

dataset	sample number	samples	note
1	15	1, 3-16	previous dataset
2	39	1-39	all samples
3	32	1,3-17,19,20,24-26, 28-37,39	removal outlier by PCA

Table 5-10. Regression models for 1-hexene incorporation efficiency in ethylene copolymerization

Dataset	Equation length	Equation	R^2	R^2_{CV}
1	3	+ 0.73 D_{10}(SEM) + 1.36 $V_{5\text{-}10}$ – 1.30 $V_{2\text{-}50}$	0.59	0.35
		+ 0.76 D_{90}(SEM) + 0.79 $V_{5\text{-}10}$ – 0.69 $V_{2\text{-}5}$	0.52	0.24
		+ 0.65 D_{10}(SEM) + 0.78 $V_{5\text{-}10}$ – 0.77 $V_{20\text{-}50}$	0.50	0.17
	4	+ 0.76 D_{10}(SEM) + 0.37 $V_{<2}$ + 1.40 $V_{5\text{-}10}$ – 1.20 $V_{2\text{-}50}$	0.70	0.25
		+ 0.75 D_{10}(SEM) + 1.18 $V_{5\text{-}10}$ – 1.13 $V_{2\text{-}50}$ – 0.32 R_C2+C6	0.68	0.43
		+ 1.04 D_{10}(SEM) + 0.75 RSF(SEM) + 0.88 $V_{5\text{-}10}$ – 0.65 $V_{2\text{-}5}$	0.65	0.34
2	3	+ 0.42 D_{10}(SEM) + 0.57 $V_{2\text{-}5}$ – 0.69 $V_{5\text{-}10}$	0.55	0.47
		+ 0.70 D_{10}(SEM) + 0.44 RSF(SEM) – 0.35 $V_{20\text{-}50}$	0.55	0.43
		+ 0.72 D_{10}(SEM) + 0.44 RSF(SEM) – 0.32 $V_{10\text{-}20}$	0.53	0.42
	4	+ 0.32 D_{10}(SEM) + 0.31 D_{90}(SEM) – 0.31 Ti cont. – 0.43 $V_{10\text{-}20}$	0.61	0.50
		+ 0.62 D_{10}(SEM) + 0.35 RSF(SEM) – 0.25 Ti cont. – 0.40 $V_{20\text{-}50}$	0.60	0.46
		+ 0.63 D_{10}(SEM) + 0.34 RSF(SEM) – 0.28 Ti cont. – 0.41 $V_{10\text{-}20}$	0.60	0.47
3	3	+ 0.68 D_{10}(SEM) + 0.49 RSF(SEM) – 0.40 $V_{20\text{-}50}$	0.61	0.49
		+ 0.47 D_{90}(SEM) + 0.21 $V_{<2}$ – 0.43 Ti cont.	0.60	0.53
		+ 0.40 D_{90}(SEM) + 0.32 $V_{2\text{-}5}$ – 0.43 $V_{5\text{-}10}$	0.59	0.52
	4	+ 0.61 D_{10}(SEM) + 0.44 RSF(SEM) + 0.37 $V_{2\text{-}5}$ – 0.40 $V_{2\text{-}50}$	0.69	0.59
		+ 0.63 D_{10}(SEM) + 0.45 RSF(SEM) + 0.29 $V_{2\text{-}5}$ – 0.39 $V_{20\text{-}50}$	0.68	0.57
		+ 0.60 D_{10}(SEM) + 0.44 RSF(SEM) + 0.30 $V_{2\text{-}5}$ – 0.37 $V_{10\text{-}20}$	0.67	0.56

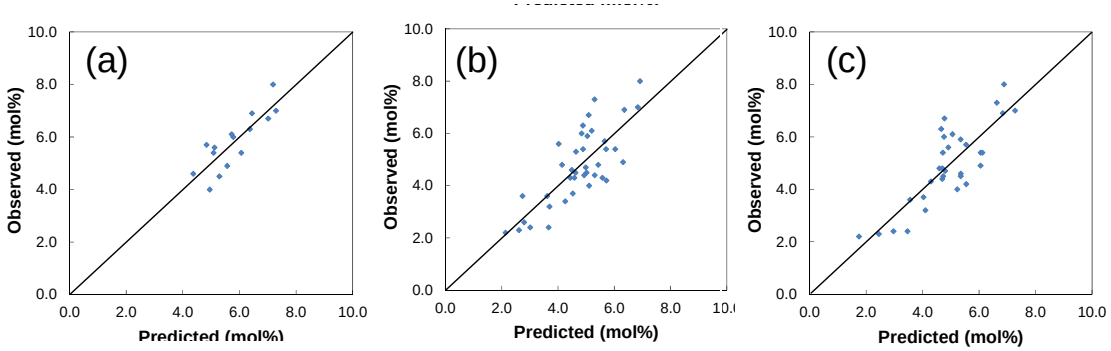

Figure 5-5. Dataset effect on regression models for 1-hexene incorporation efficiency in ethylene copolymerization; (a) dataset1, (b) dataset2, (c) dataset3

Regression equation calculated from dataset 1 showed high R^2 value and low R^2_{CV}. Comparison of the R^2 and R^2_{CV} values indicated that the small sample number for the dataset 2 led to overfitting ($R^2 >> R^2_{CV}$), while the exclusion of the outliers improved the fitting (enlarged R^2). Regression equation calculated from dataset 2 changed descriptors in equation and improved R^2_{CV} greatly. However comparison with R^2 value of dataset 3 (pretreated before analysis) R^2 did not reach same values. It suggested that increase samples improve validity of regression equations (R^2_{CV}), however outlier had worth impacts on precision of equation (R^2). From these results, that sample number and removal of outlier have positive effects on validly and preciseness for construction of regression equation models using multivariate analysis

5.3.3.3 Examination of prediction preciseness

The new catalyst was prepared and used to examine prediction preciseness of obtained equation model. The catalyst prepared newly was named Cat40 and conducted structural characterization and polymerization performances. These results were shown in Table 10~12. The predicted performance value calculated by the most precise and valid regression equation (dataset3, equation length : 4) using obtained structure characteristics were compared with experimental value. This result was shown in Figure 5-6.

Table 5-11. Particle size characteristics of Cat40

	SEM					LS			
	D_{10} (μm)	D_{50} (μm)	D_{90} (μm)	RSF	Circularity	D_{10} (μm)	D_{50} (μm)	D_{90} (μm)	RSF
Cat40	10.0	27.2	37.3	1.00	0.83	22.9	33.0	48.8	0.79

Table 5-12. Pore characteristics and chemical component of Cat40

	N_2 adsorption ($mm^3 \cdot g^{-1}$)					Chemical component analysis	
	2<D (nm)	2<D<5 (nm)	5<D<10 (nm)	10<D<20 (nm)	20<D<50 (nm)	Ti cont. (wt%)	Donor cont. (wt%)
Cat40	97.9	67.6	27.5	31.9	60.4	2.5	9.8

Table 5-13. Results of polymerization performances

	Activity (Kg-polymer$\cdot g^{-1}$-cat$\cdot$atm$^{-1}\cdot h^{-1}$)				Bu-content (mol%)		*mmmm* (mol%)
	C2 homo	C3 homo	C2 co	C3 co	C2 co	C3 co	C3 homo
Cat40	79	199	704	292	4.0	3.7	93.5

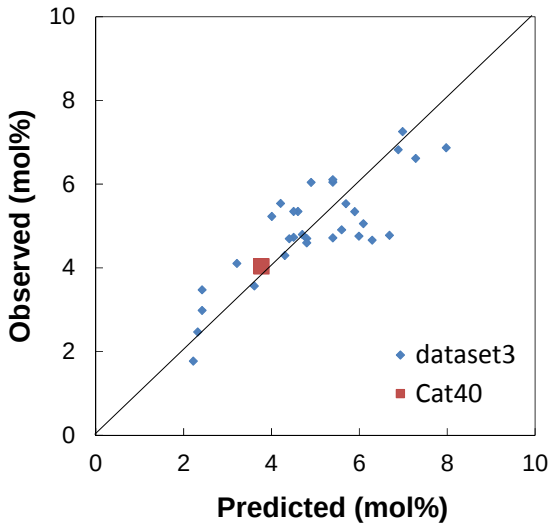

Figure 6. Validation test for best regression equation

The prediction values of 1-hexene incorporation amount in ethylene/1-hexene copolymerization was 3.77 mol%. On the contrary, experimental value was 4.04 mol%. These error was only 6.7%, suggests that obtained regression equation model has strong prediction ability without empirical assist. (Figure 5-6)

5.4 Conclusion

In this study, multivariate analysis were employed to elucidate structure performance relationship in Ziegler-Natta catalyst systems which featured extremely complex reaction mechanism.

Thirty nine kinds of catalyst were prepared and conducted structural characterization and polymerization test. These results were parameterized to form dataset. After checking dataset possessed necessary and sufficient significant difference, multivariate analysis was implemented based on genetic functional approximation method. After several examinations were conducted to obtain high valid and precise regression equation models and the importance of sample number, removal outlier and equation length were quantitatively proven. Additionally, obtained best fit regression equation model possessed high prediction ability with empirically assist were confirmed.

These results suggested that the combination of multilateral characterization and multivariate analyses were powerful tool for direct structure-performance relationships in heterogeneous Ziegler-Natta catalysis. Additionally, this established method were able to use not only Ziegler-Natta olefin polymerization but also any heterogeneous catalyst systems even if catalyst systems possesses multicomponent, complex hierarchy and/or complex reaction mechanism.

Reference

[1] S. Senkan, *Angew. Chem. Int. Ed.,* 40 (2001) 312-329

[2] M. R. Wasielewski, *Acc. Chem. Res*., 42 (2009) 1910-1921

[3] J. Jia, K. Haraki, J. N. Kondo, K. Domen, K. Tamaru, *J. Phys. Chem. B,* 104 (2000) 11153-11156

[4] T. S. Ahmadi, Z. L. Wang, T. C. Green, A. Henglein, M. A. El-Sayed, *Science,* 272 (1996) 1924-1926

[5] S. M. Csicsery, *Zeolites*, 4 (1984) 202-213

[6] R. K. Grasselli, J. D. Burrington, D. J. Buttrey, P. DeSanto Jr., C. G. Lugmair, A. F. Volpe Jr., T. Weingand, *Top. Cat*., 23 (2003) 1–4

[7] H. H. Lee, K. S. Chou, K. C. Huang, *Nanotechnology*, 16 (2005) 2436-2441

[8] S. Basri, S. K. Kamarudin, W. R.W. Daud, Z. Yaakub, *Int. J. Hydrogen Energy*, 35 (2010) 7957-7970

[9] V. Percec, C. Grigoras, H. J. Kim, *J. Polym. Sci., Part A: Polym. Chem*., 42 (2004) 505-513

[10] Y. Wei, Z. Zhao, J. Liu, S. Liu, C. Xu, A. Duan, G. Jiang, *J. Catal*., 317 (2014) 62-74

[11] R. Ryoo, S. H. Joo, S. Jun, *J. Phys. Chem. B*, 103 (1999) 7743-7746

[12] M. Kioka, N. Kashiwa, JP1981-011908

[13] M. Terano, A. Murai, M. Inoue, M.Miyoshi, JP1987-158704

[14] B. Liu, T. Nitta, H. Nakatani, M. Terano, *Macromol. Chem. Phys.,* 204 (2003) 395-402

[15] D. Fregonese, S. Mortara, S. Bresadola, *J. Mol. Catal., A* 172 (2001) 89-95

[16] J. C. Chadwick, *Macromol. React. Eng*., 3, (2009) 428-432

[17] P. Chammingkwan, V. Q. Thang, M. Terano, T. Taniike, *Top. Catal.*, 57 (2014) 911-917

[18] A. Marigo, C. Marega, R. Zannetti, G. Morini and G. Ferrara, *Euro. Polym. J.,* 36, (2000) 1921-1926

[19] X. Zheng, M. S. Pimplapure, G. Weickert, J. Loos. *Macromol. Rapid Commun.,* 27, (2006) 15-20

[20] A. Dashti, A. Ramazani, Y. Hiraoka, S.Y. Kim, T. Taniike and M. Terano, *Polym. Int.,* 58 (2009) 40-45

[21] J. C. Dearden, *J. Comput.-Aided Mol. Des*., 17 (2003) 119-127

[22] W. E. Steinmetz, C. B. Rodarte, A. Lin, *Eur. J. Med. Chem*., 44 (2009) 4485-4489

[23] X.Hu, M. L. Foo, G. K. Chuah, S. Jaenicke, *J. Catal.* 195 (2000) 412-415

[24] G. Occhipinti, H. R.´ Bjørsvik, V. R. Jensen, *J. Am. Chem. Soc*., 128, (2006), 6952-

6964

[25] T. Taniike, T. Funako, M. Terano, *J. Catal*., 311 (2014) 33-40

[26] H. Nomura, N. Kurihara, K, Higuchi, JP Patent 1991-74341 (1991) (to COLCOAT Engineering Co., Ltd.).

[27] M. Terano, A. Murai, M. Inoue, K. Miyoshi, JP Patent 1987-158704 (1987) (to Toho Catalyst Co., Ltd.).

[28] K.S.W. Sing, D.H. Everett, R.A.W. Haul, L. Moscou R.A. Pierotti, J. Rouquérol, T. Siemieniewska, *Pure & Appl. Chem.,* 57 (1985) 603–619.

[29] T. Taniike, P. Chammingkwan, V.Q. Thang, T. Funako, M. Terano, *Appl. Catal.* A: Gen. 437–438 (2012) 24-27.

[30] P. Chammingkwan, V. Q. Thang, M. Terano, T. Taniike, *Top. Catal.*, 57 (2014) 911-917

[31] J.H. de Boer, B.G. Linsen, T. J. Osinga, *J. Catal*. 4 (1965) 643-648

[32] W.B. Innes, *Anal. Chem.* 29 (1957) 1069-1073

Chapter 6

General conclusion

6.1 General Summary

This dissertation discussed the elucidation of correlation between particle structures and polymerization performances in Ziegler-Natta olefin polymerization. The results were shown in as follows briefly.

In chapter 1, general introductions introduced catalyst importance, variety of catalyst multifunctional catalyst, historical development of Ziegler-Natta catalyst, polyolefin, structure performance relationship of Ziegler-Natta catalyst and statistics based on the objectives of this dissertation.

In chapter 2, multilateral characterization was established and applied to state-of-the-art Ziegler-Natta catalysts featured with ill-defined hierarchical structures. Precise parameterization of the catalysts through scanning electron microscopy, Hg porosimetry, N_2 adsorption/desorption, and chemical analyses enabled us to tackle structure-performance relationships in heterogeneous olefin polymerization. The validity of multilateral characterization over multi length scales to depict structure-performance relationships for such a complicated catalyst whose ill-defined hierarchical structure has been empirically optimized.

In chapter 3, various data were analyzed based on statistics for the elucidation of structure performance relationship between structure and performances. Obtained results

clarified the cause of difficulty to elucidate quantitative structure performance relationship in Ziegler-Natta olefin polymerization with small number of samples and insufficient characterizations from the viewpoint of statistics.

In chapter 4, several $Mg(OR)_2$ particles with various chemical composition were synthesized as precursor using small amount of second alcohols in order to synthesis novel pore architectures in Ziegler-Natta catalyst. These results succeeded to prepare novel pore structure in Ziegler-Natta catalyst by conversion from *i*-propanol containing $Mg(OR)_2$. This knowledge will contribute development of new type Ziegler-Natta catalysts and elucidation of structure performance relationship.

In chapter 5, multivariate analysis were employed to elucidate structure performance relationship in Ziegler-Natta catalyst systems which featured extremely complex reaction mechanism. Construction of high precise and valid structure performance relationship was succeeded by various optimization based on statistical manner. Obtained best fit regression equation model possessed high prediction ability with empirically assist.

6.2 Conclusion

Enormous amount of researches and developments are tired to elucidate the structure performance relationship in Ziegler-Natta olefin polymerization, however it has not achieved. The main causes are come from three features of Ziegler-Natta catalyst systems. First is difficulty of characterization on catalyst structure. Ziegler-Natta catalyst is composed of multicomponent and irregularly hierarchic structures which ranges from angstrom scale to millimeter. Second is difficultly of systematic change of catalyst morphology because current industrial preparation methods are not able to control only one structure parameters. Third is difficulty of quantitative elucidation of structure effect because catalytic performances were determined by various structural parameters with concerted or opposed mechanism. Therefore elucidation of structure performance relationship is very difficult task from above problems.

This study aims to elucidate structure performance relationship quantitatively in Ziegler-Natta olefin polymerization with solution of three difficult problems. In concrete tem, establishment of multilateral characterizations to identify irregular hierarchy particle structure (chapter 2), establishment of new preparation methods for synthesis novel type catalyst (Chapter 4) and usage of multivariate analysis to elucidate and evaluate structure performance relationships (Chapter 3 and 5) were implemented. As a results, elucidation

of structure performance relationship were attained quantitatively by combination of above three concept. This accomplishment possesses great meaning that first establishment of quantitative structure performance relationship and to obtain knowledge of systematical catalyst development.

Especially, these results suggested that the combination of multilateral characterization and multivariate analyses were powerful tool for direct structure-performance relationships in heterogeneous Ziegler-Natta catalysis. Additionally, this established method are able to use not only Ziegler-Natta olefin polymerization but also any heterogeneous catalyst systems even if catalyst systems possesses multicomponent, complex hierarchy and/or complex reaction mechanism. Therefore, this investigation results will largely contribute developments of catalyst chemistry development.

The Study of Propylene Gas Phase Polymerization Using Ziegler-Natta Catalysts

by

Toshiki Funako

Submitted to

Japan Advanced Institute of Science and Technology

Supervisor : Professor Timothy F. McKenna

LCPP–CNRS/ESCPE-Lyon

September 2014

1. Introduction

Polypropylene is one of most famous thermoplastic resin made by polymerization of propylene, and has various remarkable characteristics such as good mechanical properties, easiness of forming process, high recyclability, cheap price and so on. Therefore it is used as a material for various kinds of commercial products currently (approximately 75 billion grams per year) and produced enormous amount in various regions [1]. From such a background, expansion of used area and increase production is desired. For this purpose, development of Ziegler-Natta catalysts and production methods must be important.

Ziegler-Natta catalysts is olefin polymerization catalyst used in industrial. Especially, it is used the 99 % of polypropylene production. This catalyst was activated simple chemical combination consist of titanium trichloride and diethyl aluminum chloride, however its activities and stereoselectivity was low in the early stage of industrial using [2]. Then a lot of investigations and developments were conducted because of commercial importance of polypropylene. In 1980, the activity and stereoselectivity were improved drastically by using multicomponent such as addition of lewis base as active site modifier and magnesium dichloride as support, and control particle structure using precipitation method [3] and chemical reaction method [4]. In recent years, the controlled performances were not only activity and stereoselectivity but also copolymerization performance, hydrogen responsibility, control polymer morphology and so on by designing of particle structure [5].

From the above catalyst developments, the establishment of high efficiency production method became desired.

Slurry polymerization was used at first for industrial manufacturing. This method was conducted by autoclave as a reactor under about 1 MPa with inert paraffin solvent such as hexane and heptane. In this way, a lot of post treatments such as separation of unreacted propylene, deashing (for removal of catalyst), water washing, centrifugation, separation of atactic component and drying were necessary to obtain a polypropylene particle. As just describe, process of work was plenty and complex, and a lot of cost was fundamental to manufacture polypropylene. Therefore saving process number and cost were desired. After a while, bulk polymerization was established and used for industrial manufacturing. This method was polymerization of propylene in liquid propylene without any solvent. The merits of this method are high polymerization rate and improving efficiency of reactor capacity by using liquid propylene as monomer. Therefore miniaturization reactor was able to be conducted. The various post treatments came to be abbreviated by high production ability of this method and catalyst performance enhancement at that time. This method is often used for industrial homopolymerization currently because of high production efficiency. However there were some problems. For example, various number of reactor must be prepared for multistage polymerization such as impact copolymer, and elution the soluble components such as low molecular weight polymer and rubber to liquid propylene. From these background, gas phase polymerization was established and used in this time. This method

was polymerization of propylene in propylene gas without any solvent. The gas phase polymerization in the early stage of development made low quality polypropylene because there was not conducted the process of separation atactic polymer. Therefore, this method was limited to be used only specialty production. After a while, it became the most available method for making high quality and various kind of polymer by drastic improvement of catalyst performances. Then, this method can produce various type of polymer with only one reactor. For example, impact copolymer that manufacturing was necessary to conduct multistage polymerization and to control rubber content was made by this method with one reactor. Because of such an advantage, many type of reactor such as fluid gas type, mixing tank type and so on were invented and widely used at recent year.

However, the operations of gas phase polymerization were difficult with extremely small scale like a laboratory because of sensitivity of catalyst. Therefore, the purpose of this research was establishment of stable procedures in laboratory scale. Then, some polymerization were carried out with various conditions using gas phase polymerization reactor to obtain knowledge for optimization.

2. Experiments

2.1. Materials

Ziegler-Natta catalyst and triethylaluminium (TEA) were donated company respectively. Heptane and Cyclohexylmethyldimethoxysilane (CMDMS) was purified and used under inert atmosphere. Propylene and ethylene were used after pass over purification column. NaCl was used as dispersing agent for catalyst after drying by heating three times at 400 °C under extremely reduced pressure. (scheme 1)

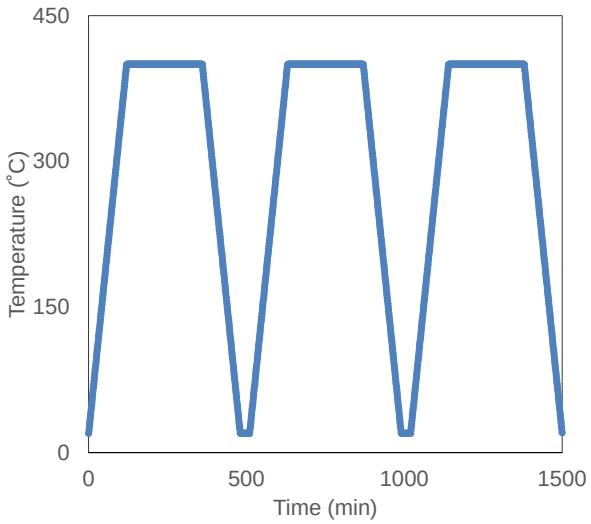

Scheme 1. The temperature behavior of NaCl in vaccum line for drying

2.2. Polymerizations

Propylene or Ethylene homopolymerization was performed in a 1 L autoclave equipped with a mechanical stirrer rotating at 350 rpm, provided with temperature control by water bath, pressure control and flow meter. (Figure 1) Monomer was introduced from connection lines into the reactor

through buffer tank and pressure record. The reactor is dried and cleaned via repeated flushing (three times) with argon at 70°C. At this temperature, 10 g of NaCl, 1 ml of 3M TEA and 20 µl of CMDMS were introduced into the reactor and stirring 10 min. Monomer was fed so as to reach the desired monomer overpressure, generally 7 bar. Once temperature and pressure have been stabilized, the catalytist mixture is fed into the reactor from a bomb by nitrogen overpressure. The homopolymerization is generally conducted at 70°C and at a total pressure of about 7 bar, usually for 1 h with continuous supply of monomer gas at 7 bar. Some trials have been performed, for example the change of introducing the catalyst mixture, using solvent and monomer etc. The produced polymer was cooled by cold water to avoid thermal fusion bonding.

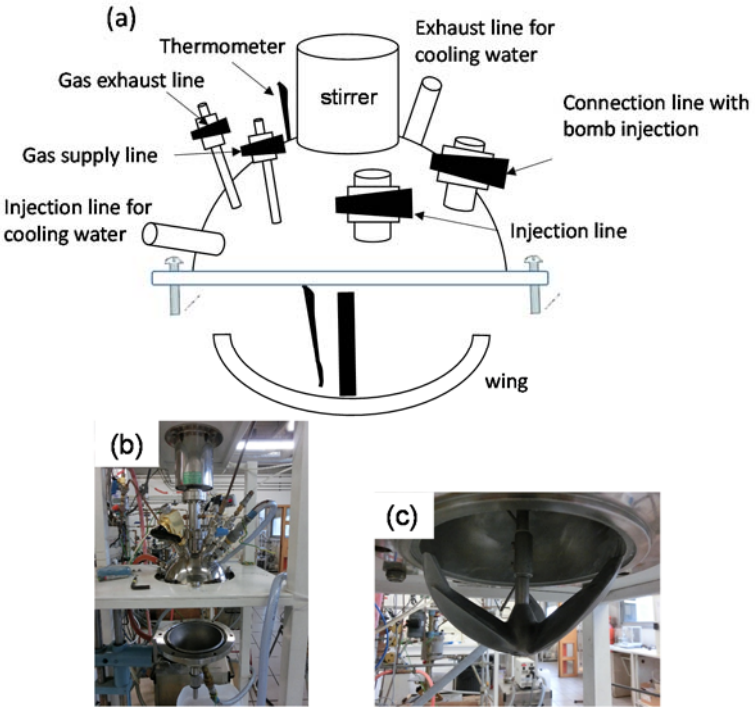

Figure 1. The images of gas phase reactor; (a) simplified reactor images , (b) reactor, (c) wing

3. Results and Discussion

3.1. Catalyst activities

The gas phase propylene polymerization was carried out in accordance with operations outlined in experimental section. The polymerization conditions and activities are shown in Table 1.

Table 1. Results of gas phase propylene polymerization[(a)]

	Catalyst (g)	NaCl (g)		Ex donor (mg)	Activity (Kg-PP·g-cat^{-1}·h^{-1})
		reactor	flask		
Run 1	30	10	2	20	0.02
Run 2	30	10	2	0	0.02
Run 3[(b)]	30	10	2	0	0.02

a) Polymerization condition; propylene, activator : TEA, activator amount : 3 mmol, pressure : 7 bar, stirring speed : 350 rpm, injection method : direct injection from flask.
b) NaCl were dried again by heating and vacuum before using.

Gas phase polymerization was carried out without any problem and reproducibility was confirmed, however catalyst activity was extremely low. (Run 1) Generally, this catalyst has more than 30times higher activity even if activity of gas phase polymerization is lower than slurry phase. Next polymerization was carried out without external donor because of avoidance the reduction effect for an activity and purity itself. (Run 2) However, the activity was not improved and value was same as Run 1. It suggested that the cause of extremely low activity was not existence of external donor. Then polymerization was carried out using NaCl which dried again by heating three times at 400 °C under extremely reduced pressure because possibility of remaining water in NaCl. (Run 3) However, Run 3

activity was as low as Run 1. It suggested that NaCl had been perfectly dried because an excess drying NaCl was inefficiency. From these results, the cause of low activity was not purity of some materials.

3.2. Injection method effects on activity

The mixture of catalyst and NaCl was transferred to reactor from round flask by argon flow so far. In order to improve injection systems much smooth and particularity, bomb injection method was adopted. The result of polymerization among different injection methods was shown in Table 2.

Table 2. Results of polymerization among different injection methods[(a)]

	Catalyst	NaCl (g)		Injection	Activity
	(g)	reactor	flask	method	(Kg-PP·g-cat^{-1}·h^{-1})
Run 4	30	10	2	direct injection	0.02
Run 5	30	10	2	bomb injection (propylene)	0.02
Run 6	30	10	2	bomb injection (H_2)	0.02

a) Polymerization condition; activator : TEA, activator amount : 3 mmol, pressure : 7 bar, stirring speed : 350 rpm, injection method : direct injection from flask.

In order to make same condition without injection method, the catalyst mixture was injected directly from flask to reactor. (Run4) Naturally, This batch had an equally low activity as Run 1~3. Then stainless steel bomb injection was used form then on. This method is expected improvement of activity by not only avoidance of contact water to catalysts by keeping high pressure but also immiscibility of inert gas in the reactor. Propylene was used as injection gas, while activity was not changed previous. (Run 5) Then, Hydrogen was used as injection gas which has an activation effect, however activity

was not improved.

3.3. Pretreatment effects on activities

The validity of polymerization activity has not been able to obtain by polymerization procedures above. It had been possibility that the cause was imperfect activation catalyst by TEA in reactor, because of big amount of NaCl as dispersion agent in comparison with TEA amount. Therefore catalyst and NaCl mixture was reacted with TEA before transfer reactor as pretreatment (Run 7). This result is shown in Table 3 with Run 4 as reference.

Table 3. Effects of pretreatment on performance[(a)]

	Catalyst	NaCl (g)	TEA (mmol)			Activity
	(g)	reactor	bomb	pretreat	reactor	(Kg-PP·g-cat^{-1}·h^{-1})
Run 4	30	10	2	0	3	0.02
Run 7	30	10	2	3	0	0.03

a) Polymerization condition; pressure : 7 bar, stirring speed : 350 rpm, injection method : direct injection from flask

The mixture of catalyst and NaCl was reacted well with TEA. The activity was slightly improved by pretreatment, however activity was too low to conclude correct value. It suggested that previous operations also activated all catalyst. Therefore activity between Run 4 and Run 7 were almost same.

3.4. Catalyst concentration in mixture effect on activities

A small amount of catalyst stuck on flask wall after a catalyst mixture transfer stainless-steel bomb from flask. It was able to be considered that sticking force come from static electricity or reaction with water from flask wall, however the direct cause of sticking catalyst was uncertain. While the amount of catalyst was increased in order to reduce catalyst loss relatively. (Run 8) In addition, another case which the mixture was treated with TEA before transfer reactor to avoid inactivation catalyst was performed. (Run 9) These results were shown in Table 4 with Run 5 as reference.

Table 4. Effects of mixture amount for activity[(a)]

	Catalyst (g)	NaCl (g) reactor	bomb	TEA pretreat	reactor	Activity (Kg-PP·g-cat^{-1}·h^{-1})
Run 5	30	10	2	0	3	0.02
Run 8	111	10	17	0	3	0.02
Run 9	89	10	14	3	3	0.03

a) Polymerization condition; activator : TEA, pressure : 7 bar, stirring speed : 350 rpm, injection method : bomb injection method.

The reduction of catalyst sticking on the wall were improved by increase catalyst/NaCl mixture amount. However, the value of activity was not increase. It suggested that catalyst loss during transfer was not major reason of low activity.

3.5. Comparison with slurry polymerization

The purity of propylene was doubted. While slurry polymerization was performed because propylene was purified by scavenger (TEA) in slurry before contact with active site. In addition, the increase of monomer contact frequency to active site, and the reduction of monomer diffusion limitation from polymer swellhead. The result is shown in Table 5 with Run 1 and Run 8 as references.

Table 5. Comparison between gas phase and slurry polymerization [(a)]

	Catalyst (g)	NaCl (g) reactor	bomb	TEA (mmol)	Ex donor (mg)	Activity (Kg-PP·g-cat^{-1}·h^{-1})
Run 1	30	10	2	3	20	0.02
Run 8	111	10	17	3	0	0.02
Run 10	136	0	0	3	20	0.99

a) Polymerization condition; activator : TEA, pressure : 7 bar, stirring speed : 350 rpm, injection method : bomb injection method.

As can be seen, the activity of slurry polymerization was very high compared with gas phase polymerization. Originally, it is well known that gas phase polymerization has lower activity than slurry polymerization, however, the difference is enormous. It is considered that this difference comes from degree of catalyst particle fragmentation and/or monomer diffusion limitation by generated polymer.

3.6. Monomer effects on activities (comparison between propylene and ethylene)

The monomer was changed from propylene to ethylene, in order to confirm previous hypothesis. It was expected that the activity would be changed by changing monomer, because the progress of particle fragmentation was changed by propagation rate. (Run 11) The result was shown in Table 6 with Run 8 as reference.

Table 6. Effect of changing monomer on activity

	monomer	Catalyst (g)	NaCl (g) reactor	bomb	TEA pretreat	reactor	Activity (Kg-PP·g-cat^{-1}·h^{-1})
Run 8	propylene	111	10	17	0	3	0.02
Run 11	ethylene	50.3	13.3	2.6	0	3	0.26

Polymerization condition; activator : TEA, pressure : 7 bar, stirring speed : 350 rpm, injection method : bomb injection method.

The gas phase ethylene polymerization activity was more than ten times higher than propylene. It can't be describe as only fragmentation effect because of many reaction situation were different such as propagation rate, diffusion limitation in polymer and/or particle. However, the difference were conformed which can't be explained only propagation rate. It suggested that the phenomenon about monomer diffusion such as fragmentation behavior and polymer film effect for activity.

4. Conclusion

The gas phase polymerization was not able to be conducted well while many trial was done. However, the results suggest that monomer diffusion control is one of most important operation for control activity. Therefore it is considered that particle fragmentation control is necessary for gas phase polymerization by pretreatment for desirable monomer diffusion.

Refference

[1] G. Natta, P. Pino, P. Corradini, F. Danusso, E. Mantica, G. Mazzaniti and G. Moraglio, *J. Am. Chem.Soc.*, 77 (1955) 1708.

[2] K. Soga and T. Shiono, *Prog. Polym. Sci.*, 22 (1997) 1503-1546.

[3] M. Kioka, N. Kashiwa, JP1981-011908

[4] M. Terano, A. Murai, M. Inoue, M.Miyoshi, JP1987-158704

[5] T. Taniike, T. Funako, M. Terano, *J. Catal*., 311 (2014) 33-40

Ackonowledgments

I would like to express my sincere gratitude to Professor Timothy F. McKenna. This work would never have been done without his kindly help.
I wish to express my gratitude to laboratory members for their kind encouragement.
Especially, I deeply appreciate to Mr Aaròn and Mr bashir for them helping and suggestions on all experiments.
Finally, I am deeply grateful to Professor Minoru Terano, associate Professor Toshiaki Taniike, associate Professor Tatsuo Kaneko and JAIST gave me an opportunity to study abroad and kindly support.

Toshiki Funako

Terano Laboratory,
School of Material Science,
Japan Advanced Institute of Technology

Achievement

Publication Paper

[1] T. Taniike, P. Chammingkwan, V. Q. Thang, T. Funako, M. Terano, "Validation of BET specific surface area for heterogeneous Ziegler-Natta catalysts based on α_s-plot" *Appl. Catal., A: Gen.*, 437-438, 26, 24-27, 2012

[2] T. Taniike, T. Funako, M. Terano, "Multilateral characterization for industrial Ziegler–Natta catalysts toward elucidation of structure-performance relationship" *J. Catal.*, 311, 33-40, 2014

[3] T. Funako, P. Chammingkwan, M. Terano, T. Taniike, "Alternation of Pore Architecture of Ziegler-Natta Catalysts through Modification of Magnesium Ethoxide" *Macromol. React. Eng.*, *accepted*

[4] T. Funako, P. Chammingkwan, T. Taniike, M. Terano, "Addition of second alcohol in magnesium ethoxide synthesis as a way to vary the pore architecture of Ziegler-Natta catalysts" *Polyolefin J.*, *accepted*

Patent

・谷池 俊明, 寺野 稔, 舟子 俊幹, 特許出願 2014-054543. " マグネシウムエトキシド結晶を含有する粒子とその製造方法"

International conference

[1] Comprehensive Structural Analysis for Magnesium Diethoxide-based Ziegler-Natta Catalysts 8th International Colloquium on Heterogeneous Ziegler-Natta catalysts, Kanazawa, Japan, Mar. 27-30, 2012

[2] Pore architecture designs of Magnesium alkoxide based olefin polymerization catalysts International Conference on the Reaction Engineering of Polyolefins, Ferrara, Italy, Sep. 2-5, 2013

Domestic conference

[1] 粒子形態の異なる Ziegler-Natta 触媒を用いたプロピレン重合
第 56 回高分子夏季大学　福井　2011 年 7 月

[2] マグネシウムエトキシドを用いて調製した Ziegler-Natta 触媒の粒子構造とプロピレン重合性能の相関

第 41 回石油化学討論会　山口　2011 年 11 月
[3] マグネシウムジエトキシド型 Ziegler-Natta 触媒粒子の定量的構造解析
第 56 回高分子学会年次会　横浜　2012 年 5 月

[4] Ziegler-Natta 触媒粒子の細孔の大きさが重合性能に及ぼす影響
第 42 回石油化学討論会　秋田　2012 年 10 月

[5] $Mg(OEt)_2$ 型 Ziegler-Natta 触媒粒子の細孔構造の同定と触媒性能
第 3 回ポリオレフィン研究会若手会　石川　2013 年 1 月

[6] 粒子状マグネシウムアルコキシドの組成が Ziegler-Natta 触媒構造に及ぼす影響
第 57 回高分子学会年次会　横浜　2013 年 5 月

[7] Ziegler-Natta 触媒粒子の多角的同定
第 4 回ポリオレフィン研究会若手会　石川　2013 年 1 月

[8] Ziegler-Natta 触媒の粒子構造分析と構造性能相関解明への統計学的アプローチ
第 58 回高分子学会年次会　名古屋　2014 年 5 月

[9] 多変量解析による不均一 Ziegler-Natta 触媒の構造と性能の相関解明
第 63 回高分子討論会　長崎　2014 年 9 月

[10] Ziegler-Natta 触媒の構造性能相関解明への統計学的アプローチ
第 4 回 CSJ 化学フェスタ 2014　東京　2014 年 10 月

Acknowledgments

I would like to express my sincere gratitude to Professor Dr. Minoru Terano and Associate professor Dr. Taniike Toshiaki. This work would never have been done without their kindly and enormously help.

I wish to express my gratitude to Professor Dr. Masayuki Yamaguchi (JAIST) and Associate Professor Dr. Tatsuo Kaneko (JAIST) who have provided valuable advice and comments. I also wish to express my gratitude to Professor Dr. Kotohiro Nomura (Tokyo Metropolitan University) for reviewing this dissertation and many valuable comments and suggestions. I also wish to express my gratitude to Professor Dr. Timothy F. McKenna, (ESCPE-Lyon in FRANCE) for their kind guidance in my minor research theme.

I wish to express my gratitude to laboratory members for their kind encouragement. Especially, I deeply appreciate to Assistant Professor Dr. Patchanee Chammingkwan, Dr. Shougo Takahashi, Keisuke Goto for them helping and suggestions on all experiments and revision of documents.

Finally, I am deeply grateful to my parents, Shigeru and Mieko for their great supports, kindness and giving an opportunity to study at JAIST.

Toshiki Funako

Terano Laboratory,
School of Material Science,
Japan Advanced Institute of Technology